R-NODE METHOD AND ITS APPLICATION IN LIMIT ANALYSIS OF STRIP FOUNDATIONS

YI YUELEI

R-Node Method and Its Application in Limit Analysis of Strip Foundations

by

©Yuelei Yi, B.E., M.E.

A thesis submitted to the School of Graduate Studies

in partial fulfillment of the requirements for the

degree of Master of Engineering

Faculty of Engineering and Applied Science

Memorial University of Newfoundland

November 18, 2004

St. John's Newfoundland

Library and Archives Canada

Published Heritage Branch

395 Wellington Street
Ottawa ON K1A 0N4
Canada

Bibliothèque et Archives Canada

Direction du Patrimoine de l'édition

395, rue Wellington
Ottawa ON K1A 0N4
Canada

Your file Votre référence
ISBN: 978-0-494-30529-4
Our file Notre référence
ISBN: 978-0-494-30529-4

Abstract

Limit analysis is very useful in the assessment and design of mechanical components and structures. Among the various methods for limit load estimation, approximate methods based on linear elastic finite element analyses are appealing to analysts and designers due to the conceptual insight, economy of computational effort and wide applicability.

In this thesis, an approximate method for determining the limit loads of foundations on homogeneous and layered cohesive soils and cohesive-frictional soil is presented in detail. The results obtained for layered soils are presented as charts to be used for foundation design. This method makes use of the results of two or more linear elastic analyses. From these linear elastic analyses, load controlled locations called r-nodes are identified and limit loads are determined. The concept of r-nodes (redistribution nodes), which are akin to plastic hinge locations in a structure, forms the basis of this method. Several possible alternative ways of applying the r-node method to pressure-sensitive materials are also presented.

The results obtained are compared with analytical results and elastic-plastic nonlinear finite element analysis results.

Acknowledgements

I want to thank my thesis supervisors, Dr. Radu Popescu and Dr. Seshu Madhava Rao Adluri for their dedication, time, and thoroughness.

I thank Dr. Arash Nobahar and Mr. Ahmad Jafari Mehrabadi, who have put up with my constant interruptions of their work and who also have been of great help in discussions on the subject of this thesis

I thank Dr. Alireza Azizian and Mrs. Neda Zangeneh for their kind assistance.

I would like to thank everyone that has been involved in my work, including all those who helped me and have made my time as a student at the department interesting.

Financial assistance provided by the Faculty of Engineering & Applied Science, the School of Graduate Studies, Memorial University of Newfoundland, in the form of scholarships and assistantships is gratefully acknowledged.

A lot of thanks go to the staffs of the Faculty of Engineering & Applied Science, who over the years have facilitated my progress.

Finally, I thank my family for their support.

Nomenclature

A	Area
B	Bulk modulus, or width of foundation
B_n	New bulk modulus of each element for the second elastic analysis
B_o	Original bulk modulus of each element for the first elastic analysis
B, n	Creep parameters for second stage creep
c, ϕ	Cohesion and friction angle
C_{ijkl}	Elastic stiffness tensor
C^p_{ijkl}	Plastic stiffness tensor
C^{ep}_{ijkl}	Elastic-plastic stiffness tensor
D_f	Depth of the foundation
e_1, e_2, e_3	Principal components of deviatoric strain tensor
e_{ij}	Deviatoric strain tensor
E_n	New elastic modulus of each element for the second elastic analysis
E_o	Original elastic modulus of each element for the first elastic analysis
E_p	Plastic modulus in uniaxial stress condition

E_t	Tangential modulus in uniaxial stress condition
F_i	Body forces
G	Shear modulus
G_n	New shear modulus of each element for the second elastic analysis
G_o	Original shear modulus of each element for the first elastic analysis
H_p	Slope of effective stress-effective plastic strain curve
$I_1 = \sigma_{ii}$	First invariant of stress tensor
$I_1^{'} = \varepsilon_{ii}$	First invariant of strain tensor
$J_2 = \frac{1}{2} s_{ij} s_{ji}$	Second invariant of deviatoric stress tensor
$J_2^{'} = \frac{1}{2} e_{ij} e_{ji}$	Second invariant of deviatoric strain tensor
$J_3 = \frac{1}{3} s_{ij} s_{jk} s_{ki}$	Third invariant of deviatoric stress tensor
k	Pure shear yield stress (kPa), Strength parameter in Drucker-Prager criterion
L	Length of the foundation (m)
M	Applied external load
m_α	Lower bound multiplier corresponding to an applied load

N_γ, N_c, N_q	Dimensionless bearing capacity coefficients
s_1, s_2, s_3	Principal components of deviatoric stress tensor
s_{ij}	Deviatoric stress tensor
P	Applied pressure
P_L	Limit pressure
$\tilde{P}$	Applied external load
$\tilde{P}_L$	Plastic collapse load or limit load
Q_f	Limit pressure of strip foundation
r	Radius
T_i	Surface tractions
u, v	Displacements
ν	Poisson's ratio
ν_n	New Poisson's ratio of each element for the second elastic analysis
ν_o	Original Poisson's ratio of each element for the first elastic analysis
V	Volume, or velocity
W	Strain energy function
Ω	Complementary energy function
α	Proportionality constant, strength parameter in Drucker-Prager criterion
$\lambda_\gamma, \lambda_c$	Shape factors of the bearing capacity of the foundation

γ	Geometric scaling factor, engineering shear strain, or unit weight
δ	Displacement in a component or structure
$\dot{\delta}$	Displacement rate
$\dot{\delta}_{ref}$	Displacement rate at the reference stress
$\varepsilon_1, \varepsilon_2, \varepsilon_3$	Principal components of strain tensor
ε_c	Creep strain
$\varepsilon_{c,m}$	Creep strain at the mean radius
$\dot{\varepsilon}_c$	Creep strain rate
$\dot{\varepsilon}_{c,ref}$	Creep strain rate at the reference stress
ε_{ij}	Strain tensor
ε_{ij}^e	Elastic strain tensor
ε_{ij}^p	Plastic strain tensor
ε_V	Volumetric strain
ϕ	Friction angle
σ_0	Initial yield stress in uniaxial tension (kPa)
$\sigma_1, \sigma_2, \sigma_3$	Principal components of stress tensor
σ_c	Uniaxial compressive yield stress (kPa)

σ_e	Effective or von Mises stress (kPa)
σ_{ei}	Pseudo elastic effective stress in an element (kPa)
$(\sigma_e)_{r-node}$	R-node effective stress (kPa)
σ_{ij}	Stress tensor
$\bar{\sigma}_n$	Combined r-node effective stress (kPa)
σ_{nj}	R-node effective stress at the plastic hinge location j (kPa)
σ_{ref}	Reference stress (kPa)
σ_t	Uniaxial tensile yield stress (kPa)
σ_y	Yield stress (kPa)
τ_0	Initial yield stress in pure shear (kPa)
κ	Hardening parameter or plastic internal variable
v_j	Unit outward normal at a point

Abbreviations

ASME	American Society of Mechanical Engineers
CSME	Canadian Society of Mechanical Engineers
GLOSS	Generalized Local Stress Strain
FEM	Finite Element Method
R-node	Redistribution Node
RSM	Reference Stress Method

Subscripts

e	External
i	Internal, tensorial index
j, k	Tensorial indices
L	Limit
r	Polar coordinate
R	Reference
s	Softened
y	Cartesian coordinate, yield
x, z	Cartesian coordinate
θ	Polar coordinate

Superscripts

c	Creep
n	Creep exponent
L	Lower bound
U	Upper bound
*	Differential change of force or moment across an element of a structure

Contents

List of Tables

List of Figures

Chapter One

Introduction

1.1 General Background

The primary objective of this thesis is to investigate the applicability of a robust approximate method, namely the r-node method, to estimate the limit load of foundations on various types of soil materials. The numerical examples are limited to strip foundations placed at ground level. At present, limit loads of strip foundation under conditions of plane strain are obtained either by analytical methods such as limit equilibrium method (Terzaghi (1943) [1] and Meyerhof (1951) [2]), slip-line method (Sokolovskii (1965) [3] and Brinch Hansen (1961) [4]) and limit analysis method (Shield (1954) [5], Chen and Davidson (1973) [6]), or numerical techniques, such as the nonlinear finite element technique.

Analytical methods for limit analysis of foundations have evolved over a long period of time as compared to computer-aided numerical techniques, such as the finite element analysis, which are comparatively recent. An examination of the literature on plastic analysis reveals that analytical solutions are available only for simple cases of loading and geometric configurations. Inelastic finite element analysis, on the other hand, has its own limitations mainly related to computational effort. The above factors thus

create the need for the development of approximate methods, which are simple, efficient and yet sufficiently accurate for analyzing limit loads of structures.

The r-node method, explained in detail in the next chapter, is an approximate method for performing limit analysis. The method, in essence, is a technique for performing limit analysis by combining the accuracy and rationale of the finite element technique, the speed and the ease of linear elastic analysis and the concept of the reference stress method. This method makes use of the statically determinate locations in a structure, called the r-nodes, for the limit analysis. The stresses at the r-node locations, called the r-node stresses, can be directly related to the load-controlled mode of failure of a structure. The r-node method can, therefore, be used to performed limit analysis of a structure in a robust manner.

1.2 Objectives of the Thesis

The objectives of this thesis are:

1. To present a robust method for the limit analyses of purely cohesive soils and provide design charts for strip foundation on layered soils.
2. To provide limits of applicability for layered cohesive soils.
3. To investigate the possibility of applying the r-node method for pressure-sensitive materials.

1.3 Organization of the Thesis

Chapter 1 briefly addresses the usefulness of limit analysis in structural design and the existing limit analysis techniques. The r-node method and its value in limit analysis

are briefly discussed in this chapter. The objectives of this thesis and its original contributions are also clearly identified in this chapter.

The fundamental concepts relating to limit analysis and r-node method are covered in chapter 2. A literature survey covering plasticity and limit analyses, the reference stress method and the r-node method is presented; the concept of robustness, which involves the development of simplified methods to predict inelastic response with reasonable accuracy, is discussed. This chapter also examines the r-node concept and the method, and brings out the relationship between the r-node stress and the reference stress.

Chapter 3 discusses constitutive equations of materials. The elastic and plastic stress-strain relations of materials are covered in this chapter. Yield criteria for the hydrostatic-pressure-independent materials, such as some metals, and hydrostatic-pressure-dependent materials, such as the brittle or granular materials, are analyzed in this chapter.

The plasticity theories applied to soil materials are briefly reviewed in Chapter 4. Finite element method and analytical methods for the determination of limit loads of soil structures are explained in this chapter. Also, the general methods for calculating the bearing capacity of shallow foundations are presented.

In Chapter 5, the r-node method is used in determining the bearing capacity of strip foundations on cohesive soils. Several numerical examples are used to validate the r-node method. The problems consist of determining the limit loads of strip foundations on homogeneous soil and layered soils. The finite element modeling methodology is explained, and the limit loads are calculated using the analytical methods, non-linear finite element method and r-node method. R-node method results are compared with

those of theoretical or other analytical methods, and nonlinear finite element results are also discussed in this chapter.

Chapter 6 presents several alternative strategies in the use of the r-node for estimating limit loads of foundations on pressure-sensitive materials (i.e. cohesive-frictional soils). While those attempts have not been entirely successful, the approaches and the results are analyzed and explained in detail to serve as a basis for future research.

Chapter 7 summarizes the present study and briefly discusses the advantages of the r-node method. Suggestions are also given for related future research.

Chapter Two

Basic Concepts and Literature Review

In view of the facts that a complete analysis including the range of plastic flow is, in general, expensive computationally, and failure by plastic collapse is the governing condition in so many problems in soil mechanics (Chen, (1975) [7]), the development of efficient methods for computing the collapse load in a more direct manner is of practical interest to engineers. Limit analysis is concerned with the development and applications of such methods.

In the field of limit analysis in soil mechanics, Chen (1975) [7] has contributed much to summarize and develop the work of previous researchers. Many significant results in theories and applications of limit analysis have been reviewed or obtained by Chen (1975) [7], such as reviewing the theorems of limit analysis, applying the slip-line and limit equilibrium methods to solve the bearing capacity of shallow foundations, analyzing the problems of stability of slopes and so on. In this thesis, many relative theories, such as concepts of limit analysis, and computer implementations, such as the principles of building the FE models are based on theorems or principles summarized by Chen (1975) [7]. In the present research, a robust approximate method, namely r-node method, would be utilized in analyzing and solving a limit analysis problem, namely bearing capacity of strip foundations.

2.1 Concept of Limit Analysis

Limit analysis is the method which enables definite statements to be made about the collapse load without carrying out the elastic-plastic analysis (Chen, (1975) [7]). Limit analysis is concerned with the calculation of the load at which plastic flow occurs in mechanical components or structures. From a design standpoint, to carry limit analysis is useful for assessing load-controlled effects in structures. The classical theorems of limit analysis are the lower and upper bound theorems.

2.1.1 Lower-bound Theorem

The load, determined from a distribution of stress alone, that satisfies the equilibrium equations, stress boundary conditions and nowhere violates the yield criterion, is not greater than the actual collapse load (Chen, (1975) [7]). The distribution of stress satisfying the above three conditions has been termed as statically admissible stress for the problem under consideration. Hence the lower-bound theorem may be restated as bellow:

If a statically admissible stress distribution can be found, uncontained plastic flow will not occur at a lower load.

2.1.2 Upper-bound Theorem

The load, determined by equating the external rate of work to the internal rate of dissipation in an assumed deformation mode (or velocity field), that satisfies velocity boundary conditions and strain and velocity compatibility conditions, is not less than the

actual collapse load (Chen, (1975) [7]). The dissipation of energy in plastic flow associated with such a field can be computed from the idealized stress-strain rate relation (or the so-called flow rule). A velocity field that satisfies the above conditions has been termed a kinematically admissible velocity field. Hence, the upper-bound theorem may be restated as bellow:

If a kinematically admissible velocity field can be found, uncontained plastic flow must impend or have taken place previously.

The upper-bound technique considers only velocity or failure modes and energy dissipation. The stress distribution need not be in equilibrium, and is only defined in the deforming regions of the mode.

By suitable choice of stress and velocity fields, the above two theorems thus enable the required collapse load to be bracketed as closely as seems necessary for the problem under consideration.

2.2 Concept of Approximate Method

The limitations of the existing analytical techniques and the nonlinear finite element analysis provide an incentive to develop inexpensive approximate methods that are simple to use, and yet can predict inelastic response with reasonable accuracy (Mangalaramanan, (1993) [8]). Such methods are termed as robust approximate methods. Approximate methods are often used to estimate the limit load of structures, which means a series of elastic analyses will be used to replace one elastic-plastic analysis in calculating the limit loads of structures.

Compared with analytical techniques and the non-linear finite element analysis methods, approximate methods are simple, inexpensive, and less time-consuming.

2.3 Classification of Approximate Methods

The approximate method being used in this thesis has roots that were first developed in creep mechanics. Carrying the general creep and relaxation analysis is normally difficult and complicated; as a result of such difficulty, several approximate techniques have been proposed and presented. These techniques are generally arranged into two broad categories. First, the reference stress method, which has been applied to problems of creep deformation under steady and variable loads, creep buckling, and creep rupture. Second, bounding techniques that emanate from the principle of virtual work have been devised for problems of creep deformation under steady and variable loads.

The reference stress method is a simplified method that attempts to minimize the effect of scatter in the creep parameters by using uniaxial test data (Kraus, (1980) [9]). This method attempts to correlate creep deformation in a structure with the creep strain that results during a simple creep test.

The bounding technique method is a simplified method that attempts to drive kinematically admissible velocity fields and statically admissible fields in the limit analysis of perfectly plastic structures by using variational principles (Kraus, (1980) [9]). The methods based on virtual work were extended to situations such as variable loads, and to interaction with plasticity by Ponter (1970) [17] and others.

2.3.1 The Reference Stress Method

One of the first approximate methods relevant to the present study is the reference stress method (RSM). In the United States, Soderberg (1941) [10] calculated the first reference stress of tubes; and then the method has been under development since the mid 1960's in the United Kingdom. Basically, the idea of the method is that a given structure can be analyzed with data obtained from a single creep test at its reference stress (Marriott, (1970) [11]).

Earlier developments of the RSM were aimed at estimating the creep deformation of a complex structure under mechanical loading by carrying out a single uniaxial test. That means there exists a transformation for a component or structure, given by

$$\delta = \gamma \varepsilon_c \left[\sigma_{ref} \right] \tag{2.1}$$

where, δ is some relevant displacement within a structure; σ_{ref} is the reference stress; γ is a geometric parameter that would depend on the overall configuration of the component or structure and the boundary conditions, and ε_c is the uniaxial creep deformation at the reference stress.

A number of the earlier investigators (e.g. Anderson, et al., (1963) [12]) also found that the reference stress is relatively insensitive to changes in the magnitude of the creep parameters, and there exists a linear proportionality between the reference stress and applied external load. The linear proportionality between the reference stress and applied external load can be expressed as

$$\sigma_{ref} = \alpha \tilde{P} \tag{2.2}$$

where, α is a function of geometry; $\tilde{P}$ is the applied external load.

The linear proportionality between the reference stress and the applied external load approximately leads to the notion of "insensitivity to the creep parameters". It also proved that the validity of RSM is not dependent on a specific form of constitutive relationship. Making use of the aspect of insensitivity to the creep parameters, several analytical methods of reference stress determination by different researchers (e.g. Anderson, et al., (1963) [12]) have been developed. The values of the reference stress and the scaling factor γ obtained by the different approaches described above are quite close.

Applying the notion that the reference stress is relatively insensitive to changes in the magnitude of the creep parameters, Sim (1971) [14] reasoned that as creep exponent approaches infinity, the stress distribution would correspond to the limit solution of perfect plasticity; therefore, the reference stress can be obtained by

$$\sigma_{ref} = \frac{\tilde{P}}{\tilde{P}_L} \sigma_y \tag{2.3}$$

where, $\tilde{P}_L$ is the rigid-plastic collapse load for a yield stress. Ponter and Leckie (1970) [17] have shown that this approximation constitutes an upper bound on the value of stress, and is therefore on the safe side for design purposes.

2.3.2 Bounding Techniques

Bounding techniques are developed based on virtual work principle. In an elastic solid, by means of the formulas $\sigma_{ij} = \frac{\partial W}{\partial \varepsilon_{ij}}$, $\varepsilon_{ij} = \frac{\partial \Omega}{\partial \sigma_{ij}}$, stresses σ_{ij} and strains ε_{ij} can be solved from the strain energy function W and the complementary energy function Ω, where, $W = \int \sigma_{ij} d\varepsilon_{ij}$, $\Omega = \int \varepsilon_{ij} d\sigma_{ij}$.

Further, by Ducker's postulate of materials stability (Drucker, (1952) [18]), a restriction is placed on them. That is, given a pair of strain states ε_{ij} and ε_{ij}^* with corresponding stress states σ_{ij} and σ_{ij}^*, it is required that

$$\int_{\varepsilon_{ij}^*}^{\varepsilon_{ij}} \left(\sigma_{ij} - \sigma_{ij}^*\right) d\varepsilon_{ij} \geq 0 \tag{2.4}$$

where, σ_{ij}^* remains constant during the integration from ε_{ij}^* to ε_{ij} over any path.

According to the virtual work principle (Drucker, (1952) [18])

$$W + \Omega = \int \left(\sigma_{ij} d\varepsilon_{ij} + \varepsilon_{ij} d\sigma_{ij}\right) = \sigma_{ij} \varepsilon_{ij} \tag{2.5}$$

The foregoing inequality may be written in another form,

$$\Omega\left(\sigma_{ij}^*\right) + W\left(\varepsilon_{ij}\right) \geq \sigma_{ij}^* \varepsilon_{ij} \tag{2.6}$$

Considering a continuum of stable elastic material, with the body forces F_i acting on the continuum, and all displacements are assumed to be small so that geometry

changes can be ignored, and that a stress field σ_{ij}^* and a strain field ε_{ij} are known for the continuum. The stress field must be in internal equilibrium with the body forces, that is,

$$\frac{\partial \sigma_{ij}^*}{\partial x_j} + F_i^* = 0 \tag{2.7}$$

The surface tractions T_i^* are defined by the requirements of external equilibrium. Thus at any surface of the continuum,

$$\sigma_{ij}^* v_j = T_i^* \tag{2.8}$$

where, v_j is the unit outward normal at a point. The strains ε_{ij} must be compatible with the displacements u_i, thus,

$$\varepsilon_{ij}^C = \frac{1}{2}\left(\frac{\partial u_i^C}{\partial x_j} + \frac{\partial u_i^C}{\partial x_i} \right) \tag{2.9}$$

Because σ_{ij}^*, ε_{ij} are completely independent of each other, T_i^*, F_i^* and σ_{ij}^* are in equilibrium and u_i^C and ε_{ij}^C are compatible, we may write by the principle of virtual work

$$\int_A T_i^* u_i^C dA + \int_V F_i^* u_i^C dV = \int_V \sigma_{ij}^* \varepsilon_{ij}^C dV \tag{2.10}$$

where, A and V are the area and volume of the continuum.

Then considering the inequality (2.6), σ_{ij}^* and ε_{ij}^C is an admissible pair of states at all points of the body, thus we may integrate over the volume retaining the inequality. Substituting the result into equation (2.10),

$$\int_V \Omega\left(\sigma_{ij}^*\right)dV + \int_V W\left(\varepsilon_{ij}^C\right)dV \geq \int_A T_i^* u_i^C dA + \int_V F_i^* u_i^C dV \tag{2.11}$$

Martin (1966) [19] derived the above inequality. He applied it to steady creep problems on the basis of the elastic analogy. As an illustration, Martin (1966) [19] applied this bounding technique to the creep of a cantilever beam subjected to a distributed load and obtained upper bound on the solution. The bound is very good for that simple example. With similar reasoning, a lower bound on the solution was developed and extended to other situations such as variable loads, and to interaction with plasticity by Ponter (1970) [17], Palmer (1967) [20], Leckie (1974) [21] and others. An excellent review of this effort had been given by Leckie (1974) [21].

In the above, two approximate analytical techniques have been presented for solving creep problems: the reference stress method and bounding techniques based on the principle of virtual work. These methods have been used mostly in the United Kingdom. It can be said that both avenues, the approximate analytical one presented here and the numerical one, are now available to those contemplating work in this field. Approximate analytical methods are presumably simpler, but digital computer solutions are more accurate. On the surface it would seem that the latter would be the preferred method. However, digital computer solutions are becoming more and more expensive so that the simpler approximate methods are becoming more appealing on the basis of cost. It is likely that eventually preliminary design will be carried out with the approximate methods while final design analysis will continue to be carried out with the digital computer.

2.4 Literature Review

Limit analysis is concerned with the calculation of the load at which uncontained plastic flow occurs in mechanical components or structures. The availability of closed form analytical expressions for limit loads is restricted to components and structures with simple geometric and loading configurations. An alternative, or a simpler recourse, is to invoke the lower and upper bound theorems and then establish bounds within which the exact solution would exist. Even this procedure can be mathematically intractable and is, therefore, limited to the analysis of simple geometric configurations.

In view of the above stated limitations of the aforementioned methods, research has more recently been directed towards estimating limit loads that are based on linear elastic FEA, which are called as robust approximate methods. Such procedures are quite straightforward and less time-and-resource consuming than inelastic FEA.

Robust approximate methods are based on the idea of creating a sequence of linear problems that closely match the conditions of the non-linear problem, which means a series of elastic analyses will be used to replace the elastic-plastic analysis in calculating the limit loads of structures. A lot of research have been done in this field; some well-known methods include R-node method by Seshadri and his co-workers (1991&1995) [22&23], Partial elastic modulus modification method by Marriott (1988) [24], m_α - multiplier method by Seshadri and Mangalaramanan (1995&1997) [25&26], elastic compensation method by Mackenzie and Boyle (1993, 1993a&1993b) [27, 28&29] and so on. Also, Ponter and co-workers (2000, 2001&2002) [30, 31&32] have developed a family of methods called 'Linear matching methods'. All these methods are robust

approximate methods, which are used to replace elastic-plastic analysis methods by using the elastic modulus adjustment procedure to simulate the inelastic flow at the plastic collapse; these methods can obtain satisfactory results in linear elastic finite element analyses.

The earliest use of elastic modulus adjustment procedures dates back to research work on classification of clamp induced stresses in a thin walled pipe wherein the secant modulus was adjusted iteratively to obtain inelastic solutions (Jones and Dhalla, (1981) [33]). In this paper, highly stressed regions of the component or structure were systematically softened by a reduction of their modulus of elasticity in an attempt to simulate local inelastic action. Rather than carry out inelastic analysis, solutions were obtained by employing several elastic analyses iteratively.

Marriott (1988) [24] developed an iterative procedure for estimating lower-bound limit loads on the basis of linear elastic finite element analysis (FEA) by generating statically admissible stress fields and used them in conjunction with established theorems of limit analysis. Marriott (1988) [24]) adopted the elastic modulus adjustment procedure to categorize stresses in pressure components where it was deemed difficult to determine the stress category by inspection alone, yet where inelastic analysis was considered to be expensive and elaborate.

Seshadri and his co-workers (1991&1995) [22&23] made use of the elastic modulus adjustment procedure to determine lower-bound limit loads by adopting reference stress concepts in creep design, they extended the concept of skeletal point to the more general inelastic component behavior by defining and locating the redistribution node (r-node) in components or structures. The method, designated as the GLOSS

(generalized local stress-strain) R-node (redistribution node) technique, had been applied to arches, frames, plates and shells. Symmetric as well as nonsymmetrical structures had been considered, and the criteria for ensuring lower bound limit loads had been provided.

Seshadri and Prasad (1996) [34] also applied r-node method for determining limit loads of foundations and slopes in saturated cohesive soils under undrained conditions. In that paper, the r-node method was applied to some problems in geotechnical engineering. Problems involving bearing capacity of footings and stability of slopes under strip loading in cohesive soils had been analyzed; both uniform and layered soils were considered. The bearing capacity or limit loads obtained for these problems were compared with results of inelastic FEA. The limit load estimates were found to be reasonably accurate and this method had been demonstrated to consume less time and resources than classical elastic-plastic analyses.

Mackenzie, et al., (1993, 1993a&1993b) [27, 28&29] applied a similar algorithm, beyond the two linear elastic iterations, to determine the lower bound limit loads of pressure vessels on the basis of Melan's theorem (Melan, (1938) [35]).

Mura, et al., (1965) [36] discussed a lower bound method for limit load determination that is based on variational concepts. On the basis of a variational formulation, traditional methods had been replaced by introducing the concept of 'integral mean of yield' by Mura and his coworkers. A variational formulation that is equivalent to the classical lower bound method, except that the use of space variables is circumvented, had been presented; improved lower bound limit loads have been obtained for symmetric and nonsymmetrical components by extending Mura's variational formulation to include local plastic collapse mechanisms.

Based on the extended variational principle, using a modulus-adjustment scheme similar to the GLOSS R-Node technique, a robust limit load estimation method, called the m_α - method, was developed by Seshadri and Mangalaramanan (1997) [26]. The m_α - method had been applied to a range of pressure component configurations, such as cylinders, torispherical heads, nozzle-sphere intersections and nonsymmetric plate structures.

The m_α - method was further extended to layered structures, cracked components and components made of anisotropic materials by Pan and Seshadri (2002) [37]. For all these applications, the multipliers and the proposed procedure were compared with those obtained by the lower bound estimation based on the elastic compensation method (ECM) and inelastic FEA. The numerical results showed that the robust method could be applied to various components and structures leading to good limit load estimates.

Ponter and coworkers (2000, 2001&2002) [30, 31&32] had provided a formal development of these methods and viewed these procedures as "linear matching method". This method was based upon principles similar to the elastic compensation method, which had been used for design calculations for some years but re-interpreted as a non-linear programming method. By matching the non-linear material behaviour to a linear material, a powerful upper bound programming method had been applied to a significant class of problems; a sufficient condition for convergence, which relates properties of the yield surface to those of the linear solutions solved at each iteration, had been derived. This method had been applied to a Drucker-Prager yield condition in terms of the von-Mises effective stress and the hydrostatic pressure by Ponter and co-workers.

Implementation was shown to be possible using the user routines in a commercial finite element code, ABAQUS. In an accompanying paper (Mangalaramanan and Seshadri, (1995) [19]) the method was extended to shakedown and related problems.

A method similar to the above robust methods has been developed without the use of r-node or m_α concepts (Adluri, 2000 [77] and Bolar & Adluri [78]). This Secant Rigidity Method realizes that r-node is essentially a cross section stress variation phenomenon. Also, the secant modification of r-node and m_α can be carried out to the stiffness directly or the rigidity as opposed to the material modulus. This allows the secant modification to be based on any relevant computed quantity that captures a scaled yield criterion. Examples can be yield criteria in terms of bending moments in plate bending. When this is done, the mesh is significantly reduced allowing for improved solutions. In this method, there is no need to identify either special nodes or special volumes.

2.5 R-Node Method

As mentioned above, Seshadri, et al., (1991&1995) [16&17]) developed a method referred to as the 'r-node method', based on two linear elastic analyses, for obtaining approximate estimates of limit loads. The r-nodes are postulated as load-controlled locations in a component or a structure. When widespread inelastic action (plasticity or creep) occurs, such as, in an entire cross-section, a redistribution of stresses occurs except at the r-nodes, which are statically determinate locations. Therefore, the effective stresses at the r-nodes are linearly proportional to externally applied loads or load-combinations as a consequence of equilibrium.

The r-node method, based upon several principles of creep mechanics, is one of the reference stress methods; it has roots that were first developed in creep mechanics.

Schuste (1960) [32] observed that in a solution of creep of beams, there were points (A and B) in the cross-section at which the stress did not change as the solution progressed from the initial elastic solution to the final stationary solution at a constant moment, shown in Figure 2.1.

Marriot and Leckic (1963-1964 and 1970) [33&34] observed that there are some points in components undergoing transient creep where the stress does not change with time. Such points are called skeletal points.

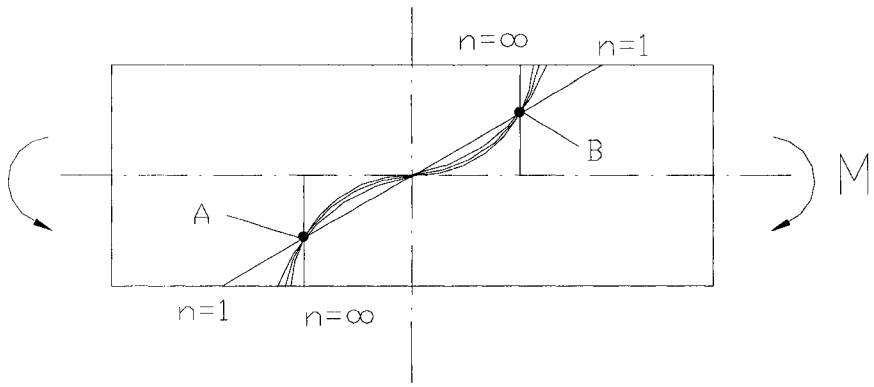

Figure 2.1 R-nodes in a Beam structure Subjected to Bending (after Kraus, (1980) [9]

Sim (1971 and 1968) [8&10] reasoned that as the creep exponent approaches infinity the stress distribution would continue to pass through the point that defines it. Since the solution for an infinite creep exponent is analogous to the limit solution corresponding to perfect plasticity. Sim (1971 and 1968) [8&10] proposed that the reference stress can de obtained from $\sigma_R = \left(\frac{P}{P_L}\right)\sigma_y$.

Based on the above principles, Seshadri and Fernando (1991)[16] explained the r-node method for limit load determination in detail. In the r-node method, limit type distribution is simulated by suitably modifying the elastic moduli of all elements in the structure. The equivalent stress at r-nodes does not change in the process of analysis. So the invariant behavior of the r-node stress and the reference stress relate the two methods.

The concept of r-nodes plays a key role in the understanding of the relationship between the concepts of reference stress, limit load and primary stress (Mangalaramanan, (1993)[8]). There is explicit recognition of load and deformation-controlled effects in the ASME codes. Load-controlled stresses are statically determinate in that they are induced in order to preserve equilibrium with externally applied forces and moments. Deformation-controlled stresses on the other hand are induced as a result of statically indeterminate actions. When widespread inelastic action (plastic or creep) occurs, the statically indeterminate stresses undergo redistribution throughout the component except at the r-nodes, which are almost statically determinate locations. On the GLOSS diagram, the follow-up angle (θ) will be equal to 90^{o} at the r-nodes.

Since the r-nodes are almost load-controlled locations within a component or structure, the induced effective stresses are linearly proportional to the externally applied loads as a consequence of equilibrium requirements; i.e.,

$$\begin{aligned} (\sigma)_{r-node} &= \gamma_1 P \\ (\sigma)_{r-node} &= \gamma_2 \langle P, M \rangle \end{aligned} \tag{2.12}$$

where, γ_1 and γ_2 are scaling parameters that would depend on the loading, geometric configuration and material behavior. For an elastic-perfectly plastic material, when

$(\sigma_e)_{r-node}$ approaches yield stress corresponding to the von Mises criterion, the externally applied load will correspond to the limit load. Equation (2.12) can therefore be expressed as

$$\begin{aligned}(\sigma)_y &= \gamma_1 P_L \\ (\sigma)_y &= \gamma_2 \langle P_L, M_L \rangle\end{aligned} \tag{2.13}$$

combining equations (2.12) and (2.13)

$$\begin{aligned}P_L &= \left[\frac{\sigma_y}{(\sigma_e)_{r-node}}\right] = P \\ \langle P, M \rangle_L &= \left[\frac{\sigma_y}{(\sigma_e)_{r-node}}\right] \langle P, M \rangle\end{aligned} \tag{2.14}$$

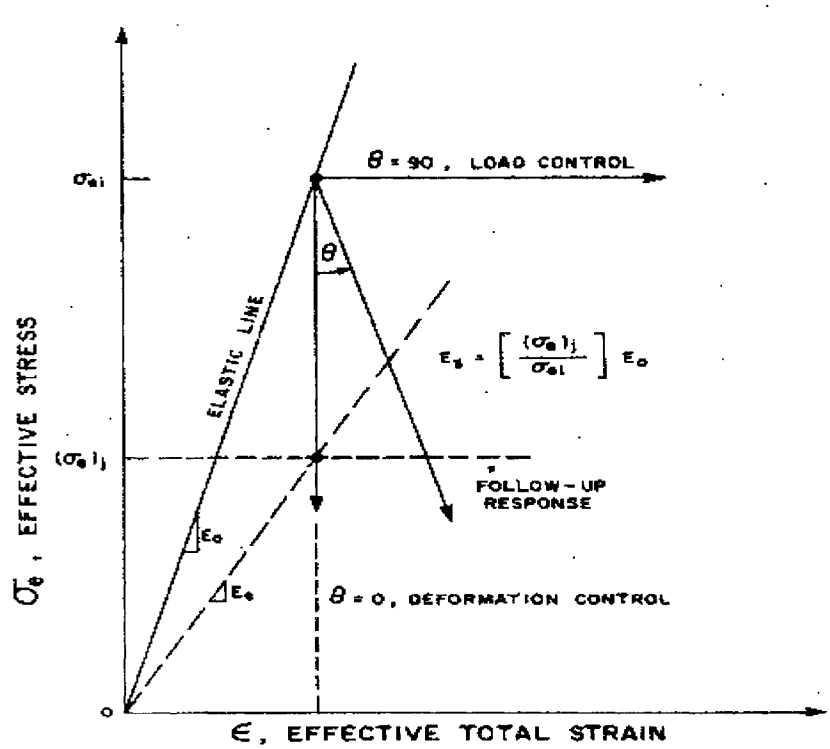

Figure 2.2 Follow-up Angle (θ) on the Gloss Diagram (after Seshadri and Fernando, (1991) [22])

1. A linear elastic finite element analysis of the given structure is carried out for the prescribed generalized loading P. The resulting equivalent stress distribution, which is pseudo elastic, is determined.

2. A location j is arbitrarily chosen within the component, the elastic modulus of all other elements are modified according to the effective stress of element j. Although the choice of this location is somewhat arbitrary, the r-nodes can be located with a reasonable degree of accuracy. The only stipulation for choosing point j is that the effective stress of element j should be nonzero.

3. A second linear analysis is then carried out which attempts to produce a limit type stress distribution, at least approximately.

4. On the basis of the two linear elastic analyses, the follow-up angle is determined for each element. The elements for which $\theta = 90^o$ are identified as the r-node elements. A practical method to determine the r-nodes is to obtain the intersections of the elastic stress distributions from the two finite element analysis. The stresses at the r-nodes are called as the r-node stresses.

5. Since the r-node stresses are load-controlled quantities, the limit load is reached when the combined r-node stress equals the yield stresses. Hence the limit load may be obtained by simply scaling the external load as $P_L = \frac{\sigma_y}{\bar{\sigma}_e} P$.

The above is the basic procedure for applying r-node method in determining the limit loads of structures.

Chapter Three

Constitutive Equations

3.1 General Discussion

The solution of a mechanics problem at each instant of time must satisfy three conditions, namely, equations of equilibrium or of motion; conditions of geometry or the compatibility of strains and displacements; material constitutive laws or stress-strain relations (Chen and Saleeb, 1982 [41]).

The first set of equations relates the stress inside a body to the body forces and external forces acting on the surface of a body. The second set of equation relates the strains inside a body to the displacements of a body. Clearly, both the equations of equilibrium and the equations of kinematics are independent of the particular material of which the body is made. The influence of this material is expressed by a third set of equations, the constitutive equations. They describe the relations between stresses and strains. In the simplest case, there are six equations expressing the strain components in terms of stress components, or vice versa. If they are linear, they are known as Hooke's law (Crawford and Armstrong, 1996 [42]).

For some materials, their behavior may be idealized as time independent, where the effects of time can be neglected. This time-independent behavior of materials can be further idealized as elastic behavior and plastic behavior.

3.2 Elastic Stress-Strain Relations

For an elastic material there exists a one-to-one coordination between stress and strain. Thus a body that consists of this material returns to its original shape whenever all stresses are reduced to zero. This reversibility is not the case for a plastic material.

3.2.1 Hooke's Law

Hooke first proposed a linear relation between stress and strain for a load applied in one direction. The generalization of Hooke's law to three dimensions is given as

$$\varepsilon_{ij} = C_{ijkl}\sigma_{kl} \tag{3.1}$$

Using the tensor subscript notation, for isotropic material this becomes

$$\varepsilon_{ij} = \frac{1}{2G}\sigma_{ij} - \delta_{ij}\frac{\nu}{E}I_1 \tag{3.2}$$

where, E is the elastic modulus; ν is Possion's ratio; G is the shear modulus related to E and ν by the well-known relation

$$G = \frac{E}{2(1+\nu)} \tag{3.3}$$

$$I_1 = \sigma_{ii} = \sigma_{11} + \sigma_{22} + \sigma_{33} \tag{3.4}$$

Equation (3.2) can be solved for the stresses to give

$$\sigma_{ij} = 2G\varepsilon_{ij} + \delta_{ij}\lambda I_1' \tag{3.5}$$

where, $I_1' = \varepsilon_{ii} = \varepsilon_{11} + \varepsilon_{22} + \varepsilon_{33}$, $\lambda = \dfrac{\nu E}{(1+\nu)(1-2\nu)}$.

In engineering notation equation (3.2) becomes

$$\varepsilon_{ij} = \frac{1+\nu}{E}\sigma_{ij} - \frac{\nu}{E}\sigma_{kk}\delta_{ij} \tag{3.6}$$

It readily follows from equation (3.6) that

$$I_1' = \frac{1-2\nu}{E} I_1 \tag{3.7}$$

or

$$\varepsilon_m = \frac{1-2\nu}{E}\sigma_m \tag{3.8}$$

where, ε_m and σ_m are the mean strain and mean stress, respectively. Finally, combining equation (3.8) and (3.2) results in

$$e_{ij} = \frac{1}{2G} S_{ij} \tag{3.9}$$

where, e_{ij} and S_{ij} are the strain deviator and stress deviator tensors, respectively. Thus the deviators of the stress and strain tensors are related to each other, in the elastic case, by the simple equation (3.9), whereas the spherical stress components are related to the spherical strain components by equation (3.8).

It should be noted that nothing in the foregoing discussion requires that E, G, ν be constant throughout the body. They may, for example, be functions of temperature, so that if the body is not at a uniform temperature, these constants may have different values at different points in the body.

3.2.2 Solution of Elastic Problems

The six stress components, six strain components, and three displacement components are connected by the three equilibrium equations, six compatibility equations,

and six constitutive equations. To solve an elastic problem, these 15 unknown quantities of stresses, strains and displacements must satisfy all the 15 equations (Sokolinikoff, (1956) [43]).

The stresses must satisfy the three equilibrium equations

$$\sigma_{ij,i} = -F_j \tag{3.10}$$

as well as the boundary conditions $S_j = l_i \sigma_{ij}$. Where, $\sigma_{ij} = \sigma_{ji}$. The strains must satisfy the six compatibility equations

$$\varepsilon_{ij} = \frac{1}{2}(\mu_{i,j} + \mu_{j,i}) \tag{3.11}$$

Finally, the stresses must be related to the strains through the stress-strain relation equation (3.2) or their equivalent. The problem of finding a set of stresses and strains satisfying the above relations is known as the first boundary-value problem of elasticity.

3.3 Plastic Stress-Strain Relations

In the previous sections the relation between stress and strain in the elastic range were discussed and also the stress states at which plastic flow or yielding will begin. These relations are the plastic stress-strain relations.

In the elastic range, the strains are linearly related to the stresses by Hooke's law, whereas the relations will generally be nonlinear in the plastic range. A more clear fact is that in the elastic range the strains are uniquely determined by the stresses. Whereas in the plastic range the strains are in general not uniquely determined by the stresses but depend on the whole history of loading or how the stress state was reached. Because the plastic strains are dependent on the loading path, it becomes necessary to compute the

differentials or increments of plastic strain throughout the loading history and then obtain the total strains by integration or summation.

The first approach to plastic stress-strain relations was suggested by Saint-Venant (1870) [44], he proposed that the principal axes of strain increments coincided with the principal stress axes. Levy (1871) [45] and von Mises (1913) [40] independently gave he general three-dimensional equations relating the increments of total strains to the stress deviations. These are known as the Levy-Mises equations. These equations are

$$d\varepsilon_{ij} = S_{ij} d\lambda \tag{3.12}$$

or

$$\frac{d\varepsilon_x}{S_x} = \frac{d\varepsilon_y}{S_y} = \frac{d\varepsilon_z}{S_z} = \frac{d\varepsilon_{xy}}{\tau_{xy}} = \frac{d\varepsilon_{yz}}{\tau_{yz}} = \frac{d\varepsilon_{zx}}{\tau_{zx}} = d\lambda$$

In these equations the total strain increments are assumed to be equal to the plastic strain increments, the elastic strains being ignored. Thus these equations can only be applied to problems of large plastic flow and cannot be used in the elastic-plastic range. The generalization of equation (3.12) to include both elastic and plastic components of strain is due to Prandtl (1925) [46] and Reuss (1930) [47], which are known as the Prandtl-Reuss equations.

Reuss (1930) [47] assumed that at any instant the plastic strain increment is proportional to the instantaneous stress deviator; i.e.,

$$d\varepsilon_{ij}^{p} = S_{ij} d\lambda \tag{3.13}$$

or

$$\frac{d\varepsilon_x^p}{S_x} = \frac{d\varepsilon_y^p}{S_y} = \frac{d\varepsilon_z^p}{S_z} = \frac{d\varepsilon_{xy}^p}{\tau_{xy}} = \frac{d\varepsilon_{yz}^p}{\tau_{yz}} = \frac{d\varepsilon_{zx}^p}{\tau_{zx}} = d\lambda$$

Equations (3.13) can be then be considered as a special case of equation (3.12) where the elastic strain components are neglected.

Equation (3.13) states that the increments of plastic strain depend on the current values of the deviatoric stress state, not on the stress increment. They also imply that the principal axes of stress and of plastic strain increment tensors coincide. The equations themselves merely give a relationship between the ratios of plastic strain increments in different directions. To determine the actual magnitudes of the increments a yield criterion is required.

3.3.1 General Derivation of Plastic Stress-Strain Relations

The Saint-Levy-Mises and Prandtl-Reuss relations were described as originating basically from an assumption that 'the maximum shear and maximum slide velocity are co-directional', as Saint-Venant expressed it. It was also shown that these relations imply the von Mises yield function. The general equations for determining the plastic stress-strain relations for any yield criterion was derived based on a unified approach due to Ducker (1950&1952) [48&18].

The general stress-strain relation is given as

$$d\varepsilon_{ij}^p = G\frac{\partial f}{\partial \sigma_{ij}} df \tag{3.14}$$

where, G is a scalar which may depend on stress, strain, and history. The scalar G, which depends in general on the stress, strain, and history, must be determined from experiment,

$f(\sigma_{ij})$ is a loading function. At each stage of the plastic deformation, a loading function $f(\sigma_{ij})$ exists so that further plastic deformation takes place only for $f(\sigma_{ij}) = 0$.

3.3.2 Perfectly Plastic Material

For this case the work done by an external agency which slowly applies and removes a set of stresses is zero over the cycle, or

$$d\sigma_{ij} d\varepsilon_{ij}^{p} = 0 \tag{3.15}$$

It should be remarked that this equation is not the same as the second of equation (3.12) with the equality sign. In equation (3.12) the equality sign is used only when $d\varepsilon_{ij}^{p} = 0$.

For ideal plasticity it is also assumed that $f(\sigma_{ij})$ exists and is a function of stress only, and that plastic flow takes place without limit when $f(\sigma_{ij}) = k$ and the material behaves elastically when $f(\sigma_{ij}) < k$. For plastic flow, therefore,

$$df = \frac{\partial f}{\partial \sigma_{ij}} d\sigma_{ij} = 0 \tag{3.16}$$

comparing equation (3.15) and (3.16) It is seen that

$$d\varepsilon_{ij}^{p} = d\lambda \frac{\partial f}{\partial \sigma_{ij}} \tag{3.17}$$

where, $d\lambda$ is a scalar.

3.3.3 Effective Stress and Effective Strain

If we want to make equation (3.14) into any practical use, it must be related somehow to the experimental uniaxial stress-strain curve. What we are looking for is some function of the stresses, which might be called effective stress, so that results obtained by different loading programs can all be correlated by means of a single curve of effective stress versus effective strain. This curve should preferably be the uniaxial tensile stress curve. Since effective stress should reduce to the stress in the uniaxial tension test, it is a quantity which will determine whether plastic flow takes place or not, and it must be a positively increasing function of the stresses during plastic flow. Now the loading function $f(\sigma_{ij})$ also, by definition, determines whether additional plastic flow takes place. It should be a positively increasing function as long as plastic flow takes place and, if unloading takes place, plastic flow is not resumed until the highest previous value of f is exceeded. The loading function $f(\sigma_{ij})$ must therefore be some constant times the effective stress to some power; i.e.,

$$f(\sigma_{ij}) = C\sigma_e^n \tag{3.18}$$

for example, if we assume again

$$f = J_2$$

then

$$J_2 = C\sigma_e^n$$

or

$$\sigma_e = \left(\frac{J_2}{C}\right)^{1/n} = \{\frac{1}{6C}[(\sigma_1 - \sigma_2)^2 + (\sigma_2 - \sigma_3)^2 + (\sigma_3 - \sigma_1)^2]\}^{1/n}$$

and for the uniaxial tensile test $\sigma_e = \sigma_1$. Therefore,

$$n = 2 \quad C = 1/3 \quad \sigma_e = \sqrt{3}J_2$$

There are two methods to define effective plastic strain, ε_p. One defines the effective strain increment in terms of the plastic work per unit volume; i.e.,

$$dW^p = \sigma_e d\varepsilon_p \tag{3.19}$$

and since $dW^p = S_{ij} d\varepsilon_{ij}^p$

$$d\varepsilon_p = \frac{1}{\sigma_e} S_{ij} d\varepsilon_{ij}^p \tag{3.20}$$

for example, if $f = J_2$, it can readily be shown that

$$d\varepsilon_p = \sqrt{\frac{2}{3} d\varepsilon_{ij}^p d\varepsilon_{ij}^p} \tag{3.21}$$

and, if $f = \sigma_1 - \sigma_3$ with $\sigma_1 > \sigma_2 > \sigma_3$ as for the Tresca criterion, then

$$d\varepsilon_p = d\varepsilon_1^p \tag{3.22}$$

Equation (3.21) expanded becomes

$$d\varepsilon_p = \sqrt{\frac{2}{3}}[(d\varepsilon_x^p)^2 + (d\varepsilon_y^p)^2 + (d\varepsilon_z^p)^2 + 2(d\varepsilon_{xy}^p)^2 + 2(d\varepsilon_{yz}^p)^2 + 2(d\varepsilon_{zx}^p)^2]^{1/2} \tag{3.23}$$

and, in terms of principal strain increment,

$$d\varepsilon_p = \sqrt{\frac{2}{3}}[(d\varepsilon_1^p)^2 + (d\varepsilon_2^p)^2 + (d\varepsilon_3^p)^2]^{1/2}$$

$$= \frac{2}{\sqrt{3}}[(d\varepsilon_1^p)^2 + (d\varepsilon_2^p)^2 + d\varepsilon_1^p d\varepsilon_2^p]^{1/2}$$

where, the incompressibility condition $d\varepsilon_1^p + d\varepsilon_2^p + d\varepsilon_3^p = 0$ has been used.

The second method is sought to find a definition of effective plastic strain increment which when integrated is a function of σ_e only. The simplest combination of plastic strain increment that is positive increasing and has the correct 'dimension' is

$$d\varepsilon^p = C\sqrt{d\varepsilon_{ij}^p d\varepsilon_{ij}^p}$$

to make this definition agree for simple tension we must have

$$d\varepsilon_x^p = d\varepsilon_p = C\sqrt{(d\varepsilon_x^p)^2 + \frac{1}{4}(d\varepsilon_x^p)^2 + \frac{1}{4}(d\varepsilon_x^p)^2} = C\sqrt{\frac{3}{2}}d\varepsilon_x^p$$

therefore,

$$C = \sqrt{\frac{2}{3}}$$

$$d\varepsilon_p = \sqrt{\frac{2}{3}d\varepsilon_{ij}^p d\varepsilon_{ij}^p}$$

and, for $f = J_2$

$$d\varepsilon_p = H(\sigma_e)d\sigma_e$$

so that the integrated effective strain is a function of effective stress only; i.e.,

$$\varepsilon_p = \int d\varepsilon_p = \int H(\sigma_e)d\sigma_e$$

It should be noted here that the definition equation (3.21) for $d\varepsilon_p$ has been derived for $f = J_2$ only. Drucker (1950&1952) [48&18] has shown that it is reasonably correct for

almost any $f(J_2, J_3)$. The second approach for defining $d\varepsilon_p$ is not based on any specific loading function.

Now we determine the function G. It should first be realized that for the previous formulation to agree with the uniaxial tensile curve, $d\sigma_e/d\varepsilon_p$ must be the slope of that curve (in the plastic range). Substituting the basic equation

$$d\varepsilon_{ij}^p = G\frac{\partial f}{\partial \sigma_{ij}}df$$

into equation (3.21) gives

$$d\varepsilon_p = \sqrt{\frac{2}{3}}G\sqrt{\frac{\partial f}{\partial \sigma_{ij}}\frac{\partial f}{\partial \sigma_{ij}}}df \tag{3.24}$$

or

$$Gdf = d\lambda = \sqrt{\frac{3}{2}}\frac{d\varepsilon_p}{\sqrt{(\partial f/\partial \sigma_{ij})(\partial f/\partial \sigma_{ij})}} \tag{3.25}$$

and the general plastic stress-strain relation becomes

$$d\varepsilon_{ij}^p = \frac{\sqrt{\frac{3}{2}}(\partial f/\partial \sigma_{ij})d\varepsilon_p}{\sqrt{(\partial f/\partial \sigma_{mn})(\partial f/\partial \sigma_{mn})}} \tag{3.26}$$

or

$$d\varepsilon_{ij}^p = \sqrt{\frac{3}{2}}\frac{(\partial f/\partial \sigma_{ij})}{\sqrt{(\partial f/\partial \sigma_{mn})(\partial f/\partial \sigma_{mn})}}\frac{d\sigma_e}{\sigma_e'} \tag{3.27}$$

where $\sigma_e' = d\sigma_e/d\varepsilon_p$ is the slope of the uniaxial stress-strain strain curve at the current value of σ_e. As an example, for $f = J_2$, equation (3.27) gives

$$d\varepsilon_{ij}^{p} = \frac{3}{2}\frac{S_{ij}}{\sigma_e}\frac{d\sigma_e}{\sigma_e^{'}}$$

$$= \frac{3}{2}\frac{S_{ij}}{\sigma_e} d\varepsilon_p \tag{3.28}$$

Equation (3.28) constitutes the flow rule (or plastic stress-strain relations) associated with the von Mises yield criterion (von Mises, (1913) [40]). They are the well-known Prandtl-Reuss relations we obtained previously. If we replace the plastic strain increments in the above equations by total strain increments, the Levy-Mises relations are obtained which are valid only if the plastic strains are so large that the elastic strains can be neglected.

As a final note, a general flow law such as (3.14) can also be obtained on the basis of a hypothesis that three exists a plastic potential (similar to the strain energy density function) which is a scalar function of stress, $g(\sigma_{ij})$, from which the plastic strain increments can be obtained by partial differentiation with respect to the stresses. Thus

$$d\varepsilon_{ij}^{p} = \frac{\partial g}{\partial \sigma_{ij}} d\beta \tag{3.29}$$

where, $d\beta$ is a nonnegative constant. The plastic potential $g\left(\sigma_{ij}\right)$ was first introduced by Melan (1938) [35]. By comparison with (3.14), it would appear that the plastic potential should play the same role as the yield function, and indeed Drucker (1952) [18] has proved that they must be the same function, so that g in (3.29) can be replaced by f; (3.29) and (3.14) are then the same.

3.3.4 Incremental and Deformation Theories

Equations such as (3.29) are called incremental stress-strain relations because they relate the increments of plastic strain to the stress. To obtain the total plastic components, we must integrate these equations over the whole history of loading. Hencky (1924) [49] proposed total stress-strain relations whereby the total strain components are related to the current stress. Thus, instead of equation (3.29), we would have

$$\varepsilon_{ij}^{p} = \frac{3}{2}\frac{S_{ij}}{\sigma_e}\varepsilon_p \tag{3.30}$$

The plastic strains then are functions of the current state of stress and are independent of the history of loading. Such theories are called total or deformation theories in contrast to the incremental or flow theories previously described. This type of assumption greatly simplifies the problem; however, as was previously shown, the plastic strains cannot in general be independent of the loading path and deformation theories cannot generally be correct. There has often been a tendency therefore to ignore all deformation theory as of little value.

It can easily be shown, however, that for the case of proportional or radial loading, i.e., if all the stresses are increasing in ratio, the incremental theory reduces to the deformation theory. For if $\sigma_{ij} = K\sigma_{ij}^{0}$, where, σ_{ij} is an arbitrary reference state of stress (nonzero) and K is a monotonically increasing function of time, then $S_{ij} = KS_{ij}^{0}$ and $\sigma_e = K\sigma_e^{0}$ and equation (3.29) becomes

$$d\varepsilon_{ij}^{p} = \frac{3d\varepsilon_p}{2\sigma_e^{0}}S_{ij}^{0}$$

which can be immediately integrated to give

$$\varepsilon_{ij}^{p} = 3\varepsilon_{p}\frac{S_{ij}^{0}}{2\sigma_{e}^{0}} = \frac{3\varepsilon_{p}S_{ij}}{2\sigma_{e}} \tag{3.31}$$

so the plastic strain is a function only of the current state of stress and is independent of the loading path.

Furthermore, it has been proposed by Budiansky (1959) [50] that there are ranges of loading paths other than proportional loading for which the basic postulates of plasticity theory are satisfied by deformation theories. Budiansky's theory (Budiansky, (1959) [50]) postulates the occurrence of corners or singular points has as yet not been established experimentally, one cannot rule out the possibility of loading paths other than proportional loading for which total plasticity theories may give satisfactory answers.

From a practical viewpoint, there are a great many engineering problems where the loading path is not far from proportional loading for which total plasticity theories may give satisfactory answers.

3.4 Yield Criteria

3.4.1 Representation of Yield Criteria

A well-defined yield stress point σ_0 on an actual stress-strain curve in uniaxial stress states can obtain the elastic limit of the material. In combined stress states, the elastic limit is defined mathematically by a certain yield criterion or yield condition (Chen and Zhang, (1991) [51]). The initial yield criterion is a function of stress state σ_{ij} and can be generally expressed as

$$f(\sigma_{ij}) = 0 \tag{3.32}$$

For isotropic materials, the stress state at a point can be uniquely represented by three principal stresses. Thus, the yield criterion for isotropic materials can be expressed as

$$f(\sigma_1, \sigma_2, \sigma_3) = 0 \tag{3.33}$$

Moreover, since principal stresses can be expressed in terms of either stress invariants, I_1, J_2, J_3, or the Haigh-Westergaard coordinates, ξ, ρ, θ, where, $\xi = \frac{1}{\sqrt{3}} I_1$; $\rho = \sqrt{2J_2}$; θ is the angle measured from the positive direction of the σ_1-axis to the vector ξ. Equation (3.33) can be written as

$$f(I_1, J_2, J_3) = 0 \tag{3.34}$$

and

$$f(\xi, \rho, \theta) = 0 \tag{3.35}$$

Equations (3.33) to (3.35) represent a surface in the principal stress space. Such a surface is referred to as the yield surface. The material behaves elastically within the yield surface; the material begins to yield on the yield surface.

To be fitted with available experimental results, the initial yield criterion generally contains several material constants. The material constants may be determined by curve fitting with simple tests, such as the uniaxial tension test and uniaxial compression test.

3.4.2 Hydrostatic-Pressure-Independent Materials

The elastic-plastic behavior of most metallic materials is essentially hydrostatic pressure insensitive. This implies that yield criteria for this type of materials do not depend on I_1. For a hydrostatic pressure insensitive material, the yield criterion can generally be expressed as

$$f(J_2, J_3) = 0 \tag{3.36}$$

or

$$f(\rho, \theta) = 0$$

The well-known yield criteria for Hydrostatic-Pressure-Independent materials include Tresca criterion and von Mises criterion.

3.4.2.1 Tresca Criterion

The Tresca criterion (Tresca, (1868) [52]) states that yielding of a material would occur when the maximum shearing stress at a point of the material reaches a critical value k. In terms of principal stresses, we have

$$Max\left(\frac{1}{2}|\sigma_1 - \sigma_2|, \frac{1}{2}|\sigma_2 - \sigma_3|, \frac{1}{2}|\sigma_3 - \sigma_1|\right) = k \tag{3.37}$$

From a uniaxial tension test, we determine $k = \sigma_0/2$, and from a pure shear test, $k = \tau_0$. Thus, if the Tresca criterion is used, the tensile strength and the shear strength of a material are related by $\sigma_0 = 2\tau_0$.

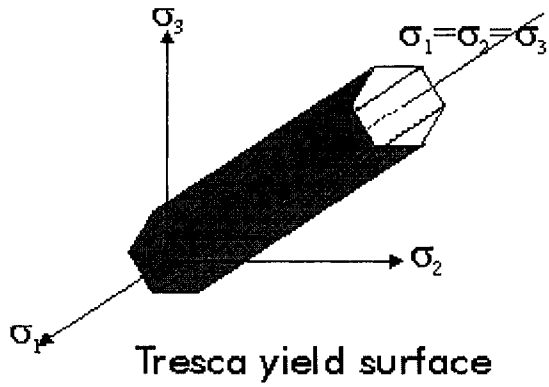

Figure 3.1 Tresca's Yield Surface (after Tresca, (1868) [52])

The Tresca's yield surface plots in principle stress space as a regular hexagonal cylinder whose axis is the space diagonal as shown in Figure 3.1.

The Tresca criterion can also be generally expressed as

$$2\sqrt{J_2}\sin\left(\theta+\frac{\pi}{3}\right)-\sigma_0=0,(0\le\theta\le\frac{\pi}{3}) \tag{3.38}$$

where $\sigma_0 = 2k$.

Since the Tresca criterion has a linear expression in the principal stress space, it is often employed for analytical solutions of elastic-plastic problems. However, the criterion does not take into account the effect of intermediate principal stress and contains singular corners causing possible troubles in numerical analysis.

3.4.2.2 Von Mises Criterion

The von Mises criterion (von Mises, (1913) [40]), states that yielding of a material would occur when the maximum shearing strain energy at a point of the material reaches

a critical value. Since the shear strain energy is proportional to the second invariant of the deviatoric stress tensor, J_2, the criterion can be expressed as

$$f(J_2) = J_2 - k^2 = 0 \tag{3.39}$$

From the uniaxial tension test, the constant k is determined as $k = \sigma_0/\sqrt{3}$, and from a pure shear test, $k = \tau_0$. Thus, if the von Mises criterion is used, the tensile strength and the shear strength of a material are related by $\sigma_0 = \sqrt{3}\tau_0$. Thus, equation (3.39) can also be written as

$$J_2 - \frac{\sigma_0}{3} = 0 \tag{3.40}$$

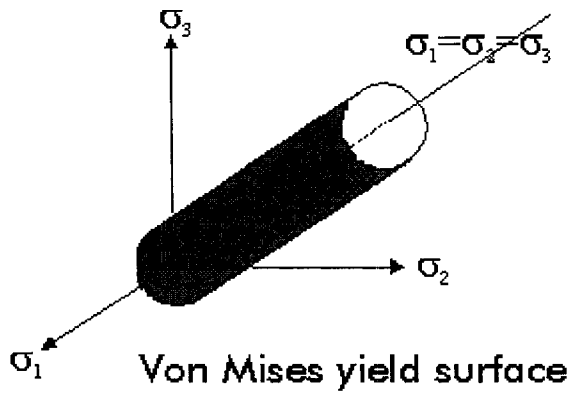

Figure 3.2 Von Mises Yield Surface (after von Mises, (1913) [40])

The von Mises's yield surface plots in principle stress space as a circular cylinder whose axis is the space diagonal as shown in Figure 3.2.

Since the von Mises criterion is of nonlinear form in terms of stress components, this criterion is somewhat harder to use for solving elastic-plastic problems.

3.4.3 Hydrostatic-Pressure-Dependent Materials

For hydrostatic-pressure-independent yield surfaces, their meridians are straight lines parallel to the hydrostatic axis. This implies that shearing stress must be the cause of yielding of this type of materials. Since the magnitude of shearing stress is important, not its direction, in governing yielding, it follows that the elastic-plastic behavior in tension and in compression should be equivalent for hydrostatic-pressure-independent materials (Chen and Saleeb, 1982, [41]). Thus, the cross-sectional shapes for his type of yield surfaces have six-fold symmetry. This will be discussed further in the following section.

3.4.3.1 Mohr-Coulomb Criterion

The Mohr-Coulomb criterion (Coulomb, (1776) [53]) can be considered as a generalization of the Tresca Criterion. Both criteria assume that the maximum shearing stress determines the yielding of a material. However, the Tresca criterion assumes that the critical value of shearing stress is a constant, while the Mohr-Coulomb criterion considers the critical value of shearing stress on a plane to be a function of the normal stress acting on the same plane

$$|\tau| = c - \sigma \tan\phi \tag{3.41}$$

where, c is the cohesion and ϕ is the angle of internal frication; σ is the normal stress; and τ is the shear stress on this plane. Both c and ϕ are material constants to be determined by experiments. Figure 3.3 shows the Mohr-Coulomb yield surface in the principal stress space.

The two parameters c and ϕ can be calibrated from two simple tests, e.g., a uniaxial tension test and a uniaxial compression test. Let σ_t be the tensile yield stress in the uniaxial tension, and σ_c the compression yield stress in the uniaxial compression test, we have

$$\sigma_t = \frac{2c\cos\phi}{1+\sin\phi}, \sigma_c = \frac{2c\cos\phi}{1-\sin\phi} \tag{3.42}$$

The ratio of σ_c and σ_t is defined as

$$m = \frac{\sigma_c}{\sigma_t} = \frac{1+\sin\phi}{1-\sin\phi} \tag{3.43}$$

In terms of m and σ_c, we have

$$\sin\phi = \frac{m-1}{m+1}, \cos\phi = \frac{2\sqrt{m}}{m+1}, 0 \le \phi \le \frac{\pi}{2} \tag{3.44}$$

and

$$c = \frac{\sigma_c}{2\sqrt{m}} \tag{3.45}$$

The general expression of the criterion has the form

$$\frac{1}{3}I_1\sin\phi + \sqrt{J_2}\sin(\theta+\frac{\pi}{3}) + \sqrt{\frac{J_2}{3}}\cos\left(\theta+\frac{\pi}{3}\right)\sin\phi - c\cos\phi = 0, 0 \le \theta \le \frac{\pi}{3} \tag{3.46}$$

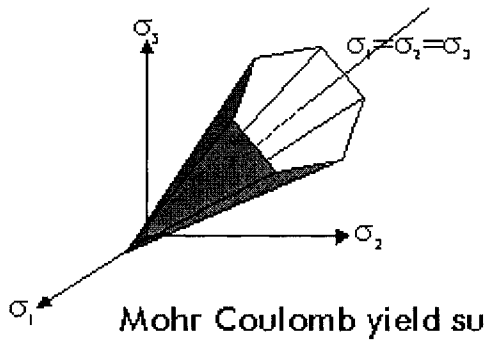

Figure 3.3 Mohr-Coulomb's Yield Surface (after Coulomb, (1776) [53])

The Mohr Coulomb's yield surface plots in principle stress space as an irregular hexagonal pyramid whose axis is the space diagonal as shown in Figure 3.3.

3.4.3.2 Drucker-Prager Criterion

The Drucker-Prager criterion (Drcuker, (1953) [54]) is a simple extension of the von Mises criterion to include the effect of hydrostatic pressure on the yielding of materials. Introducing an additional term that is proportional to I_1 to makes the extension.

$$f\left(J_2+J_3\right)=\alpha I_1+\sqrt{J_2}-k=0 \tag{3.47}$$

where, α and k are material constants. From the uniaxial tension and uniaxial compression tests, we obtain

$$\sigma_t=\frac{\sqrt{3}k}{1+\sqrt{3}\alpha},\sigma_c=\frac{\sqrt{3}k}{1-\sqrt{3}\alpha} \tag{3.48}$$

use the ratio $m=\sigma_c/\sigma_t$, we can also express the parameter α and k as

$$\alpha = \frac{m-1}{\sqrt{3}(m+1)}, k = \frac{2\sigma_c}{\sqrt{3}(m+1)} \tag{3.49}$$

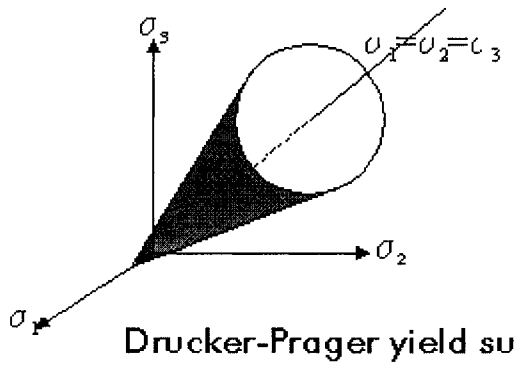

Figure 3.4 Drucker-Prager Yield Surface (after Drucker, (1953) [54])

The Drucker-Prager's yield surface plots in principle stress space as a circular cone with the space diagonal (hydrostatic stress axis, $\sigma_1 = \sigma_2 = \sigma_3$) as its axis, shown in Figure 3.4.

The Drucker-Prager yield surface can also be expressed generally as

$$\rho = \sqrt{2}k - \sqrt{6}\alpha\xi \tag{3.50}$$

For brittle or granular materials, yield criterion is often referred to as failure criterion because for such materials yielding means failure. The term failure criterion is often utilized for materials such as soils, concrete and rocks.

Chapter Four

Bearing Capacity of Strip Foundations

The soil bearing capacity can be calculated by means of the finite element (FE) method or by analytical methods.

4.1 Finite Element Method

The finite element (FE) method has been widely used in engineering analysis in the last few decades. FE is a numerical method for solving engineering and mathematical problems, such as stress-strain analysis, heat transfer and fluid flow and electromagnetic potential (William, (1990&1994) [55]). Continuum finite element method is widely used in geotechnical engineering as a general tool for all kinds of analyses. The finite element method is particularly suited to analyze foundations with unusual shapes and/or unusual loading conditions as well as in situations where the soil is highly variable. For example, the potential failure modes for the layered soils, which will require consideration of the interactions between the soft and rigid soil layers as well as between the soil layer and the foundation.

4.2 Analytical Methods

The soil ultimate bearing capacity may be estimated from a number of analytical methods, which include the methods based on the theory of elasticity, the classic earth

pressure theory, the theory of plastic equilibrium, or from experimental results. Of theses methods, the method based on the concept of plastic equilibrium extends the theory of elasticity when applied to the design of foundations and retaining structures and provides more realistic estimates of load-carrying capacities against failure and better estimates of settlements or displacements when subjected to its working load (Chen, (1975) [7]). Therefore, this method is widely used in the solutions of soil bearing capacity.

4.2.1 Soil Bearing Capacity Calculation by Means of Plastic Equilibrium

Plastic equilibrium deals with the stresses in soil masses at failure. The basic equations in plastic equilibrium consist of the equations of equilibrium and the conditions of yield or failure. The solution of these equations gives the stresses at every point in a soil mass. Such solutions are called limit equilibrium solutions.

4.2.1.1 Prandtl Mechanism

Prandtl (1921) [56] and Hencky (1923) [57] solved the problem of a rigid punch indenting metal, and this can be seen to be the 'foundation problem' for the special case of a $\phi = 0$, $\gamma = 0$ material. The solution of Prandtl is stated as below:

For soils, the Coulomb criterion is widely used for this yield condition. Combining the Coulomb criterion with the equations of equilibrium gives a set of differential equations of plastic equilibrium in this region. Together with the stress boundary conditions, this set of differential equations can be used to investigate the stresses in the soil beneath a footing or behind a retaining wall at the instant of impending plastic flow. In order to solve specific problems, it is convenient to transform this set of

equations to curvilinear coordinates whose directions at every point in this yielded region coincide with the directions of failure or slip plane. These slip directions are known as slip lines and the network is called the slip-line field. The Prandtl mechanism in fact is a slip-line mechanism.

4.2.1.1.1 Upper Bound

The Prandtl mechanism shown in Figure 4.1(a) consists of a triangular wedge, ABC, with base angles $\frac{1}{4}\pi+\frac{1}{2}\phi$ moving downwards as a rigid body with the velocity of the footing, V_p, a logspiral shear zone, ACD, of central angle $\frac{1}{2}\pi$, and a rigid wedge, ADE, with base angles $\frac{1}{4}\pi-\frac{1}{2}\phi$.

The upper-bound solution for this mechanism can be obtained in an analogous manner. In this case, the lines AC and BC in addition to the lines CDE and CFG are lines of velocity discontinuity. Referring to the left-hand side of Figure 4.1(a), the soil below the failure line CDE remains at rest so that the velocity along this line must be everywhere inclined at an angle φ to the line. The velocity of the soil, V_0, just to the left of the discontinuity line AC is perpendicular to AC and its magnitude must be such that the change in velocity, V_{op}, across AC is inclined at an angle ϕ to AC. By drawing the compatibility velocity diagram shown in Figure 4.1(b), this velocity, V_0, must have the magnitude

$$V_0=\frac{1}{2}V_p\sec(\frac{1}{4}\pi+\frac{1}{2}\phi) \tag{4.1}$$

In the logsiral shear zone ACD, the velocity increase exponentially to the value:

$$V_1 = V_0 e^{(\frac{1}{2}\pi)\tan\phi} = \frac{1}{2}V_p \sec(\frac{1}{4}\pi + \frac{1}{2}\phi) e^{(\frac{1}{2}\pi)\tan\phi} \tag{4.2}$$

On the line AD, this triangular wedge ADE moves as a rigid body in the direction perpendicular to AD with the velocity V_1. Figure 4.1(c) shows the displaced position of the Prandtl mechanism that would result if the footing moved with the downward velocity V_p for a short period of time.

Equating internal and external rates of energy for half the Prandtl mechanism and expressing all the velocities in terms of V_0 gives:

$$\begin{aligned} &\frac{1}{2}P2V_0\cos(\frac{1}{4}\pi + \frac{1}{2}\phi) = c(V_0\cos\phi)[\frac{b}{2\cos(\frac{1}{4}\pi + \frac{1}{2}\phi)}] \\ &+c[V_0 e^{(\frac{1}{2}\pi)\tan\phi}\cos\phi][\frac{be^{(\frac{1}{2}\pi)\tan\phi}}{2\cos(\frac{1}{4}\pi + \frac{1}{2}\phi)}] + \frac{c(V_0 b\cot\phi)}{2\cos(\frac{1}{4}\pi + \frac{1}{2}\phi)}(e^{\pi\tan\phi} - 1) \end{aligned} \tag{4.3}$$

collecting terms gives

$$\frac{P^u}{b} = c\cot\phi[e^{\pi\tan\phi}\tan^2(\frac{1}{4}\pi + \frac{1}{2}\phi) - 1] \tag{4.4}$$

where, c is the cohesion of the soil; k is a constant to be determined experimentally, which represents the failure (yield) stress in pure shear; ϕ is the friction angle of the soil. For the particular case of Tresca material for which $c = k$ and $\phi = 0$, from equation (4.4), we can get

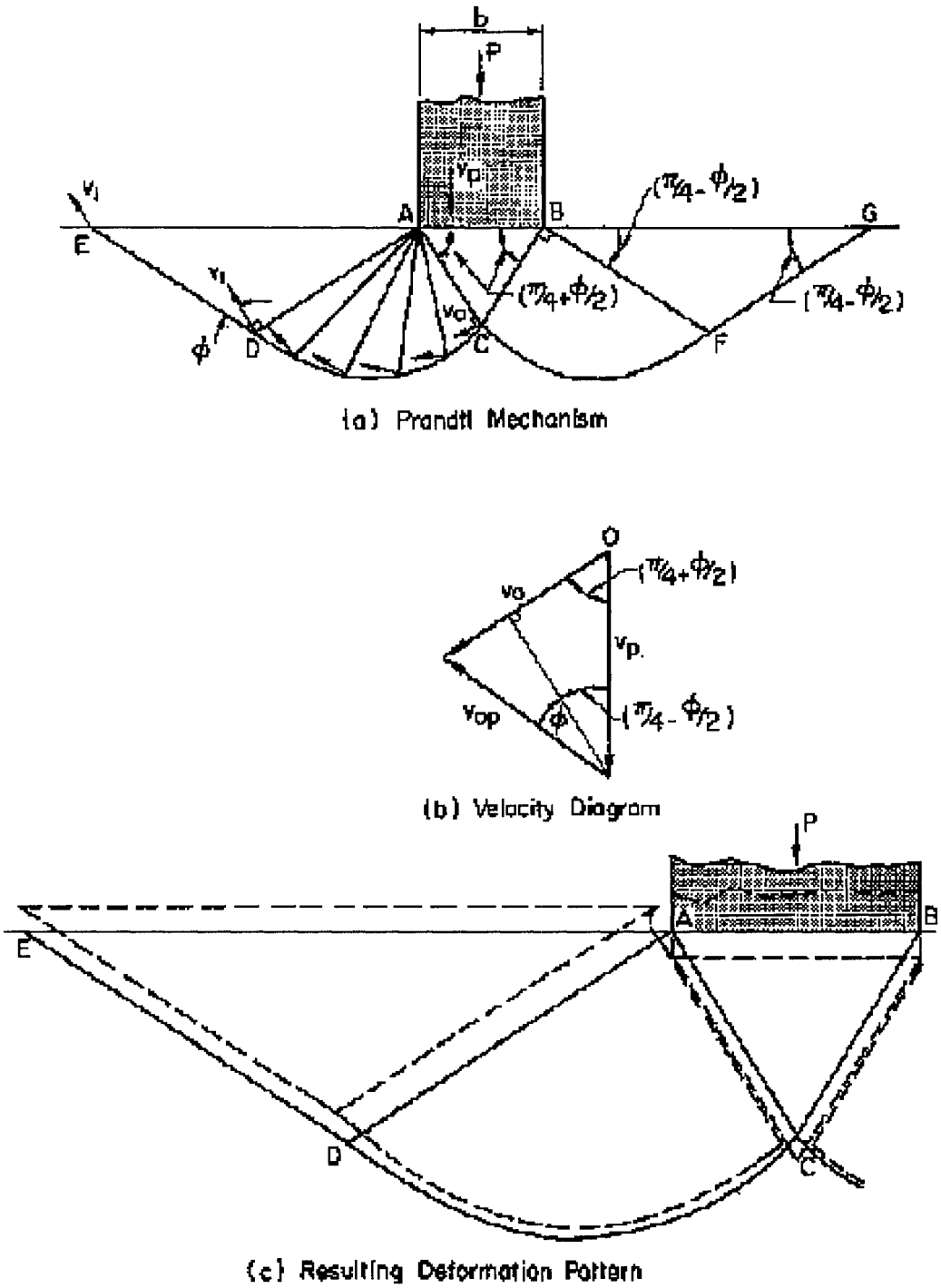

Figure 4.1 Bearing Capacity Calculation Based on Prandtl Mechanism (Upper Bound) (after Prandtl, (1921) [56])

$$\frac{P^u}{b} = c\cot\phi[e^{\pi\tan\phi}\tan^2(\frac{1}{4}\pi+\frac{1}{2}\phi)-1] = k\cos\phi\frac{[e^{\pi\tan\phi}\tan^2(\frac{1}{4}\pi+\frac{1}{2}\phi)-1]}{\sin\phi}$$

when $\phi = 0$, because

$$e^{\pi\tan\phi}\tan^2(\frac{1}{4}\pi+\frac{1}{2}\phi)-1 = 1-1 = 0$$

and

$$\sin\phi = 0$$

Therefore, use the limit method to solve the maximum value of this equation,

$$\lim_{\phi\to 0}\frac{[e^{\pi\tan\phi}\tan^2(\frac{1}{4}\pi+\frac{1}{2}\phi)-1]}{\sin\phi} = \frac{\partial[e^{\pi\tan\phi}\tan^2(\frac{1}{4}\pi+\frac{1}{2}\phi)-1]\Big/\partial\phi}{\partial\sin\phi/\partial\phi}$$

$$= \lim_{\phi\to 0}\frac{\dfrac{e^{\pi\tan\phi}\pi\tan^2(\frac{1}{4}\pi+\frac{1}{2}\phi)}{\cos^2\phi}+\dfrac{e^{\pi\tan\phi}\tan(\frac{1}{4}\pi+\frac{1}{2}\phi)}{\cos^2(\frac{1}{4}\pi+\frac{1}{2}\phi)}}{\cos\phi}$$

$$= \frac{e^{\pi\tan 0}\pi\tan^2(\frac{1}{4}\pi+\frac{1}{2}0)\Big/\cos^2 0+e^{\pi\tan 0}\tan(\frac{1}{4}\pi+\frac{1}{2}0)\Big/\cos^2(\frac{1}{4}\pi+\frac{1}{2}0)}{\cos 0}$$

$$= \frac{2+\pi}{1} = 2+\pi$$

The maximum bearing capacity, P^u, as given by equation (4.4) reduces to the value $(2+\pi)kb$. This value agrees with the well-known "exact" slip-line field solution.

In the Prandtl mechanism, there is no slip between the soil and the footing, which can be considered rough, and therefore the upper-bound solution so obtained is applicable to either a smooth or a rough footing.

4.2.1.1.2 Lower Bound

A strip foundation with a smooth base is located on the ground surface as shown in Figure 4.2(a). As the load P is increased, the penetration of the strip increases as shown in Figure 4.2(b). When the load P^l is reached the penetration increases indefinitely. At this point a bearing capacity failure is said to occur.

Here the direction of the principal stresses varies from point to point, and the slip surfaces are curves as shown in Figure 4.2(a). Since the plate is frictionless, immediately beneath the loaded plate, the major principal stress is in the vertical direction and the failure surface in ABC makes an angle $45^o + \left(\frac{\phi}{2}\right)$ with the horizontal. Also, away from the loaded plate, in zone ADE, the movement is predominantly horizontal. Along the free surface AE and BG, the major and minor principal stresses are in the horizontal and vertical directions, respectively. Therefore, the failure surfaces in AED intersect the free surface AE at an angle of $45^o - \left(\frac{\phi}{2}\right)$ with the horizontal. The slip surfaces in ACD connect those in ABC with those in AED. Thus, a series of straight lines are postulated that radiate from A (or B) and a set of curves. Noting that the two sets of slip surfaces must intersect each other at an angle of $90^o + \phi$, shown in Figure 4.2(c). From the geometric relationship between two slip surface shown in Figure 4.2(c), it can be deduced

that the normal to the curve makes an angle ϕ with the radius. This requirement is met if the curve has the shape given by

$$r = r_0 e^{\theta \tan \phi} \tag{4.5}$$

where, r_0 is the reference radius, and θ is the angle between r_0 and the radius r. Such a curve is called a logarithmic spiral.

To solve this problem we make use of the failure condition:

$$\tau = c + \sigma \tan \phi \tag{4.6}$$

and the equilibrium condition, which must now be written in differential form, in two dimensions the differential equations of equilibrium are

$$\frac{\partial \sigma_x}{\partial x} + \frac{\partial \tau_{xy}}{\partial y} = X \tag{4.7a}$$

or

$$\frac{\partial \sigma_y}{\partial y} + \frac{\partial \tau_{xy}}{\partial x} = Y \tag{4.7b}$$

Equation (4.6) defines the failure condition. In order to combine it with the equilibrium equation (4.7b), we transform equation (4.6) by the following operations. The stresses at failure are described by the Mohr circle shown in Figure 4.3(a).

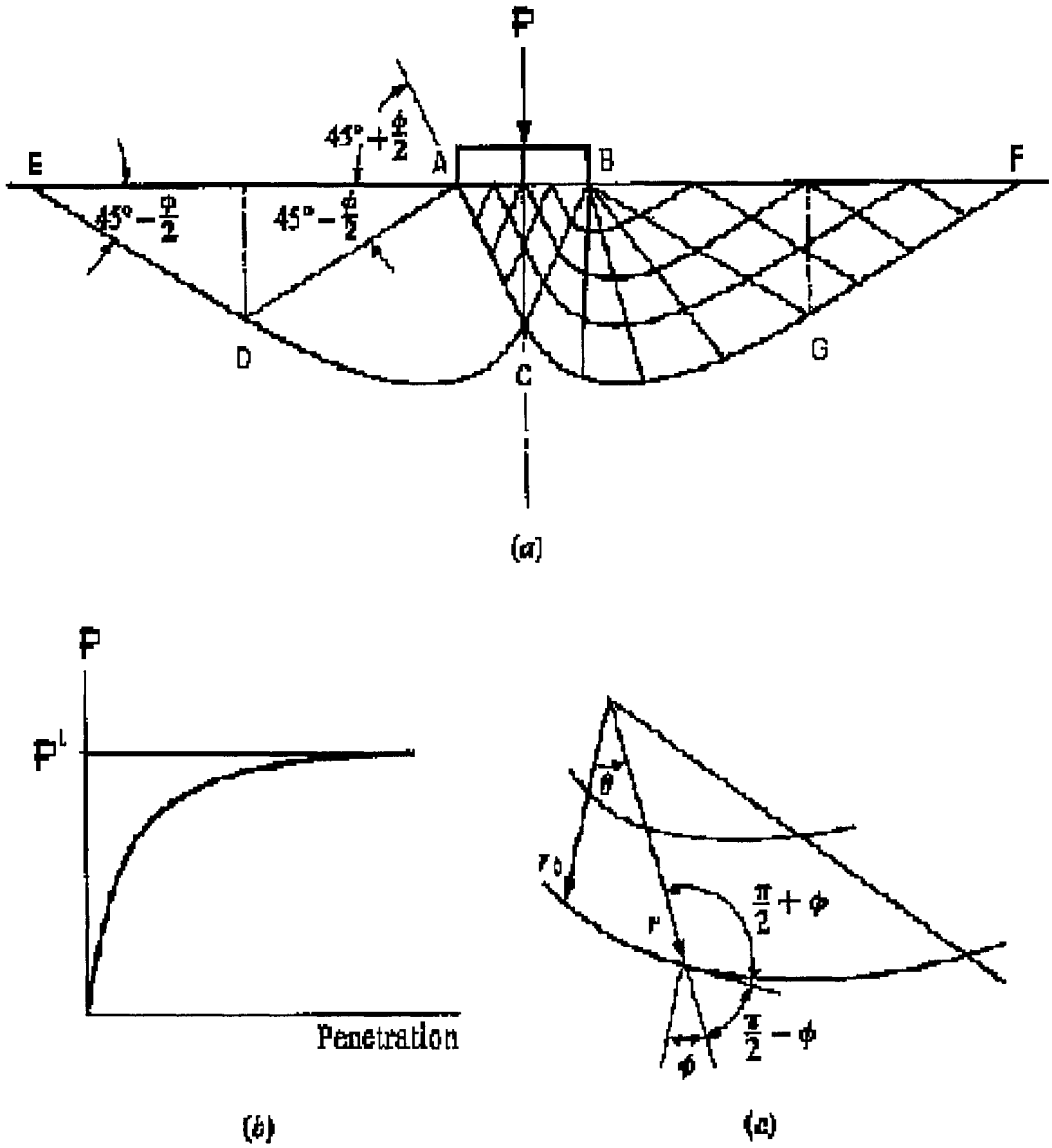

Figure 4.2 Bearing Capacity Calculation Based on Prandtl Mechanism (Lower Bound) (after Prandtl, (1921) [56])

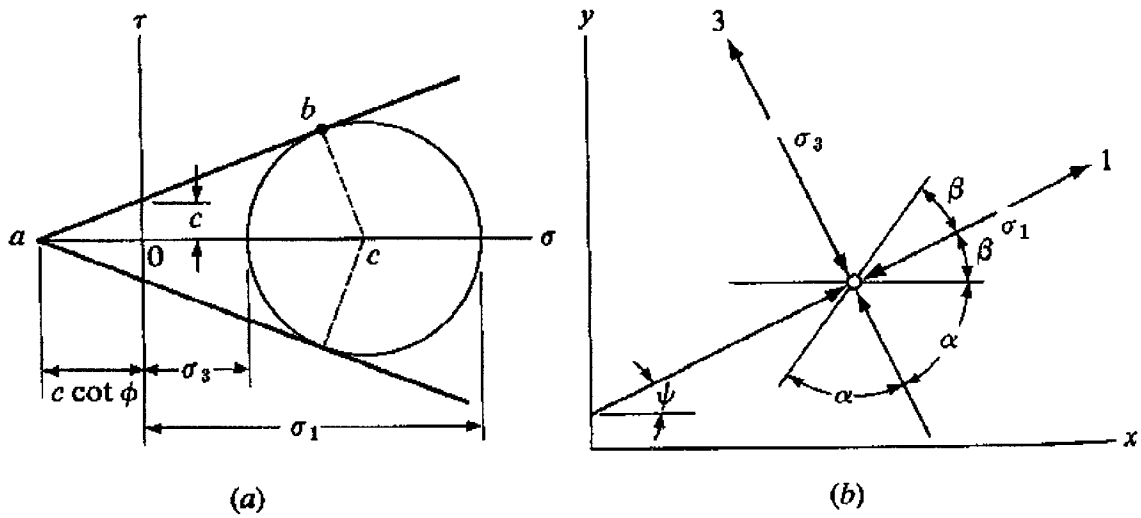

Figure 4.3 (a) Mohr's Circle of Stress at Failure.

(b) Slip Planes and Principal Axes in the XY Plane (Tien-Hsing, (1976) [58])

The distance ac is $\frac{1}{2}(\sigma_1+\sigma_3)+c\cot\phi$ and $\frac{1}{2}(\sigma_1-\sigma_3)$. From the geometric relationship, we may write

$$\begin{aligned}\frac{1}{2}(\sigma_1+\sigma_3)&=[\frac{1}{2}(\sigma_1+\sigma_3)+c\cot\phi]-c\cot\phi\\ \frac{1}{2}(\sigma_1-\sigma_3)&=[\frac{1}{2}(\sigma_1+\sigma_3)+c\cot\phi]\sin\phi\end{aligned} \tag{4.8}$$

If the principal axis is inclined at an angle ψ from the x axis ($\theta=\psi$), we also have

$$\begin{aligned}\sigma_x&=\frac{1}{2}(\sigma_1+\sigma_3)+\frac{1}{2}(\sigma_1-\sigma_3)\cos 2\psi\\ \sigma_y&=\frac{1}{2}(\sigma_1+\sigma_3)-\frac{1}{2}(\sigma_1-\sigma_3)\cos 2\psi\end{aligned} \tag{4.9a}$$

and

$$\tau_{xy}=\frac{1}{2}(\sigma_1-\sigma_3)\sin 2\psi \tag{4.9b}$$

Substituting equation (4.8) in equation (4.9) we obtain the expression for σ_x, σ_y, and τ_{xy} at failure,

$$\sigma_x = [\frac{1}{2}(\sigma_1 + \sigma_3) + c\cot\phi](1 + \sin\phi\cos 2\psi) - c\cot\phi$$
$$\sigma_x = [\frac{1}{2}(\sigma_1 + \sigma_3) + c\cot\phi](1 - \sin\phi\cos 2\psi) - c\cot\phi \quad (4.10a)$$

$$\tau_{xy} = [\frac{1}{2}(\sigma_1 + \sigma_3) + c\cot\phi]\sin\phi\sin 2\psi \quad (4.10b)$$

Equation (4.10) is the failure condition expresses in terms of σ_x, σ_y, τ_{xy}, σ_1 and σ_3 instead of σ and τ. The directions of the slip lines and the principal axes are shown in Figure 4.3(b).

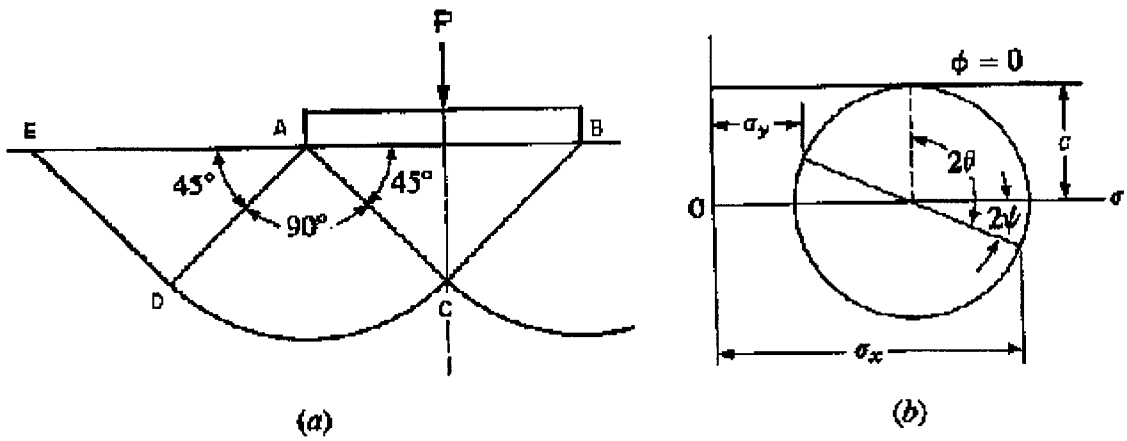

Figure 4.4 Failure of a Frictionless, Weightless Soil under a Strip Load (after Prandtl, (1921) [56])

For the case of $\phi = 0$ that is weightless ($X = 0$, $Y = 0$), the logarithmic spiral reduces to a circular arc, and the failure surfaces are as shown in Figure 4.4(a). The shear strength of the material is given by Figure 4.4(b)

$$\frac{1}{2}(\sigma_1 - \sigma_3) = c$$

Equation (4.9) then becomes

$$\sigma_x = \frac{1}{2}(\sigma_1 + \sigma_3) + c\cos 2\psi$$
$$\sigma_y = \frac{1}{2}(\sigma_1 + \sigma_3) - c\cos 2\psi$$

$$\tau_{xy} = c\sin 2\psi$$

Since the directions of the slip lines have been established, we can calculate the stress changes along the slip lines. We let θ denote the angle between the x axis and the first slip line, shown in Figure 4.4(b), then $2\theta = 2\psi + (\frac{\pi}{2})$, and the above equations become

$$\sigma_x = \frac{1}{2}(\sigma_1 + \sigma_3) + c\sin 2\theta$$
$$\sigma_y = \frac{1}{2}(\sigma_1 + \sigma_3) - c\sin 2\theta$$

$$\tau_{xy} = c\cos 2\theta$$

Substituting this into equation (4.7), we have

$$\frac{\partial}{\partial x}\frac{(\sigma_1 + \sigma_3)}{2} + 2c(\cos 2\theta\frac{\partial x}{\partial \theta} - \sin 2\theta\frac{\partial \theta}{\partial y}) = 0$$
$$\frac{\partial}{\partial x}\frac{(\sigma_1 + \sigma_3)}{2} - 2c(\cos 2\theta\frac{\partial \theta}{\partial y} + \sin 2\theta\frac{\partial \theta}{\partial x}) = 0$$

If we let the x and y axes coincide with the slip lines, then $\theta = 0$, and

$$ds_a = dx,\ \ ds_b = dy$$

in which s_a and s_b are the lengths along the a and b slip lines, respectively. The above equations then become

$$\frac{\partial}{\partial s_a}\frac{(\sigma_1+\sigma_3)}{2}+2c\frac{\partial\theta}{\partial s_a}=0 \tag{4.11a}$$

$$\frac{\partial}{\partial s_b}\frac{(\sigma_1+\sigma_3)}{2}-2c\frac{\partial\theta}{\partial s_b}=0 \tag{4.11b}$$

Equations (4.11a) and (4.11b) describe the stress changes along the failure surface and are often called Kotter's equations (Tien-Hsing, 1976 [58]). The equations are independent of our choice of the x and y axes and therefore are not restricted to the special case of $\theta=0$ assumed in the proof.

If the slip lines are straight lines, then

$$\frac{\partial\theta}{\partial s_a}=0,\ \frac{\partial\theta}{\partial s_b}=0$$

Equation (4.11) then leads to

$$\frac{\partial}{\partial s_a}(\frac{\sigma_1+\sigma_2}{2})=0,\ \frac{\partial}{\partial s_b}(\frac{\sigma_1+\sigma_2}{2})=0 \tag{4.12}$$

Thus the average normal stress $(\frac{\sigma_1+\sigma_2}{2})$ remains constant. If the slip lines consist of sets of concurrent straight lines and concentric circles as in zone *abc* (Figure 4.4(a)), then along the straight slip lines

$$\frac{\partial\theta}{\partial s_a}=0,\ \frac{\partial}{\partial s_a}(\frac{\sigma_1+\sigma_2}{2})=0 \tag{4.13}$$

Along the circular slip lines,

$$s_b = r\theta, \quad \frac{\partial \theta}{\partial s_b} = \frac{1}{r}$$

in which r is the radius of the circular slip line. Substituting in equation (4.11b)

$$\frac{1}{r}\frac{\partial}{\partial \theta}\left(\frac{\sigma_1 + \sigma_3}{2}\right) - \frac{2c}{r} = 0$$

or

$$\frac{\partial}{\partial \theta}\left(\frac{\sigma_1 + \sigma_3}{2}\right) = 2c$$

Upon integration, this yields

$$\frac{\sigma_1 + \sigma_3}{2} = A + 2c\theta \tag{4.14}$$

in which A is the constant of integration. It is given by

$$A = \left(\frac{\sigma_1 + \sigma_3}{2}\right)_{\theta=0}$$

stating at ad (Figure 4.4(a)), we have $\sigma_1 = 2c$, $\sigma_3 = 0$. Thus,

$$\frac{\sigma_1 + \sigma_3}{2} = c$$

This holds for the zone ACE by virtue of equation (4.12). In zone ACD Equation (4.13) applies along the circular are CD. On ac, $\theta = \frac{\pi}{4}$ and on AC, $\theta = \frac{3\pi}{4}$, thus,

$$\left(\frac{\sigma_1 + \sigma_3}{2}\right)_{\theta=\frac{3\pi}{4}} = \left(\frac{\sigma_1 + \sigma_3}{2}\right)_{\theta=\frac{\pi}{4}} + 2c\left(\frac{3\pi}{4} - \frac{\pi}{4}\right) = c(1+\pi)$$

in zone ACB, the term $\left(\frac{\sigma_1 + \sigma_2}{2}\right)$ is again constant and

$$\sigma_1 = \left(\frac{\sigma_1 + \sigma_3}{2}\right) + \left(\frac{\sigma_1 - \sigma_3}{2}\right) = \left(\frac{\sigma_1 + \sigma_3}{2}\right) + c = c(1+\pi) + c = 5.14c$$

Since AB is the major principal plane, σ_1 is the bearing capacity.

4.2.1.2 Trezaghi Bearing Capacity Theory

In 1921, Prandtl published results of his study regarding the penetration of hard bodies, such metal punches into a softer material. Because the strength of metal is very great compared to their weight, assumption of weightlessness is approximately valid in the case of such materials. Terzaghi (1943) [1] realized, however, that such was not the case for soils. He superimposed upon the bearing capacity of a weightless material an additional component due only to the weight of the soil and its frictional resistance.

Terzaghi's solution assumes that ab makes an angle ϕ with the horizontal. Then the spiral portion of the failure surface bc must be vertical at point b, because ab is also a failure surfaces intersect each other at angle of $90^o + \phi$. The load at failure may be calculated by considering the forces acting on the soil mass $abcd$ (Figure 4.5) (Jumikis, 1965 [59]).

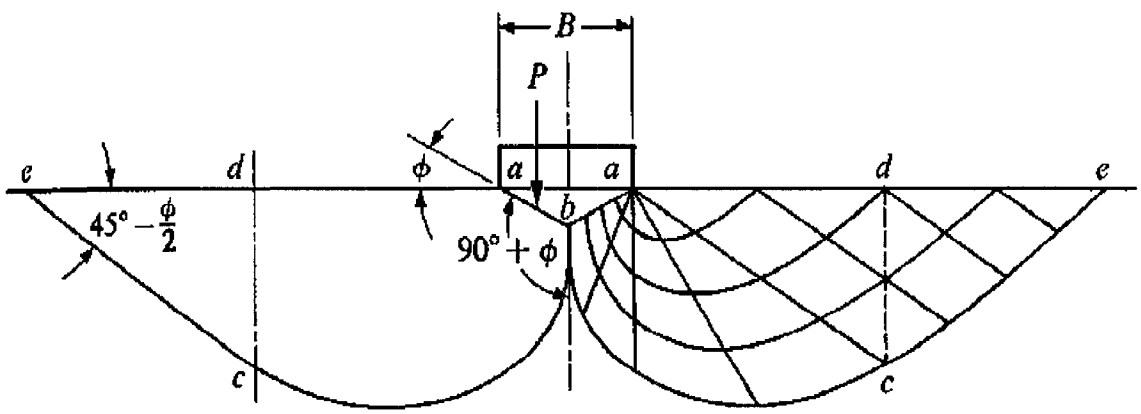

Figure 4.5 Trezaghi Bearing-capacity Theory (after Terzaghi, (1943) [1])

At failure the shear stress along the failure surface *bce* equals the shear strength of the soil as given by equation (4.6). We consider separately the resistances developed by the two components of the shear strength, c and $\sigma \tan \phi$. The forces that act on the mass *abcd* for these two cases are shown in Figure 4.6.

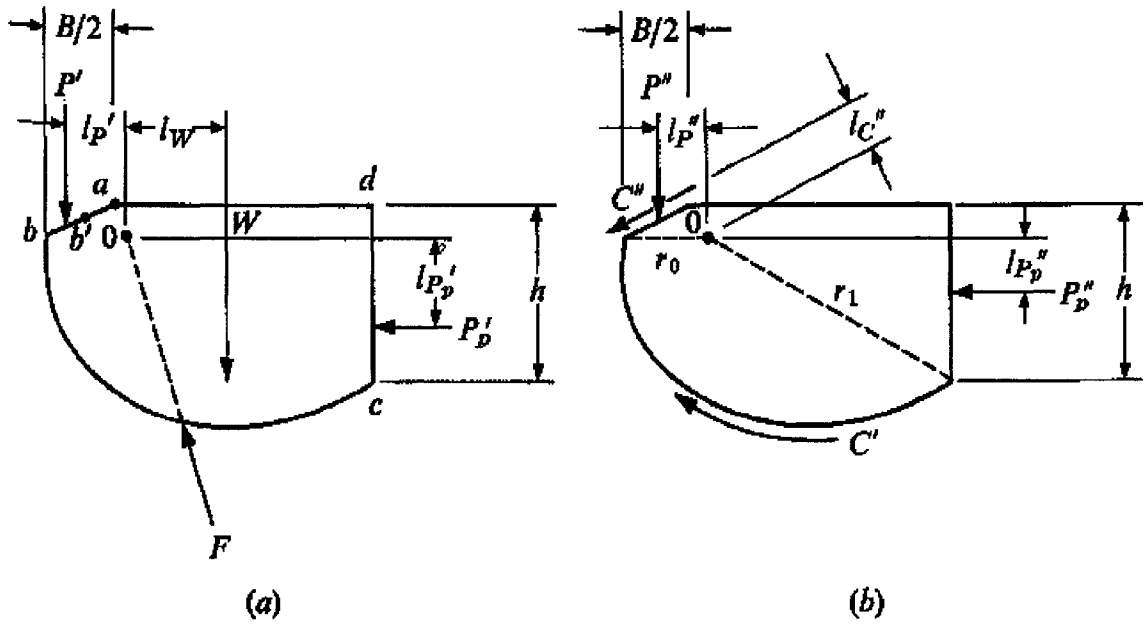

Figure 4.6 Forces on Soil Mass abcd in the Trezaghi Bearing-capacity Theory (after Terzaghi, (1943) [1])

Figure 4.6(a) shows the forces that act on the mass if the shear strength is equal to $\sigma \tan \phi$ only (or $c = 0$). Since the failure surfaces are planes in *acd*, Rankine's passive state of stress exists in this zone. The passive earth pressure P_p' on *cd* is, therefore,

$$P_p' = \frac{1}{2} h^2 \gamma \tan^2 (45^o + \frac{\phi}{2}) \qquad (4.15)$$

$P_p^{'}$ acts at a distance of $\frac{2}{3}h$ from the surface. The weight of the mass $abcd$ is equal to W and it acts through the centroid of $abcd$. On the failure surface bc there exist a normal stress σ and a shear stress equal to the shear strength of the soil, $\sigma \tan\phi$. Therefore, the resultant of σ and $\sigma \tan\phi$ makes an angle ϕ with the normal to the failure surface at every point. The resultant force F on the spiral part of the failure surface also makes an angle ϕ with the slip surface. F, therefore, passes through the center of spiral, o. The force that acts on the failure plane ab is designated by $P^{'}$, and it also acts at the lower third point. This system of forces may be solved by summation of moments about point o. The force F passes through point o and produces no moment. Hence,

$$M_0 = P_p^{'} l_{p_p}^{'} + W l_w - P^{'} l_p^{'} = 0$$

or

$$P^{'} = \frac{1}{l_p^{'}}(P_p^{'} l_{p_p}^{'} + W l_w) \tag{4.16}$$

We next consider the resistance to failure developed by c, and the forces are shown in Figure 4.5(b). The passive pressure $P_p^{''}$ is

$$P_p^{''} = 2ch\tan(45^o + \frac{\phi}{2}) \tag{4.17}$$

and acts at the midpoint of cd. The shear strength is c everywhere along curve bd, and its moment about o may be found by integrating the unit stress c along the spiral,

$$dM_c = cds\cos\phi r = rc\frac{rd\theta}{\cos\phi} = cr^2 d\theta$$

$$M_c = \int_0^{\theta_1} dM_c = \frac{c}{2\tan\phi}(r_1^2 - r_0^2) \tag{4.18}$$

the force C'' on plane ab is equal to the unit stress c times the distance ab. P'' acts at the midpoint of b^* and summation of moment about o brings

$$dM_0 = P_p'' l_{p_p}'' + M_c - C'' l_c'' - P'' l_p'' = 0$$

or

$$P'' = \frac{1}{l_p''}(P_p'' l_{p_p}'' + M_c - C'' l_c'') \tag{4.19}$$

If P' and P'' are known, the load P may be determined by considering the triangular mass aba (Figure 4.5) as the free body. The forces are P', P'', C'', P, and the weight of the mass aba'. Taking the summation of forces in the vertical direction, one finds that

$$Q_f = 2(P' + P'') + 2C'' \sin\phi - (\frac{\gamma B^2}{4})\tan\phi \tag{4.20}$$

The preceding discussion assumes that the failure surface bce is known. Actually, the failure surface is not accurately established because of the approximations mentioned at the beginning of this section. Therefore, the critical surface must be determined by trial. Computations of P should be made for a number of trial surfaces, using different locations of the center of spiral. The trial surface that results in the minimum value of P is the critical one.

4.2.2 Bearing Capacity of Shallow Foundations

The analysis presented in section 4.2.1.2 is used to determine the bearing capacity of shallow foundations. Figure 4.7 shows a section beneath a continuous footing located

at a depth D_f beneath the ground surface. In a general sense, shallow foundations are those foundations that have a depth-of-embedment-to-width ration approximately less than four (Braja, 1985 [60]). To simplify the calculations, the part of the soil mass above ad is treated as a surcharge exerting a pressure q on the surface ad. The surface of failure is assumed to terminate at d. This ignores the shearing resistance of the soil located above ad, and therefore tends to underestimate the bearing capacity.

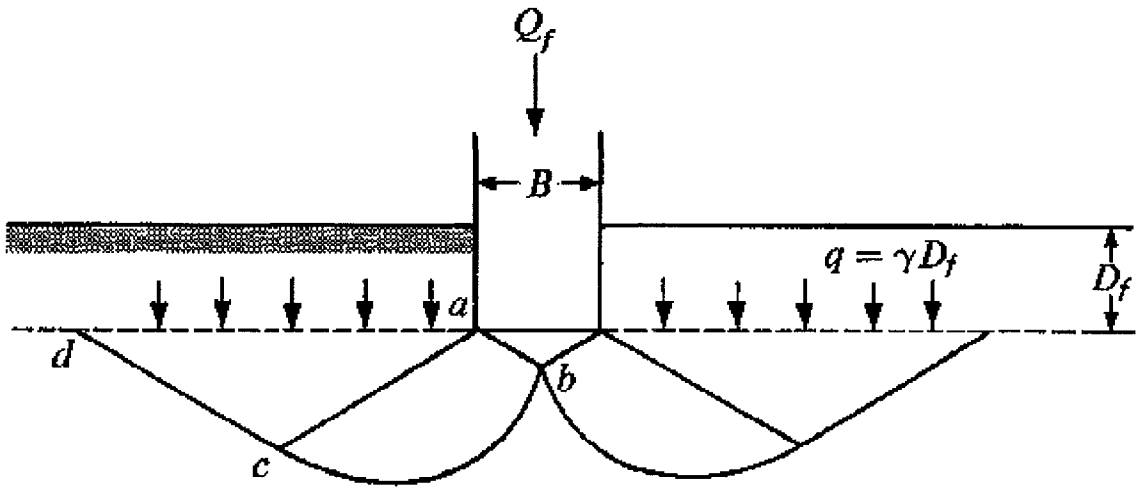

Figure 4.7 Bearing Capacity of Shallow Foundations (after Braja, 1985 [60])

It can be seen from the solution described in section 4.2.1.1.2. That the value of bearing pressure at failure $q_f = Q_f / B$ represents the sum of the following three components.

The weight of the soil mass $abcd$ and the passive earth pressure on plane dc constitute the first part of the bearing capacity. This is P' in section 4.2.1.2 (Equation 4.16). The weight W increases with the square of $B/2$. Equation (4.15) shows that the passive pressure P_p' is proportional to h^2 and hence proportional to $(B/2)^2$. Thus the

contribution to Q_f by W and $P_p^{'}$ increases with $(B/2)^2$ and their contribution to q_f increases with $(B/2)$. Furthermore, both W and $P_p^{'}$ are proportional to the unit weight γ. If this portion of the bearing capacity is denoted as q_γ, we can write for simplicity

$$q_\gamma = \frac{1}{2}\gamma B N_\gamma$$

in which N_y is the proportionality factor, called a bearing-capacity factor. Its value can be computed, after $P^{'}$ is calculated, as outlined in section 4.2.1.1.2.

By similar examination we see that $P^{''}$ and $C^{''}$ are proportional to $B/2$ and c. Therefore the contribution of the cohesion q_c to the bearing capacity is independent of B and we have

$$q_c = cN_c$$

in which N_c is the bearing-capacity factor for cohesion. The effect of the surcharge is also independent of B and is proportional to D_f and γ. Thus

$$q_q = \gamma D_f N_q$$

in which N_q is the bearing-capacity factor for surcharge.

Finally, the total bearing capacity can be expressed as

$$q_f = \frac{1}{2}B\gamma N_\gamma + cN_c + \gamma D_f N_q \qquad (4.21)$$

where N_γ, N_c and N_q are dimensionless coefficients that are governed only by the value of ϕ. This is because the shape of the failure surface depends on ϕ. It is, therefore,

possible to compute these coefficients for a set of values of ϕ, and these values may be used for all bearing-capacity calculations.

Footings with circular and rectangular shapes present very difficult mathematical problems. Various individuals have proposed semiempirical equations. The bearing-capacity equation may be written as

$$q_f = \frac{\gamma}{2}\lambda_\gamma B N_\gamma + \lambda_c c N_c + \gamma D_f N_q \tag{4.22}$$

where, λ_γ and λ_c are shape factors. Values of shape factors proposed include

$$\lambda_\gamma = 0.6$$

and

$$\lambda_c = 1.3$$

for circular footings (Terzaghi, (1943) [1])

$$\lambda_\gamma = 1 - 0.2\frac{B}{L}$$

$$\lambda_c = 1 + 0.2\frac{B}{L}$$

for rectangular foundations (Skempton, (1951) [61]), where B and L are the width and length of the foundation.

Chapter Five

Application of the R-node Method to Purely Cohesive Soils

5.1 The Problem under Consideration

The design of foundations involves two limit states: a serviceability limit state, which generally translates into a maximum settlement or differential settlement, and an ultimate limit state. The latter is concerned with the maximum load that can be placed on the footing just prior to a bearing-capacity failure (Chen, 1975 [7]).

The critical load or the total ultimate bearing capacity is the load required to produce the plastic flow or failure of the soil support. The average critical load per unit area q_u is called the bearing capacity of the soil. The value of the bearing capacity of a soil depends not only on the mechanical properties of the soil but also on the size of the loaded area, its shape, and its location with reference to the surface of the soil.

The problem under consideration in this chapter is the determination of ultimate bearing capacity of a single, strip footing bearing on a plane surface of a semi-infinite mass of soil that is assumed to be elastic-perfectly plastic material (Potts and Lidija, (1999-2001) [75]). It is further assumed that the force acting on the footing is normally and centrally loaded and increased until penetration occurs as a result of plastic flow in the soil. Also, in this chapter, the investigation is limited to the bearing capacity of the strip footings on horizontal bearing areas for purely cohesive soil (i.e., clays under

undrained conditions); in the next chapter, the investigation will be directed towards the bearing capacity of the strip footings on horizontal bearing areas for a soil with both cohesive and frictional resistance.

In the following investigation, the footing is assumed to be rigid while the interface between the soil and the footing is rough. In most parts of this chapter, the soil is assumed to be an isotropic, homogeneous and elastic-perfectly plastic material which obeys the Coulomb yield condition and the associated flow rule. The footing is assumed to be infinitely long, giving a plane strain condition is assumed in this chapter.

5.2 Limit Load Calculated by Analytical Method

Limit load of strip foundations can be solved either by general bearing capacity equation used in engineering or by nonlinear finite element analysis. Both of these two methods can give good results for bearing capacity for strip foundations.

5.2.1 Bearing Capacity Calculation by General Bearing Capacity Equation

The details about the development of bearing capacity of shallow foundations have been discussed in section 4.2. The equation is expressed as:

$$q_u = \frac{1}{2} B\gamma N_\gamma + cN_c + \gamma D_f N_q \tag{5.1}$$

In this equation, B is the width of foundation, γ is the unit weight of soil, c is the cohesion of soil, D_f is the depth of the footing; N_γ, N_c and N_q are dimensionless coefficients that are governed only by the friction angle ϕ of soil; q_u is the value of

bearing pressure at failure. This equation has been extensively used in soil mechanics to calculate the bearing capacity of strip foundations. The value obtained by this equation will be used as the theoretical solution of bearing capacity of strip foundations.

5.2.2 Bearing Capacity Calculation for Layered Soils

So far in this chapter the load-bearing capacity of homogeneous soils that support shallow foundations has been considered. However, if a footing is placed on a stratified soil deposit, soil profiles beneath footings would not be homogeneous. Studies regarding the ultimate bearing capacity of foundations on layered soils are very limited at this time; analytical solutions to the problem of footings resting on layered soils do not appear to exist (Merifieldetal, (1999) [62]). To calculate the ultimate bearing capacity for surface strip footings resting on horizontally layered soils, practitioners commonly use the approximate solutions of Button (1953) [63], Reddy and Srinivasan (1967) [64], Chen (1975) [7], Brown and Meyerhof (1969) [65] and Meyerhof and Hanna (1978) [66].

Button (1953) [63] and Chen (1975) [7] calculated upper bound solutions assuming a simple cylindrical failure surface, while Reddy and Srinivasan (1967) [64], assuming the same cylindrical mechanism, obtained results using the method of limit equilibrium. The solutions of Brown and Meyerhof (1969) [65] and Meyerhof and Hanna (1978) [66] were based upon a series of model footing tests from which empirical and semi-empirical solutions for the bearing capacity factor were derived.

Based on the assumption that the basic failure mechanism of two layered soils strata for a strip footing is a simple cylindrical failure surface for isotropic soils, the

ultimate bearing capacity of two layered purely cohesive soils may be given by (Braja, 1999 [67])

$$q_u = c_{u(1)} N_c \tag{5.2}$$

where, N_c is the bearing capacity factor and is a function of $(c_{u(2)})/(c_{u(1)})$ and H/B; $c_{u(1)}$ and $c_{u(2)}$ are the undrained cohesions of the top layer and the bottom layer; H is the depth from the interface between two layered soils to the bottom of the footing, B is the width of the footing, shown in Figure 5.1.

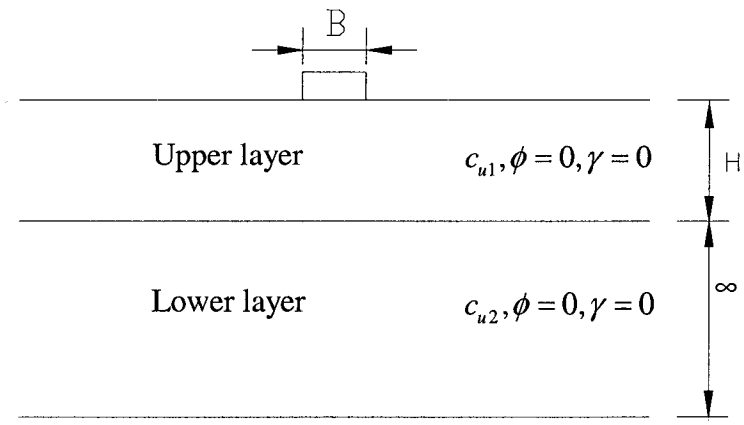

Figure 5.1 A Footing on Two-layered Cohesive Soils

5.2.3 Bearing Capacity Calculation by Finite Element Analysis

The finite element method is one of the most powerful approximate solution methods that can be applied to solve a wide range of problems represented by ordinary or partial differential equations (Fethi, 1999 [67]). It allows for different boundary conditions to be applied in such a way that an acceptable global approximate solution to

the physical problem can be achieved. Considering that closed form solutions cannot be elaborated for a large number of complex physical problems, due to the impossibility of satisfying the boundary conditions related to corresponding equilibrium equations, the finite element method therefore provides an ideal alternative (approximate) solution method.

Finite element modelling of soil-structure problems needs to be planned and undertaken carefully, so that any anomalies in the results can be spotted and remedied.

5.2.3.1 Finite Element Code, ABAQUS /Standard

The finite element code, ABAQUS/Standard v5.8, 6.1 and 6.2 (Hibbitt, et al., 1998a [69]), is used in the study. ABAQUS is a general purpose program for the static and transient responses of two and three-dimensional system; it offers standard options, or can be customized to address many of the challenges involved in a study of geotechnical structures (Nobahar, 2003 [70]), such as (1) 3-D soil-structure analysis, using complex finite strain constitutive models and accounting for large deformation effects; (2) coupled field equation capacities for two phase media; (3) contact analysis capacities for simulating the soil-structure interface; and (4) large deformation formulation capacity of capturing collapse mechanisms and strain localization.

ABAQUS is widely available, and well documented. This program has been widely used for 2D and 3D finite element analyses of soil-structure interaction involving large relative deformations, and it has been validated based on results of full-scale tests (Nobahar, (2003) [70]).

5.2.3.2 Element Type and Finite Element Model

In ABAQUS finite element code, a variety of element types are available for modeling different types of problems. For the structure under consideration, a two-dimensional solid element (CPE4R) (Hibbitt, et al., 1998a [69]) is selected for modeling. CPE4R is a quadrilateral isoparametric reduced integration element; this element type is defined by four nodal points, each having two degrees of freedom, i.e., displacements in x and y directions. Use of a reduced integration element has two reasons: firstly, fully integrated elements may suffer from "volumetric locking" behavior when the material behavior is (almost) incompressible. The cause of this problem is that the volume at each integration point must remain fixed, which puts severe constraints on the kinematically admissible displacement fields; the integration point numbers per full integration element is larger than the number of degrees of freedom, so it has more constraints than degrees of freedom, which results in overconstrained mesh (Nobahar, (2003) [70]). Because of this, the finite element solution of a structure with a perfectly plastic material cannot exhibit a limit load; instead, it shows a steadily rising load-displacement curve attaining load values far in excess of the true limit load. The use of reduced integration elements can avoid the occurrence of this problem. Secondly, reduced integration reduces the running time, especially in complicated finite element analyses (Hibbitt, et al., 1998a [76]).

For pure cohesive soil under the undrained conditions, the shear strength of the material is not affected by the effective hydrostatic stress $p' = \frac{1}{3} I_1$. Such material is

called pressure-independent. Therefore, von Mises plasticity criterion is justified for such conditions to model the undrained behavior of purely cohesive soil. This has been verified using full nonlinear analysis in comparison with the bearing capacity formula. Because the structure is symmetric, only half of structure is analyzed. Along the horizontal direction of the structure, the model is divided in 40 columns; along the vertical direction of structure, the model is divided in 40 rows. This model will be used both for obtaining limit load of structure in nonlinear finite Element analysis by using ABAQUS finite element program and for obtaining r-node elements in two linear elastic finite element analyses. When this model is used in r-node method, each column is called a segment, this model can be considered as consisting of 40 segments (columns) along the horizontal direction, with each segment consisting of 40 elements. For each segment, the stresses of all elements will be compared between two linear elastic analyses; r-node elements are represented by elements where the stresses do not change in successive analyses.

The input listing for the development of this model and subsequent analysis is given in Appendices.

5.2.4 Limit Load Calculated by R-Node method

5.2.4.1 The Failure Theory for Soil Materials

In purely cohesive soils, stability problems can be analyzed under undrained conditions. The yield of the material is assumed to be unaffected by the hydrostatic stresses $p = \frac{1}{3} I_1$ ($I_1 = \sigma_1 + \sigma_2 + \sigma_3$); the material is pressure-independent material; von

Mises yield criterion is used here to model this condition. Again, the material is assumed pressure insensitive, and isotropic.

Von Mises yield criterion is expressed as below (von Mises, (1913) [81]):

$$f(J_2,k)=\sqrt{3J_2}-k=0 \tag{5.3}$$

For pure shear,

$$\sqrt{3J_2}-\sqrt{3}\tau=0 \tag{5.4}$$

Thus, $k/\sqrt{3}$ is the shear stress at yield in pure shear experiments. From equation (5.4), we can derive $\sqrt{3J_2}=\sqrt{3}\tau$, because $\tau=c_u$, the limit load for uniform soil on the basis of the von Mises stresses according to r-node method is (Seshadri and Prasad, (1996) [34])

$$P_L=\frac{P*c_u*\sqrt{3}}{\bar{\sigma}_n} \tag{5.5}$$

where, $\bar{\sigma}_n$ is the combined r-node equivalent stress. For uniform cohesive soil, the yield stress of all elements in finite element model have the same yield stress σ_y. If there are more than one r-node peak values, the average value of these r-node equivalent stresses, $\bar{\sigma}_n=\frac{\sum_{j=1}^{N}\sigma_{nj}}{N}$ (Seshadri and Fernando, (1991) [82]), will be used in equation (5.5). Where, σ_{nj} is the peak r-node equivalent stress,

$$\sigma_{nj}=(\sqrt{3J_2})_i=\frac{1}{\sqrt{2}}[(\sigma_1-\sigma_2)^2+(\sigma_2-\sigma_3)^2+(\sigma_3-\sigma_1)^2]_j^{1/2} \tag{5.6}$$

For the layered soils, based on the basic principle of r-node method that are explained in section 2.5, equilibrium conditions for solving the limit load after obtaining the r-node equivalent stresses can be invoked in order to give the following expression (Seshadri and Prasad, (1996) [34]):

$$P_L = \frac{P(c_{u1} + c_{u2} + ... + c_{uM})\sqrt{3}}{(\sigma_{u1} + \sigma_{u2} + ... + \sigma_{uM})} \tag{5.7}$$

where, σ_{nM} is the r-node equivalent stress; c_{uM} is the corresponding cohesion of soil layer where this r-node element is located. For example, if r-node with stress σ_{nM} is located in the upper layer, the corresponding c_{uM} will be equal to the cohesion of the upper layer soil; if r-node with stress σ_{nM} is located in the lower layer, the corresponding c_{uM} will be equal to the cohesion of lower layer soil. von Mises yield criterion is used here.

5.2.4.2 The Procedure for Applying the R-node Method

The following steps are employed for limit analysis of strip foundation in purely cohesive soil under undrained conditions.

1. Choose the model parameters and mesh the model using ABAQUS/Standard.

2. Carry out the first elastic analysis using an arbitrary value of load P. The resulting equivalent stress distribution is determined.

3. Modify the Young's modulus for each element using the equation,

$$E_{ni} = \left[\frac{(\sigma_e)_j}{(\sigma_e)_i}\right] E_o \tag{5.8}$$

where, $(\sigma_e)_j$ is any arbitrary stress, $(\sigma_e)_i$ is the equivalent von Mises stress of element i, E_o is the original Young's modulus for the element, E_{ni} is the new Young's modulus for element i, which will be used in the second elastic analysis.

4. Carry out the second analysis for the same load (except for a different Young's modulus for each element) and obtain the equivalent stress in each element.

5. Compare the stress of each element between the first linear elastic analysis and the second linear elastic analysis. R-nodes are represented by locations where the equivalent stress did not change. Use equation (5.9) to find limit load.

$$P_L = \frac{\sigma_y}{\bar{\sigma}_n} P \tag{5.9}$$

where $\bar{\sigma}_n$ is the combined r-node equivalent stress, the calculation of $\bar{\sigma}_n$ has been explained in section 5.2.4.1.

Seshadri and Fernando (1991) [82] have discussed in detail the underlying concept and motivation behind equations (5.8) and (5.9). Several numerical examples involving thick-wall cylinder, rectangular beam, torispherical head, framed structures and arch have been analyzed using the r-node method with success (Seshadri and Fernando, 1991 [82], Seshadri, 1996 [83], Mangalaramanan and Seshadri, 1995 [84]).

5.2.4.2.1 Numerical Example

5.2.4.2.1.1 Bearing Capacity of Strip Foundations on Uniform Purely Cohesive Soils

For the present study, the soil is assumed to be weightless. Because the structure is symmetric, half of the foundation was analyzed. The geometry of the problem and the

finite element mesh are shown in Figure 5.2. The parameters used in numerical examples are shown in Table 5.1. Width of the footing is taken as B. The domain under analysis extends to $10B$ laterally and $5B$ vertically, an area within which most of the stress variations are expected to occur, a smaller domain might not fully exclude the influence of boundary restraints. This extension of the analysis domain is considerably larger than that used in typical plastic analyses of boundary condition (about 5 to 6B). This is due to the fact that in this study elastic analysis are performed and therefore a larger area is influenced. Chen (1975) [7] and Potts and Lidija (1999-2001) [75]) used similar or bigger domains to analyze this type of structures. The left edge of the model has the symmetry condition. The right edge of the model has vertical rollers. The bottom of the model is pinned. The behaviour of material is assumed approximately incompressible ($\nu = 0.499$) to simulate undrained loading condition; the Young's modulus of soil is set according to its undrained shear strength, such as $E = 2000c_u$ or $E = 5000c_u$ (Chen, (1975) [7]).

The results obtained with r-node method and comparisons with nonlinear FEA solution and theoretical solution methods are shown in Table 5.2. The theoretical solution is calculated according to the equation (5.1) and tables given by Das (Das, (1999) [68]), and the nonlinear FEA solution is calculated by using ABAQUS/Standard. Von Mises yield criterion has been used for nonlinear analysis. Large deformation analysis is used to calculate the limit load of structure; the input listing for the development of this model and subsequent analysis is given in Appendices 1.3.

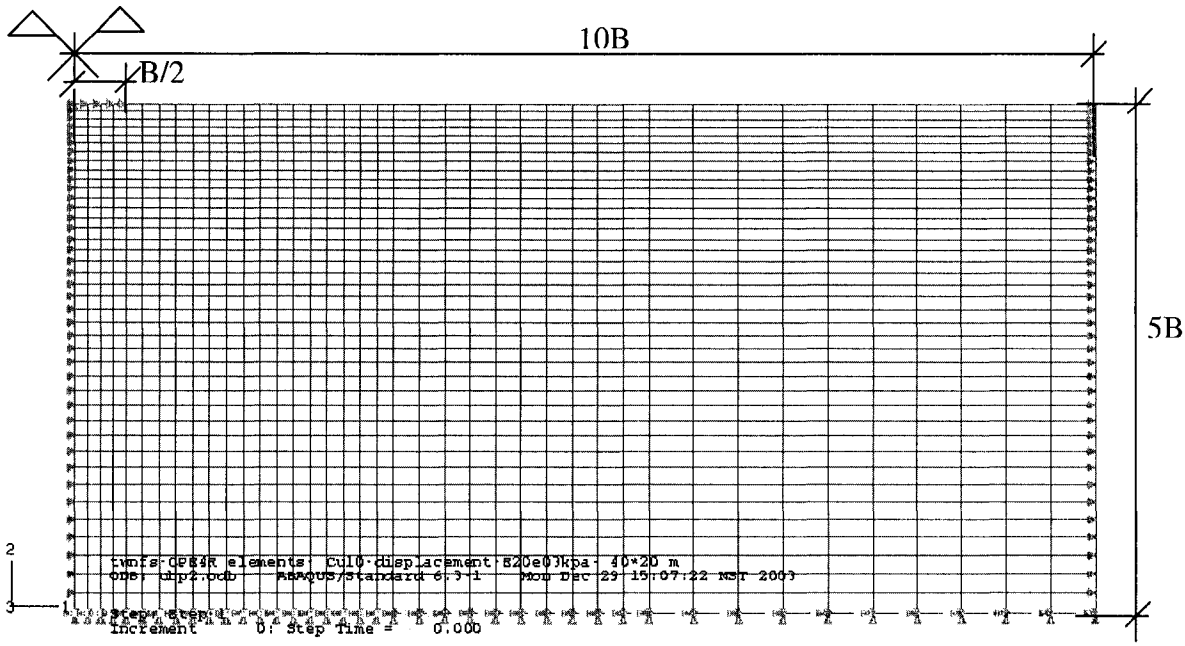

Figure 5.2 Geometry and Finite Element Model for Uniform Purely Cohesive Soil

Table 5.1 The Parameters Used in Numerical Examples

Case #	Width of foundation, B (m)	Young's modulus (MPa)	Poisson's ratio	Undrained shear strength, Cu (kPa)	Applied pressure (kPa)
1	3	20	0.499	10	100
2	4	20	0.499	10	100
3	3	50	0.499	10	100
4	4	50	0.499	10	100
5	3	20	0.499	10	50
6	4	20	0.499	10	50
7	3	20	0.499	20	100
8	4	20	0.499	20	100

The r-node locations and corresponding von Mises stresses for case one are shown in Figure 5.3 and 5.4 as an example to explain how to calculate the limit load based on r-node peak stresses. From Figure 5.3, we can find two distinct r-node peaks; the average value of von Mises stresses of them are used to calculate the limit load of structure according to the method explained in section 5.2.4.1, hence the limit load

$$P_L = \frac{P * c_u * \sqrt{3}}{\bar{\sigma}_n} = \frac{100 * 10 * \sqrt{3}}{(46.3 + 18.6)/2} = 53.38 KN/m^2$$

Figure 5.4 shows the r-node element locations in FE model.

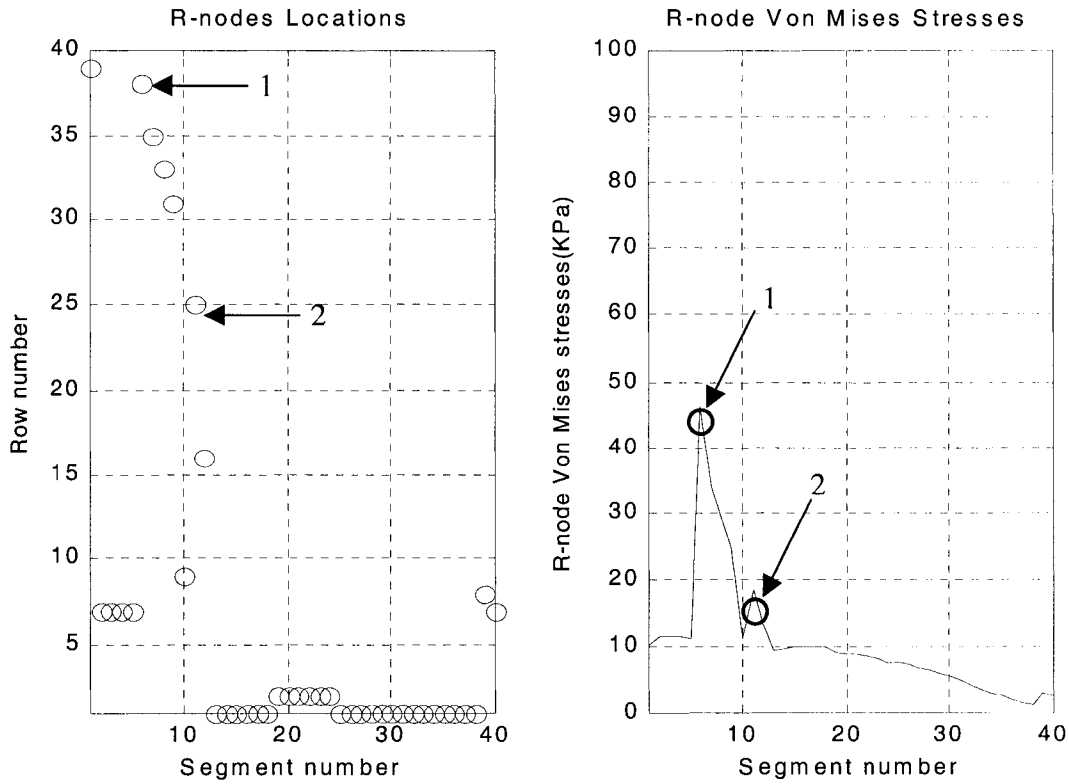

Figure 5.3 R-node Locations and Corresponding von Mises Stresses (case one)

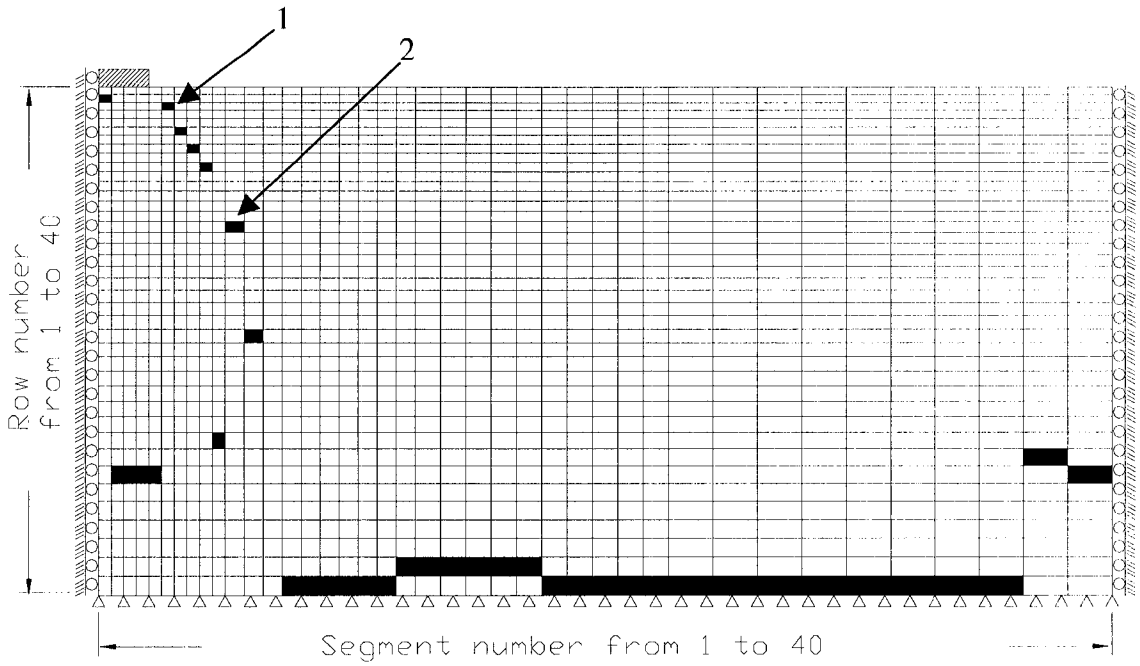

Figure 5.4 R-node Locations in FE Model (case one)

Similarly, the results of other cases are obtained and shown in Table 5.2.

Table 5.2 Results and Comparisons (in kPa)

Case #	R-node method	Nonlinear solution (von Mises criterion)		Bearing Capacity (formula equation 5.1)	
		Capacity	Error bound (percent)	Capacity	Error bound (percent)
1	53.38	54.9	2.77	51.4	3.85
2	53.38	54.9	2.77	51.4	3.85
3	53.38	54.9	2.77	51.4	3.85
4	53.38	54.9	2.77	51.4	3.85
5	53.38	54.9	2.77	51.4	3.85
6	53.38	54.9	2.77	51.4	3.85
7	106.76	109.7	2.68	102.8	3.85
8	106.76	109.7	2.68	102.8	3.85

From the Table 5.2, we can see accurate limit load estimates have been obtained for the uniform purely cohesive soil by using the r-node method.

5.2.4.2.1.2 Bearing Capacity of Strip Foundations on Layered Purely Cohesive Soils

The bearing capacity of footings on layered purely cohesive soils by using r-node method is examined in this section. Several different cases are considered. The finite element model and the soil properties under consideration are presented in Figure 5.5 and Table.5.3. Layer 1 has a depth of H while layer 2 lies below layer 1. The cohesion values for the layers are c_{u1} and c_{u2}, respectively. The corresponding modulus are E_1 and E_2.

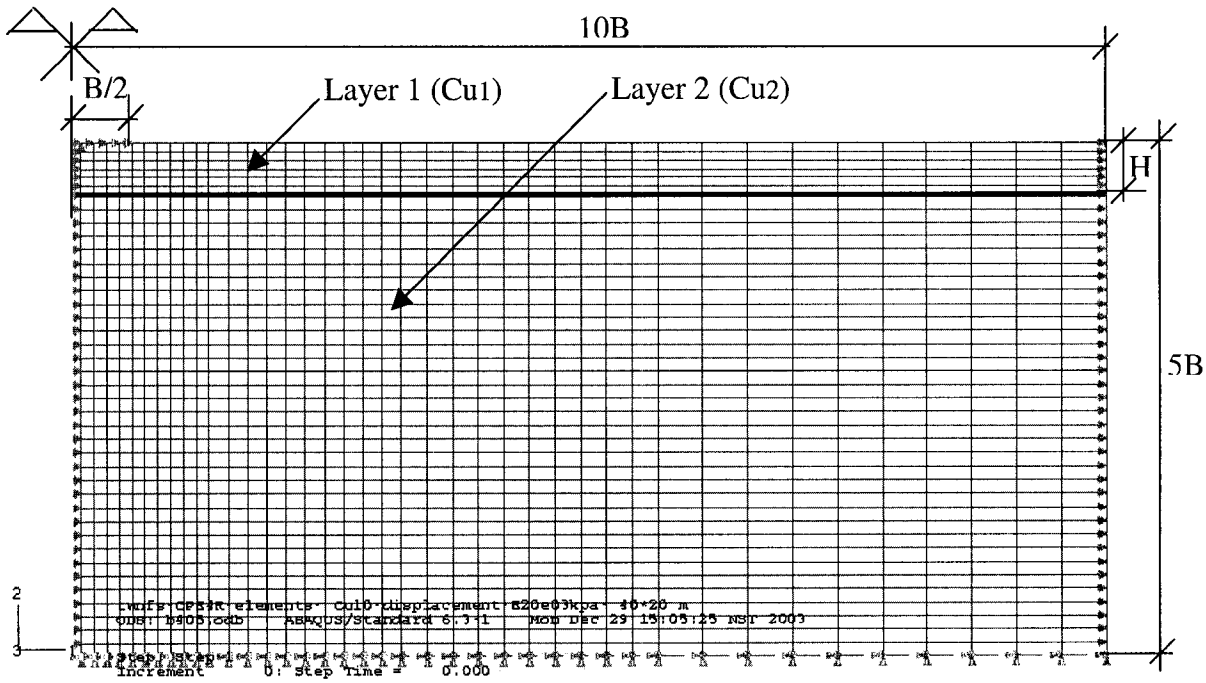

Figure 5.5 Geometry and Finite Element Model

for Layered Purely Cohesive Soils

The results obtained with r-node method and comparison with several kinds of analytical methods and nonlinear solution are shown in Table 5.6. The solutions of analytical methods are calculated according to the equations and tables provided in Merifield's paper (Merifield, (1999) [62]), and the nonlinear FEA solution is calculated by using ABAQUS/Standard. Large deformation analysis is used to calculate the limit

load of structure; the input listing for the development of this model and subsequent analysis is given in Appendices 1.2.

Table 5.3 The Parameters Used in the Examples

Case #	Cu1/Cu2	Cu1 (kPa)	Cu2 (kPa)	E1 (MPa)	E2 (MPa)	v1	v2
1	4	40	10	80	20	0.499	0.499
2	2	20	10	40	20	0.499	0.499
3	1.5	15	10	30	20	0.499	0.499
4	1	10	10	20	20	0.499	0.499
5	0.66	10	15	20	30	0.499	0.499
6	0.5	10	20	20	40	0.499	0.499
7	0.25	10	40	20	80	0.499	0.499

The r-node locations and corresponding von Mises stresses for case one ($H/B=2, c_{u1}/c_{u2}=4$) are shown in Figure 5.6 and 5.7 as an example to explain how to calculate the limit load based on r-node peak stresses. From Figure 5.6, we can find two distinct r-node peaks; both of them are located at the upper layer soil, hence the corresponding cohesions of them all are $40kPa$. According to the equation (5.7) given in section 5.2.4.2, the limit load of structure is calculated as follow:

$$P_L = \frac{P(c_{u1}+c_{u2}+...+c_{uM})\sqrt{3}}{(\sigma_{u1}+\sigma_{u2}+...+\sigma_{uM})} = \frac{40*2*\sqrt{3}}{(51.3+19)} = 197.1kPa$$

Figure 5.7 shows the r-node element locations in FE model.

Similarly, the results of other cases are obtained and shown in Table 5.4.The value of bearing capacity ($N_c^{'}$) obtained for different H/B with r-node method and comparison with several kinds of analytical methods and nonlinear solution are given in Table 5.5.

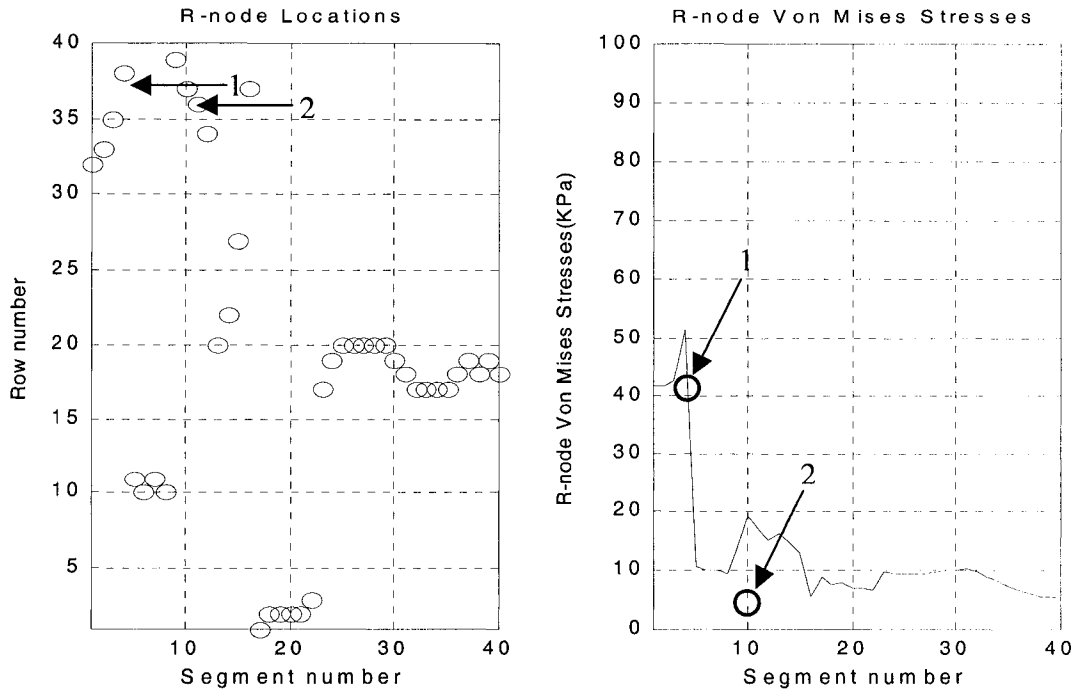

Figure 5.6 R-node Locations and Corresponding von Mises Stresses (case one)

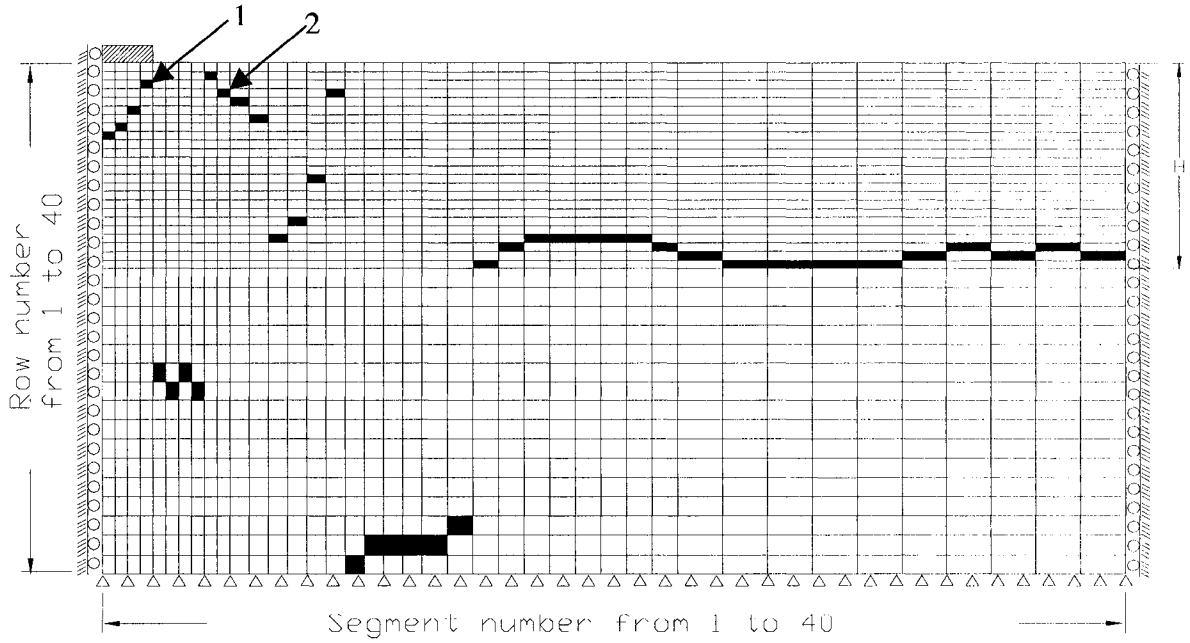

Figure 5.7 R-node Locations in FE Model (case one)

Table 5.4 Resulting Ultimate Bearing Capacity (in kPa)

H/B	Cu1/Cu2	Average (Merifield et al., 1999)	Upper Bound (Chen, 1975)	Meyerhof&Hanner (1978)	R-node method	Nonlinear solution
2	4	202.4	221.2	184	197.1	220.5
	2	100.8	110.6	102.8	90.21	110.65
	1.5	75.6	82.95	77.1	74.23	82.85
	1	51.3	55.3	51.4	53.38	54.9
	0.66	51.2	55.3	51.4	52.97	55.05
	0.5	51.2	55.3	51.4	54.55	54.85
	0.25	51.2	55.3	\	43.09	55.15
1.5	4	181.6	218.4	150.8	189.55	190.65
	2	101.8	110.6	92	98.04	110
	1.5	76.35	82.95	77.1	83.81	82.65
	1	51.3	55.3	51.4	53.38	54.9
	0.66	51.2	55.3	51.4	39.64	55.15
	0.5	51.2	55.3	51.4	54.38	55.3
	0.25	51.2	55.3	\	47.98	54.65
1	4	146	165.9	117.6	160.99	151.8
	2	92.6	102.2	89.2	99.97	99.25
	1.5	74.55	82.95	77.1	81.34	82.35
	1	51.3	55.3	51.4	53.38	54.9
	0.66	51.2	55.3	51.4	46.1	55.15
	0.5	51.2	55.3	51.4	53.39	55.05
	0.25	51.2	55.3	\	59.1	55.05
0.75	4	124.8	141.2	101.2	160.93	132.35
	2	83.6	88.6	79.8	99.83	90.05
	1.5	70.35	73.05	73.5	83.01	75.25
	1	51.3	55.3	51.4	53.38	54.9
	0.66	51.7	55.3	51.4	46.07	54.6
	0.5	51.7	55.3	51.4	53.38	54.9
	0.25	51.7	55.3	\	59.11	56.88
0.50	4	103.6	113.2	84.4	56.05	109.5
	2	74	78.8	70.2	89.74	80.05
	1.5	64.2	67.8	66.15	68.19	69.55
	1	51.3	55.3	51.4	53.38	54.9
	0.66	52.4	57.8	53.3	48.11	57
	0.5	52.4	57.8	54.3	51.86	57.1
	0.25	52.4	57.8	\	55.93	57.2
0.25	4	79.6	84.8	68	46.07	86.1
	2	63.4	68	68.4	60.46	69.05
	1.5	58.05	62.1	69.15	51.86	69.45
	1	51.3	55.3	51.4	53.38	54.9
	0.66	59.8	76.1	58.1	40.75	69.45
	0.5	62.6	76.1	60	79.94	71.2
	0.25	62.6	76.1	\	129.26	72.15

Table 5.5 Values of Bearing Capacity Factor (N'c) and Comparisons

H/B	Cu1/Cu2	Value of Bearing Capacity of N'c					
		Average (Merifield et al., 1999)	Upper bound (Chen, 1975)	Meyerhof&Hanner (1978)	R-node method	Nonlinear solution	Error bound
2	4	5.06	5.53	4.6	5.9	5.51	7.08
	2	5.04	5.53	5.14	4.51	5.53	18.44
	1.5	5.04	5.53	5.14	4.95	5.52	10.33
	1	5.13	5.53	5.14	5.08	5.49	7.47
	0.66	5.12	5.53	5.14	5.3	5.51	3.81
	0.5	5.12	5.53	5.14	5.53	5.49	0.73
	0.25	5.12	5.53	\	4.31	5.52	21.92
1.5	4	4.54	5.46	3.77	4.74	4.77	0.63
	2	5.09	5.53	5.14	4.97	5.5	9.64
	1.5	5.09	5.53	5.14	5.59	5.51	1.451
	1	5.13	5.53	5.14	5.08	5.49	7.47
	0.66	5.12	5.53	5.14	5.45	5.52	1.27
	0.5	5.12	5.53	5.14	5.44	5.53	1.63
	0.25	5.12	5.53	\	4.8	5.47	12.25
1	4	3.65	4.14	2.94	4.02	3.8	5.79
	2	4.63	5.11	4.46	5	4.96	0.81
	1.5	4.97	5.53	5.14	5.42	5.49	1.28
	1	5.13	5.53	5.14	5.08	5.49	7.47
	0.66	5.12	5.53	5.14	4.61	5.52	16.49
	0.5	5.12	5.53	5.14	5.34	5.51	3.09
	0.25	5.12	5.53	\	5.91	5.51	7.26
0.75	4	3.12	3.53	2.53	4.12	3.31	24.47
	2	4.18	4.43	3.99	4.61	4.5	2.44
	1.5	4.69	4.87	4.9	4.73	5.02	5.78
	1	5.13	5.53	5.14	5.08	5.49	7.47
	0.66	5.17	5.53	5.14	4.69	5.46	14.1
	0.5	5.17	5.53	5.14	5.08	5.49	7.47
	0.25	5.17	5.53	\	5.89	5.49	7.29
0.5	4	2.59	2.83	2.11	1.4	2.74	48.91
	2	3.7	3.94	3.51	4.49	4	12.25
	1.5	4.28	4.52	4.41	4.55	4.64	1.94
	1	5.13	5.53	5.14	5.08	5.49	7.47
	0.66	5.24	5.78	5.33	4.82	5.7	15.44
	0.5	5.24	5.78	5.43	5.37	5.71	5.95
	0.25	5.24	5.78	\	5.53	5.72	3.32
0.25	4	1.99	2.12	1.7	1.05	2.15	51.16
	2	3.17	3.4	3.42	3.02	3.45	12.46
	1.5	3.87	4.14	4.61	3.45	4.63	25.49
	1	5.13	5.53	5.14	5.08	5.49	7.47
	0.66	5.98	7.61	5.81	7.72	6.95	11.08
	0.5	6.26	7.61	6	7.98	7.12	12.08
	0.25	6.26	7.61	\	17.68	7.22	144.88

Based on the results in table 5.4 and 5.5, the error bound for variation bearing capacity factor N'c is shown in Figure 5.8, contour of N'c for nonlinear analysis, contour of N'c for r-node method and contour of error bound between nonlinear analysis and r-node method are shown in Figure 5.9, 5.10 and 5.11.

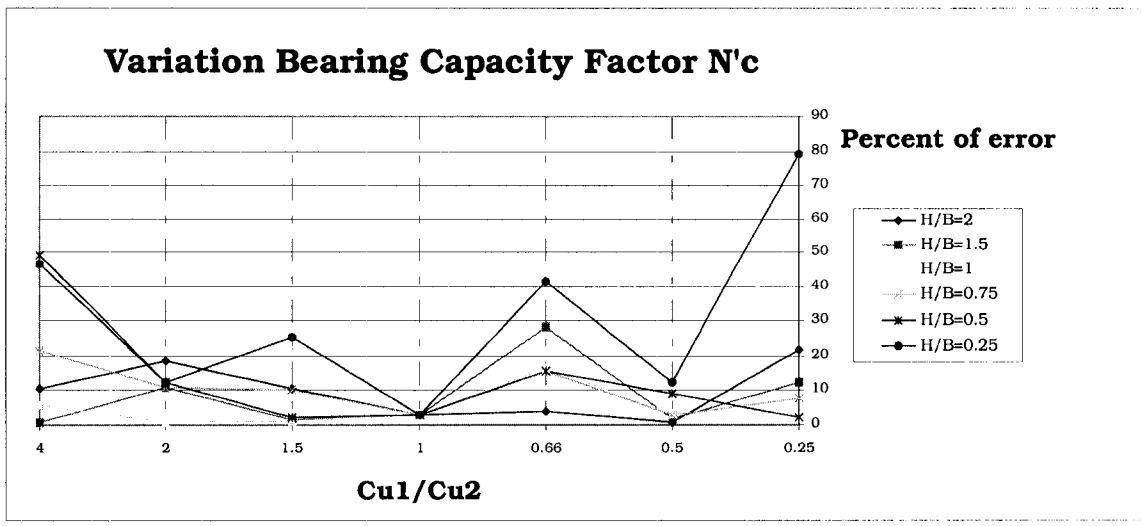

Figure 5.8 Error Bound for Variation in Bearing Capacity Factor N'c

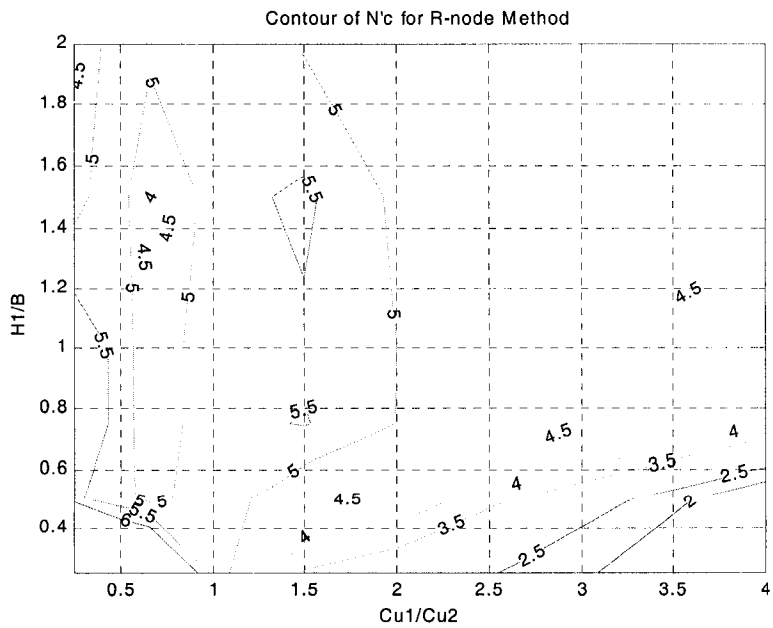

Figure 5.9 Contour of N'c for R-node Method

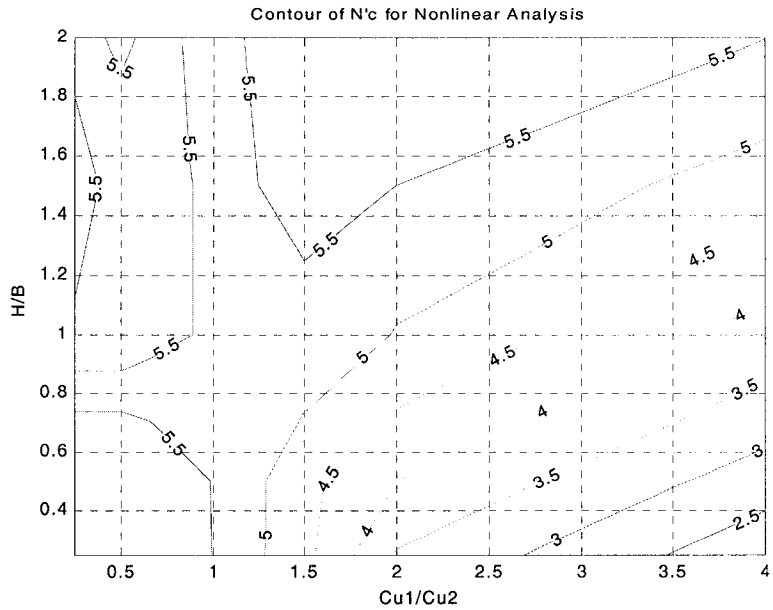

Figure 5.10 Contour of N'c for Nonlinear Analysis

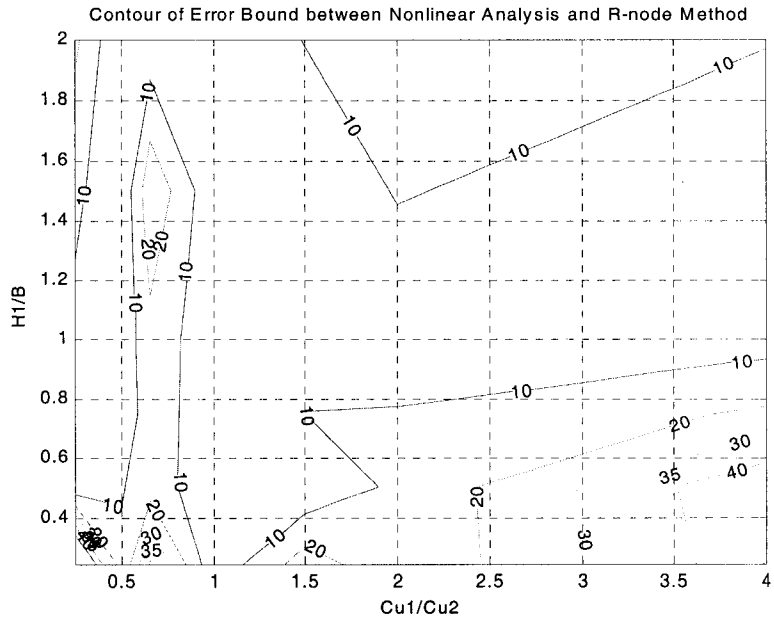

Figure 5.11 Contour of Error Bound

between Nonlinear Analysis and R-node Method

From the results, it can be seen that as compared to the results of full nonlinear solution, the method works well for uniform purely cohesive soils (homogeneous

materials); for layered soils it seems to provide less accurate results if the main resistant layer is on top (i.e. the failure surface is more likely to pass through both layers) and as the degree of inhomogeneity increase (e.g. $c_{u1}/c_{u2}=4$ vs $c_{u1}/c_{u2}=2$) and the division between soil layers is close to the foundation (e.g. $H/B=0.25$ vs $H/B=1.5$).

The reason for such tendencies is locating of r-nodes becomes difficult because there exists a sudden change of soil properties across the division between soil layers; the increasing of the degree of inhomogeneity aggravates this influence. Specially, when the main resistant layer is on top and thin, the locations of r-node elements having the peak stresses are normally close to the interface of two soil layers. Under such condition, not all r-node peak values can be found or located accurately, which leads to the poor or wrong results. By using more iterations to find r-nodes, one can somehow improve this problem, but for the condition that top soil layer is thin, the improvement is smaller than when the top soil layer is thick. Several cases are show below:

H/B	Cu1/Cu2	R-node Iteration 2 (kPa)	R-node Iteration 3 (kPa)	Nonlinear solution (kPa)
2	4	197.31	224.21	220.25
0.75	4	164.58	147.41	132.35
0.25	4	46.07	59.7	86.1

Chapter Six

Application of R-Node Method

to Cohesive-Frictional Soils

6.1 Failure Theory

Mohr (1900) [72]) presented a shear strength theory for pressure-sensitive materials called Mohr-Coulomb theory, which has been found to be very successful in defining shear failure in soils. The theory states that failure in a material occurs if the shear stress on any plane equals the shear strength of the material. Furthermore, the shear strength τ_f, along a plane is a function of the normal effective stress σ' on that plane, or

$$\tau_f = f(\sigma') \tag{6.1}$$

This function plots as a curve in a normal versus shear stress plane. Coulomb (1776 [53]) defined the function f as a linear function of the normal effective stress called as failure line or failure envelope. Equation (6.1) then becomes

$$\tau_f = c + \sigma_n' \tan\phi \tag{6.2}$$

If the major and minor principal effective stresses in an element of material are equal to σ_1' and σ_3', these stresses can be calculated graphically by means of Mohr's circle of stress. A Mohr's circle with principal effective stresses σ_1' and σ_3' is plotted in

Figure 6.1. If the Mohr circle is tangent to the failure envelope, there is a plane defined by angle ϕ where the shear stress τ_A is equal to the shear strength τ_f, and failure occurs.

$$\tau_f = \frac{1}{2}(\sigma_1' - \sigma_3')\cos\phi$$

$$\sigma_n' = \frac{1}{2}(\sigma_1' + \sigma_3') - \frac{1}{2}(\sigma_1' - \sigma_3')\sin\phi \tag{6.3}$$

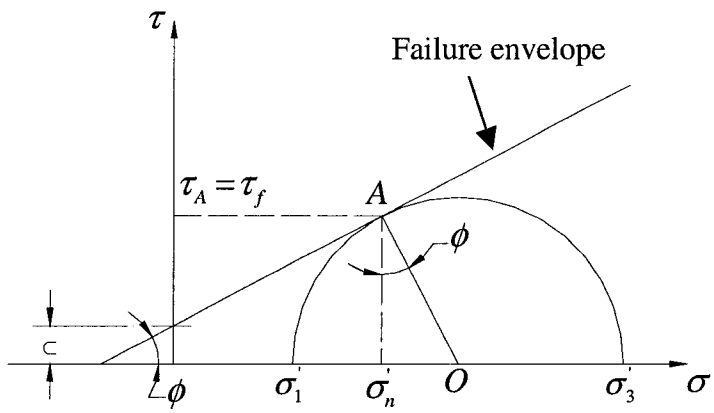

Figure 6.1 Mohr-Coulomb Failure Envelope (after Mohr, 1900 (72))

For purely cohesive soils under undrained condition, the failure envelope is a horizontal line. The failure theory becomes

$$\tau_f = c_u \tag{6.4}$$

where, c_u is the undrained shear strength and equal to the radius of the Mohr's circle at failure.

6.2 Yield Criterion for Cohesive-Frictional Soils

For cohesive-frictional soils, the shear strength of the material is affected by the effective hydrostatic stresses $p' = \frac{1}{3} I_1$. The material is called pressure-dependent. Mohr-Coulomb and Drucker-Prager yield criteria are normally used to include the effect of hydrostatic pressure on the yielding of materials.

The Mohr-Coulomb Criterion (Coulomb, (1776) [53]) is expressed as

$$|\tau| = c + \sigma' \tan\phi \tag{6.5}$$

The general expression of the criterion in three dimensions has the form

$$f(I_1, J_2, \phi, \theta) = \frac{1}{3} I_1 \sin\phi + \sqrt{J_2}\sin(\theta + \frac{\pi}{3}) + \sqrt{\frac{J_2}{3}}\cos(\theta + \frac{\pi}{3})\sin\phi - c\cos\phi = 0,$$
$$0 \le \theta \le \frac{\pi}{3} \tag{6.6}$$

The function in equation (6.6) is called yield (or failure) surface and plots as an irregular hexagonal pyramid in the ($3D$) principal effective stress space. The apex of the pyramid is located on the hydrostatic line ($\sigma_1' = \sigma_2' = \sigma_3'$). Drucker (1953) introduced a simpler failure surface, which plots as a circular cone in the principal effective shear space and is tailored to be tangent (internally or externally) to the more realistic Mohr-Coulomb failure surface. Drucker-Prager criterion is expressed as:

$$f(I_1, J_2, \alpha, k) = -\alpha\frac{I_1}{3} + \sqrt{J_2} - k = 0 \tag{6.7}$$

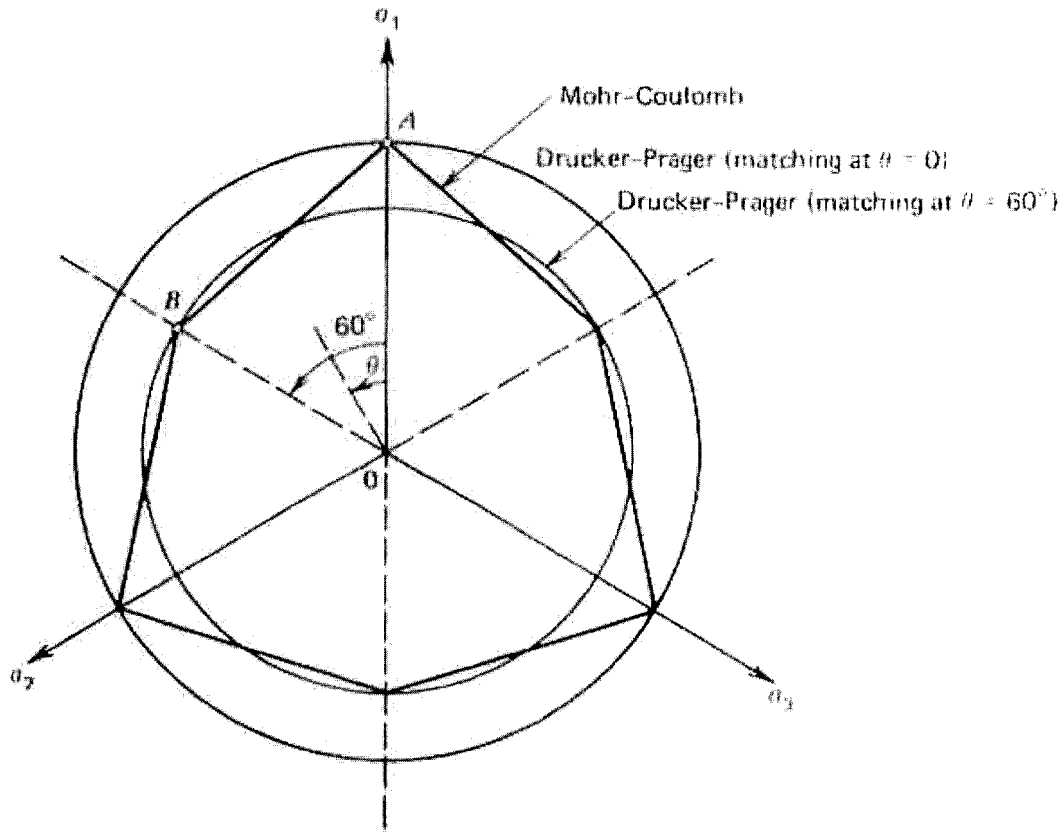

Figure 6.2 Drucker-Prager and Mohr-Coulomb Failure Criteria with Different Matching Conditions (after Chen and Saleeb, (1982) [41])

where, α and k are positive material parameters; $I_1 = \sigma_{ii}$ is the first invariant of stress tensor; $J_2 = \frac{1}{2} s_{ij} s_{ji}$ is the second invariant of deviatoric stress tensor; θ can be measured from Figure 6.2, and θ is the polar angle measured from the positive direction of the projection of the σ_1 axis. By matching the predictions of both yield criteria in given test condition, the values of α and k can be expressed in terms of the cohesion c and friction

angle ϕ (Chen and Saleeb, (1982) [41]). For instance, in axial compression ($\sigma_2 = \sigma_3$ and $\theta = 0$) (Prevost, (1989) [73]):

$$\alpha = \frac{2\sin\phi}{\sqrt{3}(3-\sin\phi)}, \quad k = \frac{6c\cos\phi}{\sqrt{3}(3-\sin\phi)} \tag{6.8}$$

Similarly, in axial extension ($\sigma_2 = \sigma_3$ and $\theta = +\frac{\pi}{3}$):

$$\alpha = \frac{2\sin\phi}{\sqrt{3}(3+\sin\phi)}, \quad k = \frac{6c\cos\phi}{\sqrt{3}(3+\sin\phi)} \tag{6.9}$$

If the Drucker-Prager and Mohr-Coulomb criteria are expected to give an identical limit load (or plastic collapse load) for the case of plane strain, the following two conditions must be satisfied to determine the constants α and k (Chen and Saleeb, (1982) [41]):

1. The condition of plane strain deformation.

2. The condition of the same rate of dissipation of mechanical energy per unit volume. Based on these two conditions,

$$\alpha = \frac{3\tan\phi}{\sqrt{(9+12\tan^2\phi)}}, \quad k = \frac{3c}{\sqrt{(9+12\tan^2\phi)}} \tag{6.10}$$

Under this condition, the Drucker-Prager cone is internally tangential to the Mohr-Coulomb yield surface (Chen and Saleeb, (1982) [41]), the angle θ in equation (6.6) is defined by $\tan\theta = \frac{\sin\phi}{\sqrt{3}}$ (Prevost, (1989) [73]).

6.3 Application of R-Node Method to Cohesive-Frictional Soils

The r-node method has been developed for the limit analysis of structures made of elastic- perfectly plastic material corresponding with the one-parameter failure criteria, such as metals. The elastic-plastic behavior of most metallic materials is essentially hydrostatic pressure insensitive. The one-parameter failure criteria, such as Tresca criterion or von Mises criterion, have generally been used for this type of materials. Purely cohesive soils loaded under undrained conditions match this type of material.

In this chapter, the r-node method is applied to cohesive-frictional soils, which are pressure-sensitive materials. This implies that the effect of hydrostatic pressure on the yielding of materials must be considered. Two-parameters failure criteria are normally used, such as Mohr-Coulomb criterion or Drucker-Prager criterion, as the yielding condition for this type of materials. Hence, before applying the r-node method to it, there are some particular discussions below:

Firstly, the failure shear stress of the cohesive-frictional soils depends on the confining stress as opposed to the purely cohesive soil that is independent of the confining stress.

The purely cohesive soils match the type of pressure-insensitive material; the shear strength of this material is independent of the confining stress and is a constant, which is expressed as $\tau_f = c_u$. When the r-node method is applied, a unique reference stress is used to modify the Young's moduli of all elements in the modulus-modified procedure. But for cohesive-frictional soils, when Mohr-Coulomb criterion is, the shear strength of material depends on the normal effective stress. Therefore, dependence of

shear strength on confining stress should be considered in analysis. Instead of working with a unique reference stress, for the cohesive-frictional soils the Young's modulus of each element is modified according to the corresponding shear strength, which is expressed below:

$$E_{ni} = \frac{(\tau_f)_i}{(\tau_e)_i} E_o \tag{6.11}$$

where, $(\tau_f)_i$ is shear strength of element i; $(\tau_e)_i$ is the shear stress of element i; E_o is the original Young's modulus; E_{ni} is the new Young's modulus for element i, which will be used in the second elastic analysis.

Secondly, for cohesive-frictional soils, there are two parameters (c and ϕ) characterizing shear strength of materials as opposed to one parameter (e.g., c_u) for undrained clays or for metals (yield stress σ_y).

When equation (6.11) is used, the shear strength of each element is solved according to $(\tau_f)_i = c + (\sigma_n^{'})_i \tan\phi$, which is based on the normal effective stress obtained from the first elastic analysis.

The problem here is how to calculate the shear stress $(\tau_e)_i$ of that element knowing only the normal effective stress of it. One can somehow address this problem using mobilized cohesion c_d and mobilized friction angle ϕ_d as scaling factors.

For getting the mobilized cohesion and mobilized friction angle of that element, it is necessary to establish some functional relation between mobilized cohesion and

mobilized friction angle. It is assumed that the failure surface and the mobilized stress surface have the same apex, shown in Figure 6.3 and explained below:

For the material with cohesion c and friction angle ϕ, the Mohr-Coulomb yield criterion is used and shown as a straight line in the $\tau - \sigma$ stress space, see Figure 6.3. The principal effective stresses in each element are obtained from the first analysis; the mobilized stress Mohr-Coulomb circle and line are shown in Figure 6.3. The mobilized shear strength is calculated as $\tau_d = c_d + \sigma_n' \tan\phi_d$, where, ϕ_d (mobilized friction angle) is the slope of the mobilized stress line; c_d is the mobilized cohesion, $c_d = a\tan\phi_d$; the quantity $a = \dfrac{c}{\tan\phi}$, shown in Figure 6.3, is called attraction.

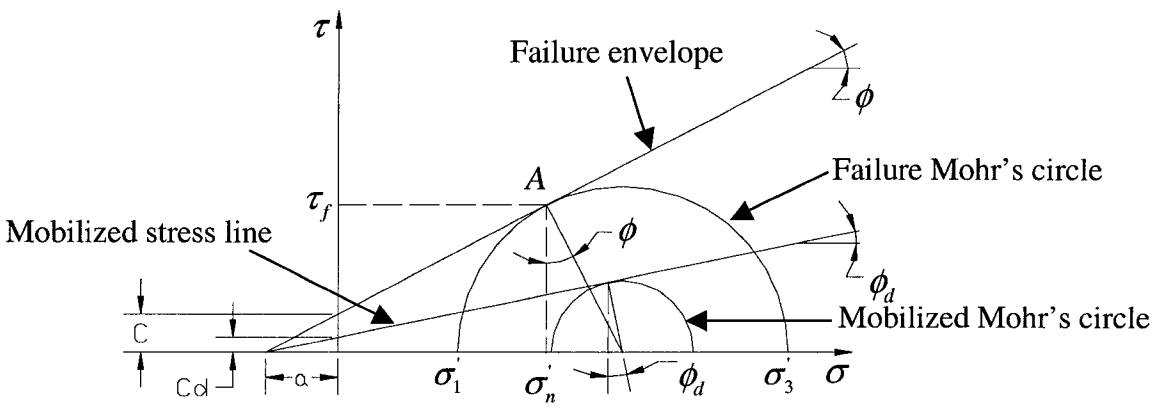

Figure 6.3 Failure and Mobilized Stress Mohr's Circle (after Prevost, (1989) [89])

The Mohr-Coulomb yield criterion, $\tau_f = c + \sigma_n' \tan\phi$, is expressed as $c = \tau_f - \sigma_n' \tan\phi$, therefore, the modulus of each element will be modified by using

$E_n = \frac{c}{(c_d)_i} E_o$, where, c is the cohesion of soil; $(c_d)_i$ is the mobilized cohesion of each element.

Thirdly, stresses caused by the self-weight of soil affect the shear strength.

Normally metals and purely cohesive soils are taken as weightless materials when calculating the load-carrying capacities against failure. But for cohesive-frictional soils, the self-weight of them cannot be ignored in limit load calculation. When applying r-node method, the procedures given below are employed to consider the effect of self-weight of soil for different trials.

Soil is still considered weightless in the two elastic analyses, but the self-weight stresses are added when calculating shear strength and estimating the Young's modulus. But in some trials, stresses induced by self-weight are deleted when calculating limit loads. That's because for the condition in practice, before the foundation is submitted to load, the stresses caused by self-weight have existed in the soil as the initial stresses. The limit load of structure in fact is the limit-applied load. Thus, Limit load solved in last step should only depend on the additional stresses produced by applied load.

Fourthly, for the failure of soil in shear, deformability is characterized by shear modulus rather than by Young's modulus.

For metallic materials, the stress-strain behavior is normally exhibited by normal stress versus normal strain; for soils, the failure of soil is determined by shear strength, the shear stress-strain curve is presented to exhibit this behavior. Hence instead of working with Young's modulus, E, the shear modulus, $G = \frac{E}{2(1+\nu)}$, is used as the

quantity to be modified from the first to the second elastic analysis. The values of Young's modulus and Possion's ratio for the second analysis are estimated from the new shear modulus and the condition that bulk modulus, $B = \frac{E}{3(1-2\nu)}$, is constant. It is mentioned here that in soil nonlinear behaviour, bulk modulus is approximately constant during plastic flow if the confining stress does not change significantly. Hence, for the second elastic analysis, each element in the structure has the new Young's modulus and Possion's ratio in order to simulate the inelastic flow at the plastic collapse of structure.

All those modifications to the original method used in chapter 5 for purely cohesive soils have been gradually introduced, and their effects have been analyzed in a series of trials, as described hereafter.

6.4 Numerical Example

For the analysis of this problem, plane strain conditions are assumed. Because the structure is symmetric, half of the foundation was analyzed. The Mohr-Coulomb plasticity model is selected in this study for modelling cohesive-frictional soils. The geometry of the problem and finite element mesh are shown in Figure 6.4. The parameters used in numerical examples are shown in Table 6.1.

6.4.1 Trial one

The first two elements mentioned in section 6.3, namely, relation between cohesion and frictional angle (Figure 6.3) and effect of self-weight of soil, are considered in trial one; the self-weight of soil is also considered when calculating limit loads. The following steps are employed for trial one:

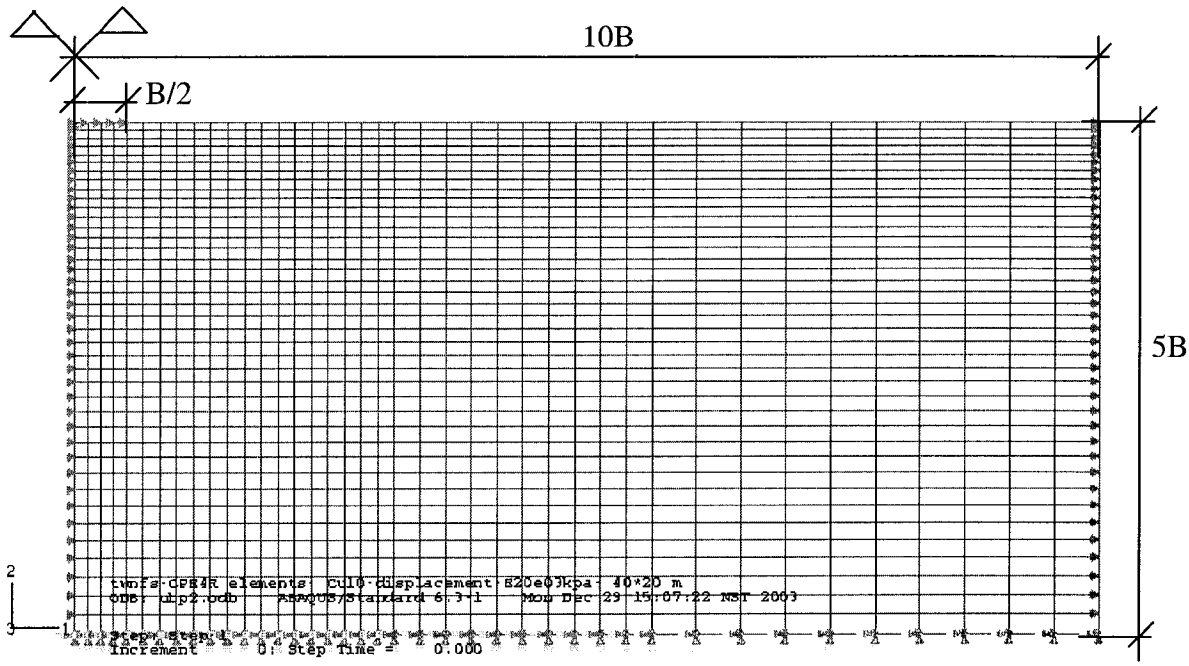

Figure 6.4. Geometry and Finite Element Model for Cohesive-Frictional Soils

Table 6.1 The Parameters Used in Numerical Examples

Case Number	Width of Foundation (m)	Young's Modulus (MPa)	Poisson's ratio	Cohesion (kPa)	Friction Angle (Degree)
1	4	20	0.3	10	10
2	4	20	0.3	10	20
3	4	100	0.3	50	10
4	4	100	0.3	50	20
5	4	100	0.3	50	30

1. Carry the first elastic analysis, then using

$$E_{ni} = \frac{c}{(c_d)_i} E_o = \frac{c}{a\tan(\phi_d)_i} E_o = \frac{c}{\frac{c}{\tan\phi}\tan(\phi_d)_i} E_o = \frac{\tan\phi}{\tan(\phi_d)_i} E_o \qquad (6.12)$$

to modify Young's modulus of each element, where, $\phi_d = \sin^{-1}(\frac{q}{p+a})$, $q = \frac{\sigma_1' - \sigma_3'}{2}$, $p = \frac{\sigma_1' + \sigma_3'}{2}$, σ_1' and σ_3' are the maximum and minimum entire effective principle stresses, which including the stresses caused by applied load and self-weight, of each element. How to calculate the entire stress has been explained in section 6.3.

2. Carry out the second elastic analysis for the same load, mesh except for a different elastic modulus and obtain $\tan\phi_d$ in each element.

3. Compare $\tan\phi_d$ of each element between the first linear elastic analysis and the second linear elastic analysis. R-node elements are represented by locations where the $\tan\phi_d$ did not change between two elastic analyses.

4. Use

$$P_L = \frac{\tan\phi}{\sum_{j=1}^{N}(\tan\phi_d)_{nj}\Big/N} P = \frac{c}{\sum_{j=1}^{N}(c_d)_{nj}\Big/N} P \tag{6.13}$$

to find limit load. Where, $\sum_{j=1}^{N}(c_d)_{nj}\Big/N$ is the combined r-node equivalent stress. If there are more than one r-node peak values, the average value of them will be used in equation (6.13).

The results obtained with r-node method and comparison with nonlinear FEA solution and theoretical solution methods are shown in Table 6.2. The theoretical solution is calculated according to the equation (5.1) and tables given by Das (Das, (1999) [68]),

and the inelastic FEA solution is calculated by using ABAQUS/Standard. Large deformation analysis is used to calculate the limit load of structure; the input listing for the development of this model and subsequent analysis is given in Appendices 1.3.

The r-node locations and corresponding von Mises stresses for case one are shown in Figure 6.5 and 6.6 as an example to explain how to calculate the limit load based on r-node peak stresses. Based on the principle that an r-node peak located away from the "critical region" of the component or structure is not a virtual peak, from Figure 6.5, two distinct r-node peaks can be found; the average value of mobilized cohesions of them are used to calculate the limit load of structure according to the method explained in equation (6.13), hence the limit load

$$P_L = \frac{c}{\sum_{j=1}^{N}(c_d)_{nj}\Big/N} P = \frac{10}{(19.2+19.4)/2}100 = 51.81kPa$$

Figure 6.6 shows the r-node element locations in true FE model.

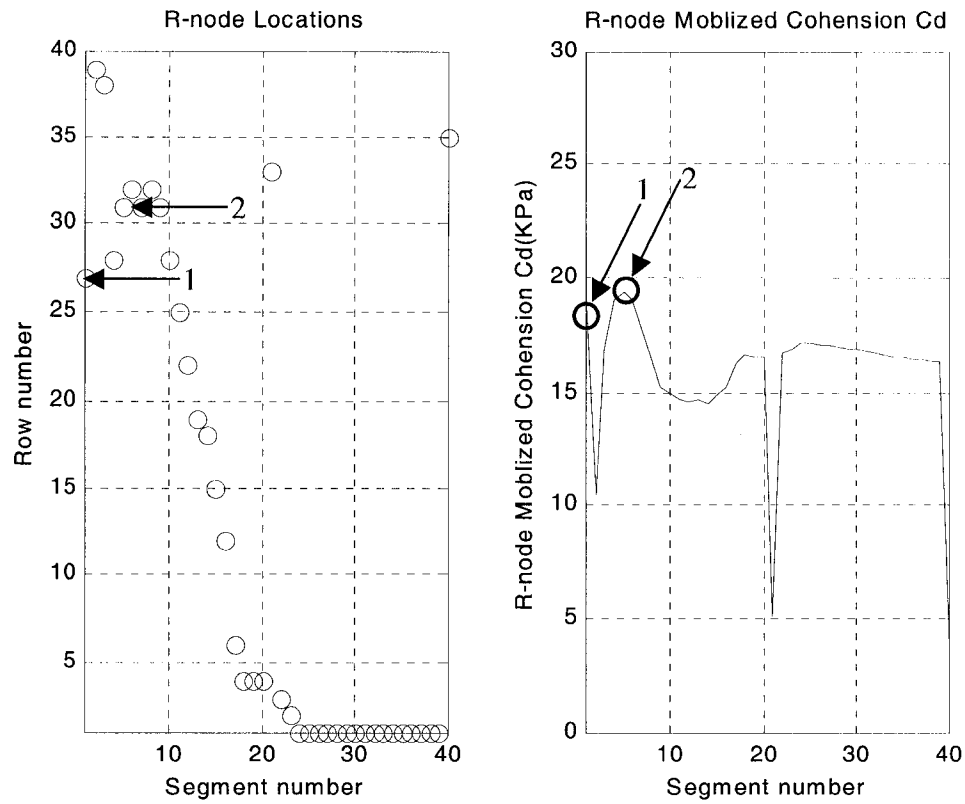

Figure 6.5 R-node Locations and Corresponding Mobilized Cohesion C_d (case one)

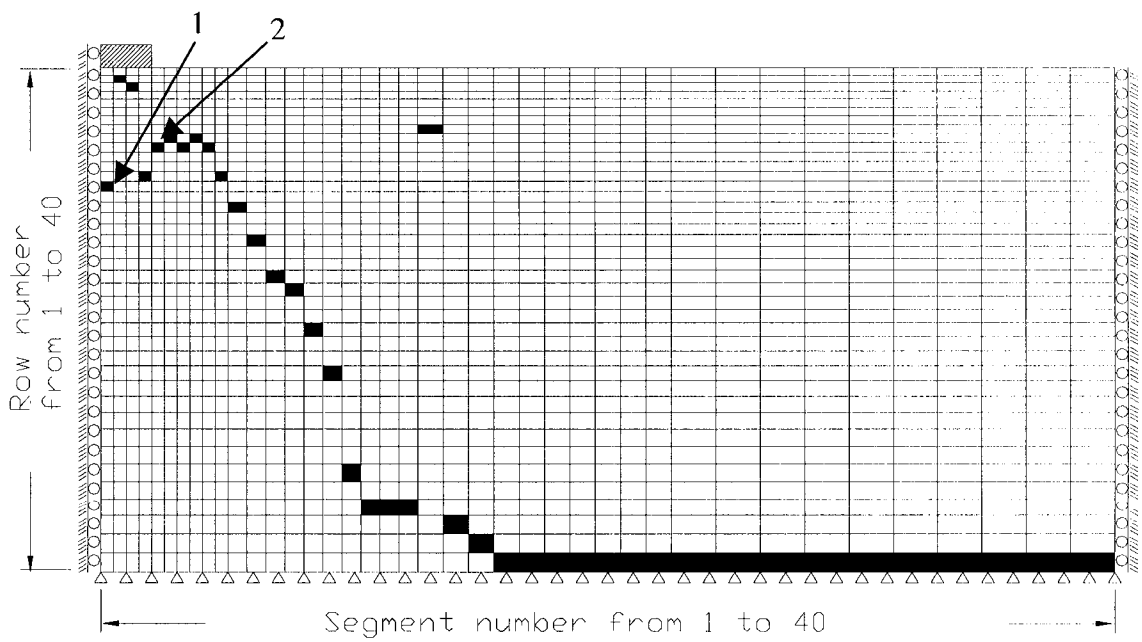

Figure 6.6 R-node Locations in FE Model (case one)

Similarly, the results of other cases are obtained and shown in Table 6.2.

Table 6.2 Results and Comparisons

Limit Load (kPa)			
Case #	R-node	Theoretical Solution	Nonlinear (Mohr-Coulomb)
1	51.81	105.46	111.2
2	54.92	245.32	246.4
3	167.22	439.46	464.6
4	192.31	838.52	853
5	222.22	1910.2	1693.5

The possible reason of poor results is that for the failure of soil in shear, deformability is characterized by shear modulus rather than by Young's modulus. Hence in trial two, the shear modulus is used as the quantity to be modified from the first to the second elastic analysis instead of Young's modulus.

6.4.2 Trial two

The main difference between trial two and trial one is the shear modulus, $G = \frac{E}{2(1+\nu)}$, is used as the quantity to be modified from the first to the second elastic analysis instead of working with Young's modulus, E. In order to solve the values of Young's modulus and Possion's ratio for the second analysis, another condition is introduced here, namely the bulk modulus, $B = \frac{E}{3(1-2\nu)}$, is a constant during the whole analysis. The reason has been explained in section 6.3.

So two new equations are obtained as below:

$$B_{ni} = \frac{E_{ni}}{3(1-2\nu_{ni})} = B_o = \frac{E_o}{3(1-2\nu_o)}$$

$$G_{ni} = \frac{E_{ni}}{2(1+\nu_{ni})} = G_o \frac{\tan\phi}{(\tan\phi_d)_i} = \frac{E_o}{2(1+\nu_o)} \frac{\tan\phi}{(\tan\phi_d)_i} \tag{6.14}$$

where, B_o, G_o are the original shear modulus and bulk modulus; B_{ni} and G_{ni} are the new shear modulus and bulk modulus of elements, which will be used in the second elastic analysis. Based the above two equations, the new Young's modulus and Possions' ratio will be

$$E_n = (1+\nu_n)\frac{E_0}{1+\nu_o}\frac{\tan\phi}{\tan\phi_d} \tag{6.15a}$$

and

$$\nu_n = \frac{3}{(2+\frac{\tan\phi}{\tan\phi_d}\frac{1-2\nu_0}{1+\nu_0})} - 1 \tag{6.15b}$$

For the new analysis, the other steps are the same as trial one except the elastic modulus and Possions' ratio will be modified according to (6.15a) and (6.15b).

1. Carry the first elastic analysis, then use equations (6.15a) and (6.15b) to modify Young's modulus and Possion's ratio of each element. Equation (6.15a) and (6.15b) are obtained based on the principles explained in point four, namely, the shear modulus, $G = \frac{E}{2(1+\nu)}$, is modified according to shear strength with the condition that bulk modulus, $B = \frac{E}{3(1-2\nu)}$, is constant; $\phi_d = \sin^{-1}(\frac{q}{p+a})$, $q = \frac{\sigma_1' - \sigma_3'}{2}$, $p = \frac{\sigma_1' + \sigma_3'}{2}$, σ_1' and σ_3' are the maximum and minimum entire effective principal stresses, which include the

stresses caused by applied load and self-weight and are obtained from the first elastic analysis.

2. Carry out the second elastic analysis for the same load, mesh except for a different Young's modulus and Possion's ratio and obtain $\tan\phi_d$ in each element.

3. Compare $\tan\phi_d$ of each element between the first linear elastic analysis and the second linear elastic analysis. R-nodes are represented by locations where the $\tan\phi_d$ did not change.

4. Use

$$P_L = \frac{\tan\phi}{\sum_{j=1}^{N}(\tan\phi_d)_{nj}\Big/N} P = \frac{c}{\sum_{j=1}^{N}(c_d)_{nj}\Big/N} P \tag{6.16}$$

to calculate the limit load of structure.

The parameters used in numerical examples are shown in table 6.1. The results obtained with r-node method and comparison with nonlinear FEA solution and theoretical solution methods are shown in Table 6.3. The theoretical solution is calculated according to the equation (5.1) and tables given by Das (Das, (1999) [68]), and the inelastic FEA solution is calculated by using ABAQUS/Standard. Large deformation analysis is used to calculate the limit load of structure; the input listing for the development of this model and subsequent analysis is given in Appendices 1.3

For the above two trials, the possible problem of incorrect results may appear at last step, in which the stresses caused by self-weight of soil also are considered in calculating the limit load of structure. Since the limit load of structure is actually the

limit-applied load, such consideration is obviously incorrect. Hence for new trials, the stressed induced by self-weight will be deleted when calculating limit loads.

Table 6.3 Results and Comparisons

Limit Load (kPa)			
Case #	R-node	Theoretical Solution	Nonlinear (Mohr-Coulomb)
1	79.86	105.46	111.2
2	117.5	245.32	246.4
3	163.3	439.46	464.6
4	269.4	838.52	853
5	590.62	1910.2	1693.5

6.4.3 Trial three

The steps 1 to 3 are same as that used in trial one; the difference is in step 4, in step the stresses induced by self-weight are taken out when calculating limit loads. A safety factor K is set and calculated in order to consider this effect. Equation

$$P_L = KP \tag{6.17}$$

is used to solve the limit load at last step. The calculation of K is derived below:

Considering the self-weight of soil, assuming the mobilized friction angle under the applied load P_1 is ϕ_{d1}, from the Figure 6.3, $\phi_d = \sin^{-1}(\frac{q'}{p'+a})$, where, $q' = \frac{\sigma_1' - \sigma_3'}{2}$, $p' = \frac{\sigma_1' + \sigma_3'}{2}$, σ_1' and σ_3' are the maximum and minimum entire effective principal stresses, including the stresses caused by applied load and self-weight, of each element. The method how to calculate the entire stress has been explained in section 6.3. Hence,

$\phi_{d1} = \sin^{-1}(\frac{q_1^{'} + q_s^{'}}{p_1^{'} + p_s^{'} + a})$, where, $q_1^{'} = \frac{\sigma_1^{'} - \sigma_3^{'}}{2}$, $p_1^{'} = \frac{\sigma_1^{'} + \sigma_3^{'}}{2}$, which are the maximum and minimum effective principle stresses caused by applied load P_1, $q_s = \frac{\sigma_{sw}^{'} - \sigma_{sw}^{'}}{2}$,

$p_s = \frac{\sigma_{sw}^{'} + \sigma_{sw}^{'}}{2}$, which are the maximum and minimum effective principle stresses caused by self-weight, in which $a = \frac{c}{\tan\phi}$.

Set $K = \frac{P_L}{P_1}$, P_L is the limit load of structure; K can be looked as the safety factor of the structure. For elastic analysis, $p^{'}$, $q^{'}$ are linear proportional to the applied load, thus $K = \frac{P_L}{P_1} = \frac{p_L^{'}}{p_1^{'}} = \frac{q_L^{'}}{q_1^{'}}$, where, $p_L^{'}$, $q_L^{'}$ are caused by limit load P_L. When $P_1 = P_L$, K equals one and the mobilized friction angle will equal the failure friction angle, namely

$$(\phi_d)_L = \sin^{-1}(\frac{q_L^{'} + q_s^{'}}{p_L^{'} + p_s^{'} + a}) = \phi \tag{6.18}$$

At this time, the failure occurs.

Substitute $p_L^{'} = Kp_1^{'}$ and $q_L^{'} = Kq_1^{'}$ into equation (6.18), we can get

$$\sin^{-1}(\frac{Kq_1^{'} + q_s^{'}}{Kp_1^{'} + Kp_s^{'} + a}) = \phi,$$

so

$$\sin\phi = \frac{Kq_1^{'} + q_s^{'}}{Kp_1^{'} + Kp_s^{'} + a} \tag{6.19}$$

Set $\sin\phi = \alpha$, from equation (6.19), we can derive

$$K = \frac{\alpha(p_1' + a) - q_s'}{q_1' - \alpha p_s'} \tag{6.20}$$

For the new analysis, the other steps are the same as trial one except in the last step equation (6.17) will be used to calculate the limit load of structure.

The parameters used in numerical examples are shown in table 6.1. The results obtained with r-node method and comparison with nonlinear FEA solution and theoretical solution methods are shown in Table 6.4. The theoretical solution is calculated according to the equation (5.1) and tables given by Das (Das, (1999) [68]), and the inelastic FEA solution is calculated by using ABAQUS/Standard. Large deformation analysis is used to calculate the limit load of structure; the input listing for the development of this model and subsequent analysis is given in Appendices 1.3.

The r-node locations and corresponding von Mises stresses for case one are shown in Figure 6.7 and 6.8 as an example to explain how to calculate the limit load based on r-node peak stresses. From Figure 6.5, one distinct r-node peaks is located according to the method explained in equation (6.12); the limit load

$$P_L = KP = 0.321 * 100 = 32.1kPa$$

Figure 6.8 shows the r-node element locations in true FE model.

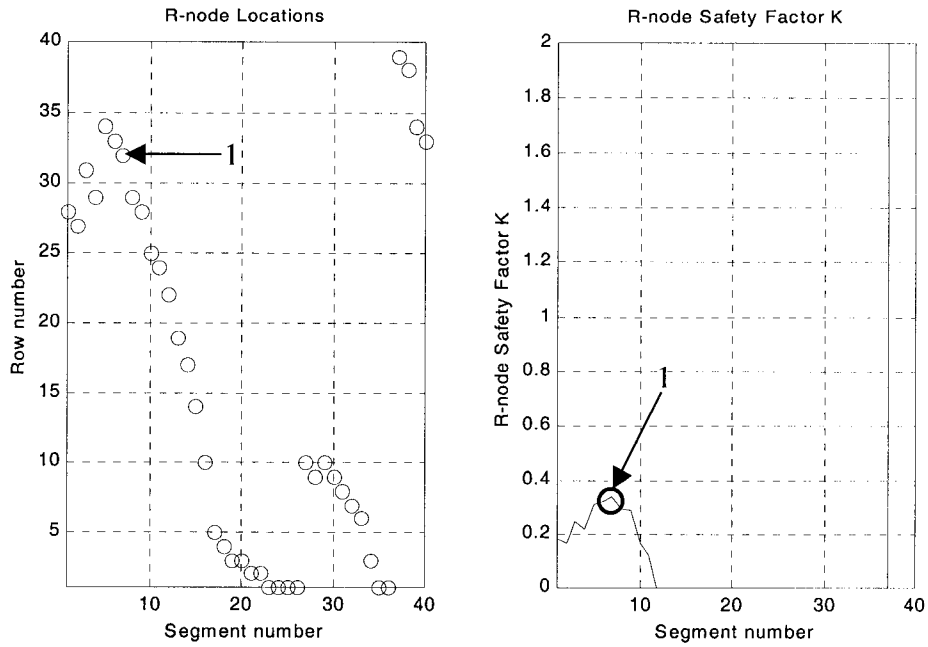

Figure 6.7 R-node Locations and Corresponding von Mises Stresses (case one)

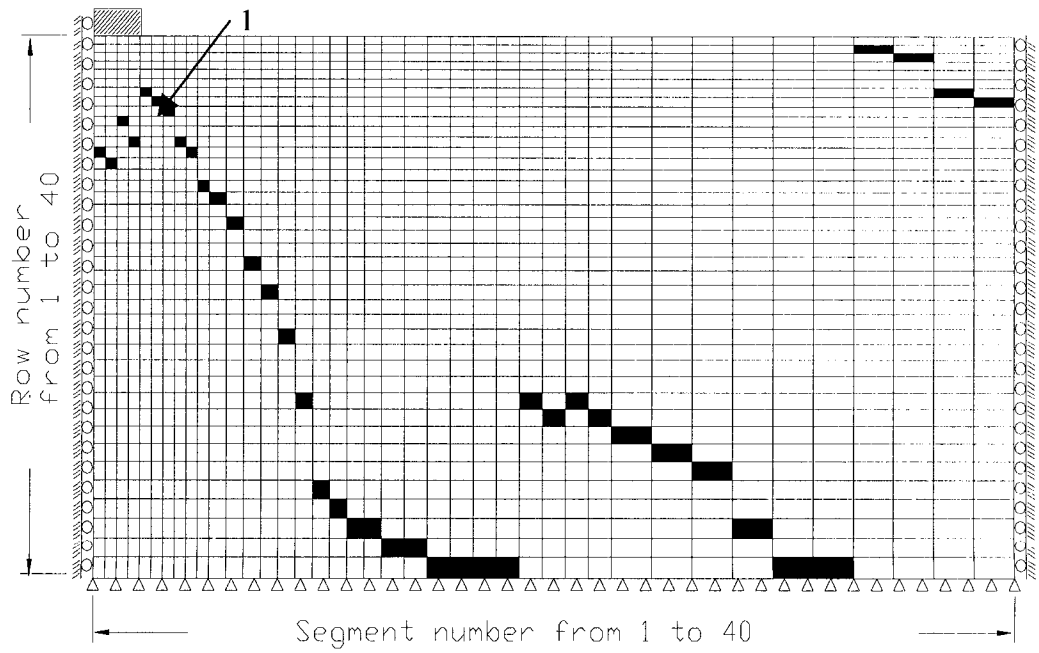

Figure 6.8 R-node Locations in FE Model (case one)

Similarly, the results of other cases are obtained and shown in Table 6.2.

Table 6.4.Results and Comparisons

Limit Load (kPa)			
Case #	R-node	Theoretical Solution	Nonlinear (Mohr-Coulomb)
1	32.1	105.46	111.2
2	73.37	245.32	246.4
3	278.8	439.46	464.6
4	319.8	838.52	853
5	390.4	1910.2	1693.5

6.4.4 Trial Four

For trial four, the shear modulus is used as the quantity to be modified from the first to the second elastic analysis instead of Young's modulus and the stressed induced by self-weight will be deleted when calculating limit loads in last step.

1. Carry the first elastic analysis, then use

$$E_n = (1+\nu_n)\frac{E_0}{1+\nu_o}\frac{\tan\phi}{\tan\phi_d} \tag{6.15a}$$

and

$$\nu_n = \frac{3}{(2+\frac{\tan\phi}{\tan\phi_d}\frac{1-2\nu_0}{1+\nu_0})} - 1 \tag{6.15b}$$

to modify Young's modulus and Possion's ratio of each element.

2. Carry out the second elastic analysis for the same load, mesh (except for a different elastic modulus and Possion's ratio) and obtain $\tan\phi_d$ in each element.

3. Compare $\tan\phi_d$ of each element between the first linear elastic analysis and the second linear elastic analysis. R-nodes are represented by locations where the $\tan\phi_d$ did not change.

4. Use

$$P_L = \frac{\tan\phi}{\sum_{j=1}^{N}(\tan\phi_d)_{nj}\Big/N}P = \frac{c}{\sum_{j=1}^{N}(c_d)_{nj}\Big/N}P \tag{6.13}$$

to find limit load.

The parameters used in numerical examples are shown in table 6.1. The results obtained with r-node method and comparisons with nonlinear FEA solution and theoretical solution methods are shown in Table 6.5. The theoretical solution is calculated according to the equation (5.1) and tables given by Das (Das, (1999) [68]), and the nonlinear FEA solution is calculated by using ABAQUS/Standard. Large deformation analysis is used to calculate the limit load of structure; the input listing for the development of this model and subsequent analysis is given in Appendices 1.3.

Table 6.5 Results and Comparisons

Limit Load (kPa)			
Case #	R-node	Theoretical Solution	Nonlinear (Mohr-Coulomb)
1	41.8	105.46	111.2
2	71.33	245.32	246.4
3	117.84	439.46	464.6
4	150.88	838.52	853
5	159.57	1910.2	1693.5

For the all trials above, the anticipated results have not been obtained. One possible reason is the assumption that the apex of all mobilized stress surfaces coincide with the apex of the yield surface

Chapter Seven

Conclusions and Prospects

Robust approximate methods are often used to estimate limit load of structures due to the conceptual insight, economy of computational effort and wide applicability. Many of these methods have been readily applicable to conventional structures made of homogeneous isotropic materials. The r-node method, which is an approximate method for determining the limit loads of structures, has been presented in detail in this thesis. This method has been applied to the bearing capacity problem in soil mechanics, and the results obtained are found to compare well with analytical results and elastic-plastic finite element analysis results for uniform purely cohesive soils. The bounds for errors compared with elastic-plastic analysis are shown in Table 5.5 and Figure 5.8; it can be seen that for uniform purely cohesive soils, the results of r-node method are in close agreement with the nonlinear FEA solutions.

Relatively close results, but less accurate for some cases, have been obtained for layered purely cohesive soils (less accurate results correspond to small H/B and large c_{u1}/c_{u2} ratios). In most cases with H/B from 0.5 to 2, the bounds of errors are within 12%, but for cases of $H/B=0.5$ and $H/B=0.75$ and large c_{u1}/c_{u2} ($c_{u1}/c_{u2}=4$), the results are less accurate. For smaller H/B ($H/B=0.25$), also the results are less accurate; bounds of errors are large, especially for large c_{u1}/c_{u2} ($c_{u1}/c_{u2}=4$). From the comparisons of results, for layered soils, with the decreasing of the ratio H/B and the

increasing of the ratio c_{u1}/c_{u2}, the results are less and less accurate. The reason for such tendencies consists in difficulty in locating the r-nodes when the upper layer of soil is thin and the degree of inhomogeneity increases. The error bounds of different ratios of H/B and c_{u1}/c_{u2} have been given in Table 5.5 and Figure 5.8. From them, the applicable range of r-node method for layered soils can be determined. Within this range, the results obtained by using r-node method can be thought as approximatly accurate and accepted.

The method has also been extended to analyze the bearing capacity problems of footings on cohesive-frictional soils. Several trials were proved to be unsuccessful. The reasons for these trials and various proposed procedures have been detailed in chapter 6. The procedure for applying r-node method to cohesive-frictional materials has not been solved, more attention should be given to establishing a reasonable relation between mobilized cohesion and mobilized friction angle of cohesive-frictional soils, and correctly estimate the shear strength of each element in the foundation. Also, as seen from the analysis results, the r-nodes of the soil foundation seem to lie along the pressure bulb for cohesive soils; and for cohesive-frictional soils, they seem to lie along the frustum of a cone. Further research toward this assumption may go along the lines of a concept developed by Wolf (Wolf and Deeks (2004) [76]).

Reference

[1] Terzaghi, K., (1943), *Theoretical Soil Mechanics*, Willey, New York.

[2] Meyerhof, G.G., (1951), The Bearing Capacity of Foundations, *Geotechnique*, Vol.2(4), pp.301-332.

[3] Sokolovskii, V.V., (1965), *Static of Granular Media*, Pergamon Press, New York.

[4] Brinch Hansen, J., (1961), A General Formula for Bearing Capacity, *Bull. Dan.Geotech. Inst.*, Vol.11, pp.38-46.

[5] Shield, R.T., (1954), Stress and Velocity Fields in Soil Mechanics, *J. Math. Phys.*, Vol.33(2), pp.144-156.

[6] Chen, W.F. and Davidson, H. L., (1973), Bearing Capacity Determination by Limit Analysis, *J. Soil Mech.Found.Div, ASCE*, Vol.99(SM6) proc. pap, 6742, pp.955-978.

[7] Chen, W. F., (1975), *Limit Analysis and Soil Plasticity*, American Elsevier Scientific Publishing Company Inc, New York.

[8] Mangalaramanan, S. P., (1993), *Robust Limit Loads for Plate Structures*, Master Thesis, University of Regina.

[9] Kraus, Harry., (1980), *Creep Analysis*, John Wiley & Sons Inc, New York.

[10] Soderberg, C. R., (1941), Interpretation of Creep Tests on Tubes, *Trans. ASME*, Vol.63, pp.737-748.

[11] Marriott, D. L., (1970), A Review of Reference Stress Methods for Estimating Creep Deformations, *Second IUTAM Symposium on Creep Of Structures*, Gothenburg.

[12] Anderson, R. G., Gardner, L. R. T. and Hodgkins, W. R., (1963), Deformation of Uniformly Loaded Beams Obeying Complex Creep Laws, *Journal of Mechanical Engineering Science*, Vol.5, pp.238-244.

[13] Mackenize, A. C., (1968), On the Use of a Single Uniaxial Test to Estimate Deformation Rates in Some Structures Undergoing Creep, *International Journal of Mechanical Science*, Vol.10, pp.441.

[14] Sim, R. G., (1971). Evaluation of Reference Stress Parameters for Structures Subject to Creep, *Journal of Mechanical Engineering Science*, Vol.13, pp.47-50.

[15] Johnsson, A., (1974). An Alternative Definition of Reference Stress for Creep. *Int. Conf. On Creep and Fatigue in Elevated Temperature Application*, Institute of Mechanical Engineering, Paper No C205/23.

[16] Sim, R. G., (1968), P.H.D Dissertation, University of Cambridge.

[17] Ponter, A. R. S. and Leckie, F. A., (1970), Application of Energy Theorems to Bodies Which Creep in the Plastic Range. *Journal of Applied Mechanics*, Vol.37, pp.753-758.

[18] Drucker, D. C., (1952), A More Fundamental Approach to Plastic Stress-strain Relations, *1st U.S. Congress of Applied Mechanics, ASME*, New York, pp.487-491.

[19] Martin, J. B., (1966), A Note on the Determination of an Upper Bound on Displacement Rates for Steady Creep Problems, *J. Appl. Mech.,* Vol.33, pp.216-217.

[20] Palmer, A. C., (1967), A Lower Bound on Displacement Rates in Steady Creep, *J.Appl. Mech.*, Vol.34, pp.216-217.

[21] Leckie, F. A., (1974), A Review of Bounding Techniques in Shakedown and Ratcheting at Elevated Temperatures, *Welding Research Council Bulletin*, No.195, pp. 1-32.

[22] Seshadri, R. and Fernando. C P. D., (1991), Limit Loads of Mechanical Components and Structures Based on Linear Elastic Solutions Using GLOSS R-Node Method, *ASME PVP*, Vol.210-2, pp.125-134.

[23] Seshadri, R., (1996), Robust Stress-Classification of Pressure Components Using the GLOSS and GLOSS R-Node Methods, *Journal of Pressure Vessel Technology, Transactions of the ASME*, Vol.118, n2, May 1996, pp.208-215

[24] Marriott, D. L., (1988), Evaluation of Deformation or Load Control of Stresses under Inelastic Conditions Using Elastic Finite Element Stress Analysis, *ASME PVP*, Vol. 136, pp.3-9.

[25] Mangalaramanan, S. P. and R.Seshadri., (1995), Robust Limit Load Determination Based on Extended Variation Principles. *American Society of Mechanical Engineers, Pressure Vessels and Piping Division (Publication) PVP*, Vol.318, pp.353-363.

[26] Seshadri, R., and Mangalaramanan, S.P., (1997), Lower Bound Limit Loads Using Variational Concepts: The $m\alpha$-method, *International Journal of Pressure Vessels and Piping*, Vol.71, pp.93-106.

[27] Mackenzie, D., and Boyle, J.T., (1993), A Method of Estimating Limit Loads by Iterative Elastic Analysis I: Simple Examples, *International Journal of Pressure Vessels and Piping*, Vol.53, pp.77-95.

[28] Nafaraiah, C., Mackenzie, D., Boyle, J. T., (1993a), A Method of Estimating Limit Loads by Iterative Elastic Analysis I: Nozle Sphere Intersections with Internal Pressure and Radial Load, *International Journal of Pressure Vessels and Piping*, 53,pp.97-119.

[29] Shi, Jinhua, Mackenzie, D. and Boyle, J. T., (1993b), A Method of Estimating Limit Loads by Iterative Elastic Analysis I: Torispherical Heads under Internal Pressure, *International Journal of Pressure Vessels and Piping*, 53, pp.121-142.

[30] Ponter, A. R. S., Fuschi, P. and Engelhardt, M., (2000), Limit Analysis for a General Class of Yield Conditions, *European Journal of Mechanics, A/Solids*, (2000), Vol.19, No3, pp.401-422.

[31] Ponter, A. R. S., Chen, H., Boulbibane, M. and Habibullah, M., (2002), The Linear Matching Method for the Evaluation for Limit Loads, Shakedown Limits and Related Problems, *Proceedings of the Fifth World Congress on Computational Mechanics* (WCCM V), July 7-12, 2002.

[32] Parrinello, F. and Ponter, A. R. S., (2001), Shakedown Limit Analysis Based on Linear Elastic Solutions, for a Hydrostatic Pressure Dependent Material", *Proc. 2nd European Conference on Computational Mechanics*, Cracow, June 2001.

[33] Jones, G. L. and Dhalla, A. K., (1981), Classification of Clamp Induced Stresses in Thin Walled Pipe, *Proc. ASME PVP Conf.*, Denver, CO, Vol. 81,pp.17–23.

[34] Seshadri, R. and Prasad, Y. V. S. N., (1996), Lower Bound Limit Loads for Foundations and Slopes Using The R-Node Method, *49th Canadian Geotechnical*

Conference of the Canadian Geotechnical Society. 23-25 September, 1996, St. John's, Newfoundland.

[35] Melan, E., (1938), Zur Plastizitaaet des raeumlichen Kontinuums, *Ingr. -Arch.*, 9,1938, pp.116-126.

[36] Mura, T., Rimawi, W. H. and Lee, S. L., (1965), Extended Theorems of Limit Analysis, *Quarterly of applied mathematics*, Vol. 3, pp.171-179.

[37] Pan, L. and Seshadri, R., (2002), Limit Loads for Layered Structures Using Extended Variational Principles and Repeated Elastic Finite Element Analysis, *Journal of Pressure Vessel Technology*, Vol.124, pp.425-432.

[38] Schulte, C. A., (1960), Interpretation of Creep Tests on Tubes, *Trans. ASME*, Vol.63, pp.737-748.

[39] Marriott, D. L. and Leckie, F. A., (1963-1964), Some Observations on the Deflections of Structures During Creep, *Proc. I. Mech. E.*, Vol.178, Pt. 3l, pp.115-125.

[40] von Mises, R., (1913), Mechanik der festen Koerper in Plasticisch deformablem Zustand, Goettinger Nachr. *Math. Phys.*, Kl., pp.582-592.

[41] Chen, W. F. and Saleeb, A. F., (1982), *Constitutive Equations for Engineering Materials*, Canada, John Wiley & Sons, Inc.

[42] Benham, Crawford and Armstrong, (1996), *Mechanics of Engineering Materials* (second edition), England, Longman Group Limited.

[43] Sokolinikoff, I. S., (1956), *Mathematical Theory of Elasticity*, McGraw-Hill, New York.

[44] Saint-Venant, B., (1870), Memoire sur l'etablissement des equations differentielles des mouvements interieurs operas dans les corps solides ductiles au dela des limites ou l'elasticite pourrait les ramener a leur premier etat, *Compt, Rend*, Vol.70, pp 473-480.

[45] Levy, M., (1870), Memoire sur les equations generales des mouvements interieurs des corps solides ductile au dela limites ou l'elasticite pourrait les ramener a leur premier etat, *Compt. Rend,* Vol.70, pp.1323-1325.

[46] Prandtal, L., (1925), Spannungsverteilung in plastischen Koerpern, Proceedings of the 1st International Congress on Applied Mechanics, Delft, *Technishe Boekhandel en Druckerij*, J. Waltman, Jr., pp.43-54.

[47] Reuss, E., (1930), Beruecksichtigung der elastischen Formaederungen in der Plastizitaetstheorie, Z. Angew. *Math. Mech.*, 10, pp 266-274.

[48] Drucker, D. C., (1950), Some Implications of Work Hardening and Ideal Plasticity, *Quart.Appl.Math.*, Vol.7, pp.411-418.

[49] Hencky, H. Z., (1924), Zur Theorie Plasticher Deformationen und der herdurch im Material hervorgerufenen Nachspannungen, Z. Angew. *Math. Mech.*, Vol.4, pp.323-334.

[50] Budiansky, B., (1959), A Reassessment of Deformation Theories of Plasticity, *J. Appl. Mech.*, Vol.26, pp.259-264.

[51] Chen, W. F. and Zhang, H., (1991), *Structural Plasticity: Theory, Problem, and CAE Software*,Springer-Verlag New York Inc, USA.

[52] Tresca, H., (1868), Memoire sur l'econlement des corps solides, Memoires presentes par divers savants a Academie des Sciences, Vol.18, pp.733-799.

[53] Coulomb, C. A., (1776), Essai sur une application des regles de Maximums et Minimis a quelques Problemes de Statique, relatifs a l'Architecture, Memories de Mathematique et de Physique, Presentes, a l'Academie Royale des Sciences, Paris, Vol.3, pp.38.

[54] Drcuker, D. C., (1953), Limit Analysis and Design, *Appl. Mech., Rev.*, Vol.7, pp.421.

[55] William, B. Bickford, (1990 & 1994), *A First course in the Finite Element Method*, Richard D. Irwin, Inc., USA.

[56] Prandtl, L., (1921), Hauptaufsatze Uber die Eindringungsfestigkeit (Harte) plastischer Baustoffe und die Festigkeit von Schneiden, Zeitschrift fur Angewandte, Mathematik und Mechanik, Vol.1, No.1, pp.15-20.

[57] Hencky, H., (1923), Uber einige statisch bestimmte Falle des Gleichgewichts in plastichen Korpern, Zeitschrift fur Angewandte, Mathematik und Mechanik, Vol.3, No. 4, pp.241-251.

[58] Tien-Hsing, Wu., (1976), *Soil Mechanics*, Allyn and Bacon Inc, USA.

[59] Jumikis, A. R., (1965), *Soil Mechanics*, D. Van Nostrand Company Inc, New York

[60] Braja M. Das., (1985), *Principles of Geotechnical Engineering*, PWS Publishers, Boston.

[61] Skempton, A. W., (1951), The Bearing Capacity of Clays, Proc. 3^{rd} *Intern. Conf. Soil Mech. Found. Eng.*, Vol.1, pp.57.

[62] Merifield, R. S., Sloan, S. W. and Yu, H. S., (1999), Rigorous Plasticity Solutions for the Bearing Capacity of Two-Layered Clays, *Geotechnique*, Vol.49, No.4, pp.471-490.

[63] Button, S. J. (1953). The Bearing Capacity of Footings on a Two-layer Cohesive Subsoil. *Proc. 3rd Int. Conf. Soil Mech. Found. Engng*, Zurich 1, pp.332-335.

[64] Reddy, A. S. and Srinivasan, R. J., (1967), Bearing Capacity of Footings on Layered Clays. *J. Soil Mech. Found. Div., ASCE 93*, SM2, pp.83-99.

[65] Brown, J. D. and Meyerhof, G. G., (1969), Experimental study of bearing capacity in layered clays, *Proc., 7th Int. Conf. on Soil Mechanics and Foundation Engineering*, Mexico, Vol. 2, pp. 45-51.

[66] Meyerhof, G. G. and Hanna, A. M., (1978), Ultimate Bearing Capacity of Foundations on Layered Soils under Inclined Load. *Can. Geotech.* J.15, pp.565-572.

[67] Fethi.Azizi, (1999), *Applied Analysis in Geotechnics*, E & FN Spon, New York.

[68] Braja, M. Das, (1999), *Principles of Geotechnical Engineering*, PWS Publishers, Boston.

[69] Hibbitt, Karlsson & Sorensen, Inc. (1998a), *ABAQUS/Standard User's Manual; Version 5.8 (Vols. I-III)*. Rhode Island: Author.

[70] Nobahar, Arash, (2003), *Effects of Soil Spatial Variability on Soil-Structure Interaction*, P.H.D Thesis, Memorial University of Newfoundland, St John's, Newfoundland.

[71] Braja M. Das, (1997), *Advanced Soil Mechanics*, Taylor & Francis, USA.

[72] Mohr, O., (1900), Welche Umstande Bendingen die Elastizitatsgrenze und den Brucheines Materials, *Zeitschrift des Vereines Deutscher Ingenieure*, Vol.44, pp.1524-1530, 1572-1577.

[73] Prevost, Jean H., (1989), A Computer Program for Nonlinear Seismic Site Response Analysis Technical Documentation, *Technical Report NCEER-89-0025*, Princeton University, New Jersey.

[74] Seshadri, R. and Fernando, C P. D., (1992), Limit Loads of Mechanical Components and Structures Based on Linear Elastic Solutions Using GLOSS R-Node Method, *Journal of Pressure Vessel Technology*, Vol.114, pp.201-208.

[75] David M, Potts and Lidija, Zdravkovi, (1999-2001), *Finite Element Analysis in Geotechnical Engineering*, Thomas Telford, London.

[76] J.P. Wolf and A.J.Deeks, (2004), *Foundation Vibration Analysis: A Strength of Materials Approach*, Elsevier Science & Technology, U.S.A.

[77] S.M.R. Adluri, (2000), Direct Estimation of Limit Loads Using Secant Rigidity and Scaled Yield Criteria, *Proc. Canadian Conf. On Applied Mechanics -CANCAM*, St. John's, NL

[78] A.A. Bolar and S.M.R. Adluri, (2000), Limit Loads of Plates Estimated Using Secant Rigidity, *Proc. Canadian Conf. On Applied Mechanics -CANCAM*, St. John's, NL

Appendices

ABAQUS Finite Element Input Files

1 Nonlinear Analysis

1.1 Input Files for Uniform Cohesive Soils

1.1a Input File for Uniform Cohesive Soils (Width of Foundation B=2m)

*HEADING

****

**Bearing capacity of strip foundation on uniform cohesive soil*

**Element type: CPE4R; Cohesion=10kPa; Friction angle=0^o; Self-weight γ=0*

**Elastic modulus=20MPa; Possions' ratio=0.499; Area=40m*20m*

**Von Mises yield criterion*

****

** NODES DEFINING

****

**All dimension in meter and stress is kPa*

*NODE, NSET=NA1

1001,0,0

1011,5,0

1021,12.5,0

1031,22.5,0

1041,40,0

5001,0,20

5011,5,20

5021,12.5,20

5031,22.5,20

5041,40,20

**Define the analysis domain*

*NGEN, NSET=NBOT

1001,1011,1

1011,1021,1

1021,1031,1

1031,1041,1

*NGEN, NSET=NTOP

5001,5011,1

5011,5021,1

5021,5031,1

5031,5041,1

*NFILL, BIAS=1.025, NSET=NSOIL

NBOT, NTOP,40,100

*NSET, NSET=NSIDE, GENERATE

1001,5001,100

1041,5041,100

*NSET, NSET=F1

5001,

*NSET, NSET=F2, GENERATE

5002,5005

**Mesh the model*

****

** SOIL ELEMENT DEFINING

****

*ELEMENT, TYPE=CPE4R, ELSET=ELSOIL

1001,1001,1002,1102,1101

*ELGEN, ELSET=ELSOIL

1001,40,1,1,40,100,100

*SOLID SECTION, ELSET=ELSOIL, MATERIAL=MSOIL

*MATERIAL, NAME=MSOIL

*ELASTIC

20E3,0.499

**Young's modulus and Possions' ratio*

*PLASTIC

17.32

**Yield stress*

*ELSET, ELSET=ELST, GENERATE

4901,4940

*ELSET, ELSET=ELOAD, GENERATE

4901,4904,1

**Define the area of loading*

****

*RESTART, WRITE, FREQUENCY=1

*EQUATION

2

F2,2,1.0,5001,2,-1

*BOUNDARY

NBOT, ENCASTRE

NSIDE,1,1

F2,1

**Boundary condition*

*STEP, INC=1000, UNSYMM=YES

*STATIC

0.001,1,,0.005

*CONTROLS, ANALYSIS=DISCONTINUOUS

*CONTROLS, PARAMETERS=LINE SEARCH

20

**Analysis control*

*BOUNDARY

5001,2,2,-1

**Apply displacement, large deformation analysis*

*EL PRINT, FREQUENCY =0

*NODE PRINT, NSET=F1, FREQUENCY=1, SUMMARY=NO, TOTAL=YES

U2,RF2

*NODE PRINT, FREQUENCY=0

*END STEP

**Output the results*

****

**The input file 1.1 also can be used for nonlinear analyses of bearing capacity of strip*

**foundation on uniform cohesive soil with different elastic modulus, cohesion.*

****

1.1b Input File for Uniform Cohesive Soils (Width of Foundation B=3m)

*HEADING

****

**Bearing capacity of strip foundation on uniform cohesive soil*

**Element type: CPE4R; Cohesion=10kPa; Friction angle=0^o; Self-weight γ=0*

**Elastic modulus=20MPa; Possions' ratio=0.499; Area=40m*20m*

**Von Mises yield criterion*

****

** NODES DEFINING

****

*******All dimension in meter and stress is kPa*

*NODE, NSET=NA1

1001,0,0

1011,7.5,0

1021,18.75,0

1031,33.75,0

1041,60,0

5001,0,30

5011,7.5,30

5021,18.75,30

5031,33.75,30

5041,60,30

*NGEN, NSET=NBOT

1001,1011,1

1011,1021,1

1021,1031,1

1031,1041,1

*NGEN, NSET=NTOP

5001,5011,1

5011,5021,1

5021,5031,1

5031,5041,1

*NFILL, BIAS=1.025, NSET=NSOIL

NBOT, NTOP,40,100

*NSET, NSET=NSIDE, GENERATE

1001,5001,100

1041,5041,100

*NSET, NSET=F1

5001,

*NSET, NSET=F2, GENERATE

```
5002,5005
**********************************
** SOIL ELEMENT DEFINING
**********************************
*ELEMENT, TYPE=CPE4R, ELSET=ELSOIL
1001,1001,1002,1102,1101
*ELGEN, ELSET=ELSOIL
1001,40,1,1,40,100,100
*SOLID SECTION, ELSET=ELSOIL, MATERIAL=MSOIL
*MATERIAL, NAME=MSOIL
*ELASTIC
20E3,0.499
PLASTIC
17.32
*ELSET, ELSET=ELST, GENERATE
4901,4940
*ELSET, ELSET=ELOAD, GENERATE
4901,4904,1
**********************************************************
*RESTART, WRITE, FREQUENCY=1
*EQUATION
2
F2,2,1.0,5001,2,-1
```

*BOUNDARY

NBOT, ENCASTRE

NSIDE,1,1

F2,1

*STEP, INC=1000, UNSYMM=YES

*STATIC

0.001,1,,0.005

*CONTROLS, ANALYSIS=DISCONTINUOUS

*CONTROLS, PARAMETERS=LINE SEARCH

20

*BOUNDARY

5001,2,2,-1

*EL PRINT, FREQUENCY=0

*NODE PRINT, NSET=F1, FREQUENCY=1,SUMMARY=NO, TOTAL=YES

U2, RF2

*NODE PRINT, FREQUENCY=0

*END STEP

****

**The input file 1.1b also can be used for nonlinear analyses of bearing capacity of strip*

**foundation on uniform cohesive soil with different elastic modulus, cohesion.*

****

1.2 Input Files for Layered Cohesive Soils

1.2a Input File for Layered Cohesive Soils (H/B=1.5)

*HEADING

****

**Bearing capacity of strip foundation on layered cohesive soil*

**Element type: CPE4R; Cohesion: $cu_1/cu_2=2$; $cu_1=20kPa$; $cu_2=10kPa$.*

**Friction angle=0^o; Self-weight $\gamma_1= \gamma_2= 0$*

**Elastic modulus: $E_1=40MPa$, $E_2=20MPa$; Possions' ratio=0.499.*

**Area=40m*20m*

**von Mises yield criterion*

****

** NODES DEFINING

****

*******All dimension in meter and stress is kPa*

*NODE, NSET=NA1

1001,0,0

1011,5,0

1021,12.5,0

1031,22.5,0

1041,40,0

3201,0,14

3211,5,14

3221,12.5,14

3231,22.5,14

3241,40,14

5001,0,20

5011,5,20

5021,12.5,20

5031,22.5,20

5041,40,20

*NGEN, NSET=NBOT

1001,1011,1

1011,1021,1

1021,1031,1

1031,1041,1

*NGEN, NSET=NMID

3201,3211,1

3211,3221,1

3221,3231,1

3231,3241,1

*NGEN, NSET=NTOP

5001,5011,1

5011,5021,1

5021,5031,1

5031,5041,1

*NFILL, BIAS=1.00, NSET=NSOIL

NBOT, NMID,22,100

*NFILL, BIAS=1.00, NSET=NSOIL

NMID, NTOP,18,100

*NSET, NSET=NSIDE, GENERATE

1001,3201,100

3201,5001,100

1041,3241,100

3241,5041,100

*NSET, NSET=F1

5001,

*NSET, NSET=F2, GENERATE

5002,5005

****

** SOIL ELEMENT DEFINING

****

*ELEMENT, TYPE=CPE4R, ELSET=ELSOIL

1001,1001,1002,1102,1101

*ELGEN, ELSET=ELSOIL

1001,40,1,1,22,100,100

*ELEMENT, TYPE=CPE4R, ELSET=ELSOIL1

3201,3201,3202,3302,3301

*ELGEN, ELSET=ELSOIL1

3201,40,1,1,18,100,100

*ELSET, ELSET=ELST, GENERATE

4901,4940

*SOLID SECTION, ELSET=ELSOIL, MATERIAL=MSOIL

*MATERIAL, NAME=MSOIL

*ELASTIC

20.0E3,0.499

*PLASTIC

17.32

*SOLID SECTION, ELSET=ELSOIL1, MATERIAL=MSOIL1

*MATERIAL, NAME=MSOIL1

*ELASTIC

40.0E3,0.499

*PLASTIC

34.641

*ELSET, ELSET=ELOAD, GENERATE

4901,4904,1

****

*RESTART, WRITE, FREQUENCY=1

*EQUATION

2

F2,2,1.0,5001,2,-1

*BOUNDARY

NBOT, ENCASTRE

NSIDE,1,1

F2,1

*STEP, INC=1000, UNSYMM=YES

*STATIC

0.001,1,,0.005

*CONTROLS, ANALYSIS=DISCONTINUOUS

*CONTROLS, PARAMETERS=LINE SEARCH

20

*BOUNDARY

5001,2,2,-1

*EL PRINT, FREQUENCY=0

*NODE PRINT, NSET=F1, FREQUENCY=1, SUMMARY=NO, TOTAL=YES

U2, RF2

*NODE PRINT, FREQUENCY=0

*END STEP

****

**The input file 1.2a also can be used for nonlinear analyses of bearing capacity of strip*

**foundation on layered cohesive soil with same H/B and different cu_1/cu_2.*

****

1.2b Input File for Layered Cohesive Soils (H/B=1)

*HEADING

****

**Bearing capacity of strip foundation on layered cohesive soil*

**Element type: CPE4R; Cohesion: $cu_1/cu_2=2$; $cu_1=20kPa$; $cu_2=10kPa$.*

**Friction angle=$0^{o;}$ Self-weight $\gamma_1= \gamma_2= 0$*

***Elastic modulus: E_1=40MPa, E_2=20MPa; Possions' ratio=0.499.*

***Area=40m*20m*

***von Mises yield criterion*

****

** NODES DEFINING

****

*******All dimension in meter and stress is kPa*

*NODE, NSET=NA1

1001,0,0

1011,5,0

1021,12.5,0

1031,22.5,0

1041,40,0

3801,0,16

3811,5,16

3821,12.5,16

3831,22.5,16

3841,40,16

5001,0,20

5011,5,20

5021,12.5,20

5031,22.5,20

5041,40,20

```
*NGEN, NSET=NBOT
1001,1011,1
1011,1021,1
1021,1031,1
1031,1041,1
*NGEN, NSET=NMID
3801,3811,1
3811,3821,1
3821,3831,1
3831,3841,1
*NGEN, NSET=NTOP
5001,5011,1
5011,5021,1
5021,5031,1
5031,5041,1
*NFILL, BIAS=1.00, NSET=NSOIL
NBOT, NMID,28,100
*NFILL, BIAS=1.00, NSET=NSOIL
NMID, NTOP,12,100
*NSET, NSET=NSIDE, GENERATE
1001,3801,100
3801,5001,100
1041,3841,100
```

3841,5041,100

*NSET, NSET=F1

5001,

*NSET, NSET=F2, GENERATE

5002,5005

****

** SOIL ELEMENT DEFINING

****

*ELEMENT, TYPE=CPE4R, ELSET=ELSOIL

1001,1001,1002,1102,1101

*ELGEN, ELSET=ELSOIL

1001,40,1,1,28,100,100

*ELEMENT, TYPE=CPE4R, ELSET=ELSOIL1

3801,3801,3802,3902,3901

*ELGEN, ELSET=ELSOIL1

3801,40,1,1,12,100,100

*ELSET, ELSET=ELST, GENERATE

4901,4940

*SOLID SECTION, ELSET=ELSOIL, MATERIAL=MSOIL

*MATERIAL, NAME=MSOIL

*ELASTIC

20.0E3,0.499

*PLASTIC

```
17.32
*SOLID SECTION, ELSET=ELSOIL1, MATERIAL=MSOIL1
*MATERIAL, NAME=MSOIL1
*ELASTIC
40.0E3,0.499
*PLASTIC
34.641
*ELSET, ELSET=ELOAD, GENERATE
4901,4904,1
**********************************************************
*RESTART, WRITE, FREQUENCY=1
*EQUATION
2
F2,2,1.0,5001,2,-1
*BOUNDARY
NBOT, ENCASTRE
NSIDE,1,1
F2,1
*STEP, INC=1000, UNSYMM=YES
*STATIC
0.001,1,,0.005
*CONTROLS, ANALYSIS=DISCONTINUOUS
*CONTROLS, PARAMETERS=LINE SEARCH
```

20

*BOUNDARY

5001,2,2,-1

*EL PRINT, FREQUENCY=0

*NODE PRINT, NSET=F1, FREQUENCY=1,SUMMARY=NO, TOTAL=YES

U2, RF2

*NODE PRINT, FREQUENCY=0

*END STEP

****

**The input file 1.2b also can be used for nonlinear analyses of bearing capacity of strip*

**foundation on layered cohesive soil with same H/B and different cu_1/cu_2.*

****

1.2c Input File for Layered Cohesive Soils (H/B=0.75)

*HEADING

****

**Bearing capacity of strip foundation on layered cohesive soil*

**Element type: CPE4R; Cohesion: cu_1/cu_2=2; cu_1=20kPa; cu_2=10kPa.*

**Friction angle=0^o; Self-weight γ_1= 0, γ_2= 0*

**Elastic modulus: E_1=40MPa, E_2=20MPa; Possions' ratio=0.499.*

**Area=40m*20m*

**von Mises yield criterion*

****

** NODES DEFINING

****

*******All dimension in meter and stress is kPa*

*NODE, NSET=NA1

1001,0,0

1011,5,0

1021,12.5,0

1031,22.5,0

1041,40,0

4101,0,17

4111,5,17

4121,12.5,17

4131,22.5,17

4141,40,17

5001,0,20

5011,5,20

5021,12.5,20

5031,22.5,20

5041,40,20

*NGEN, NSET=NBOT

1001,1011,1

1011,1021,1

1021,1031,1

1031,1041,1

```
*NGEN, NSET=NMID
4101,4111,1
4111,4121,1
4121,4131,1
4131,4141,1
*NGEN, NSET=NTOP
5001,5011,1
5011,5021,1
5021,5031,1
5031,5041,1
*NFILL, BIAS=1.00, NSET=NSOIL
NBOT, NMID,31,100
*NFILL, BIAS=1.00, NSET=NSOIL
NMID, NTOP,9,100
*NSET, NSET=NSIDE, GENERATE
1001,4101,100
4101,5001,100
1041,4141,100
4141,5041,100
*NSET, NSET=F1
5001,
*NSET, NSET=F2, GENERATE
5002,5005
```

```
**********************************
** SOIL ELEMENT DEFINING
**********************************
*ELEMENT, TYPE=CPE4R, ELSET=ELSOIL
1001,1001,1002,1102,1101
*ELGEN, ELSET=ELSOIL
1001,40,1,1,31,100,100
*ELEMENT, TYPE=CPE4R, ELSET=ELSOIL1
4101,4101,4102,4202,4201
*ELGEN, ELSET=ELSOIL1
4101,40,1,1,9,100,100
*ELSET, ELSET=ELST, GENERATE
4901,4940
*SOLID SECTION, ELSET=ELSOIL, MATERIAL=MSOIL
*MATERIAL, NAME=MSOIL
*ELASTIC
20.0E3,0.499
*PLASTIC
17.32
*SOLID SECTION, ELSET=ELSOIL1, MATERIAL=MSOIL1
*MATERIAL, NAME=MSOIL1
*ELASTIC
40.0E3,0.499
```

```
*PLASTIC
34.641
*ELSET, ELSET=ELOAD,GENERATE
4901,4904,1
**********************************************************
*RESTART, WRITE, FREQUENCY=1
*EQUATION
2
F2,2,1.0,5001,2,-1
*BOUNDARY
NBOT, ENCASTRE
NSIDE,1,1
F2,1
*STEP, INC=1000, UNSYMM=YES
*STATIC
0.001,1,,0.005
*CONTROLS, ANALYSIS=DISCONTINUOUS
*CONTROLS, PARAMETERS=LINE SEARCH
20
*BOUNDARY
5001,2,2,-1
*EL PRINT, FREQUENCY=0
*NODE PRINT, NSET=F1, FREQUENCY=1, SUMMARY=NO, TOTAL=YES
```

U2, RF2

*NODE PRINT, FREQUENCY=0

*END STEP

****

**The input file 1.2c also can be used for nonlinear analyses of bearing capacity of strip*

**foundation on layered cohesive soil with same H/B and different cu_1/cu_2.*

****

1.2d Input File for Layered Cohesive Soils (H/B=0.5)

*HEADING

****

**Bearing capacity of strip foundation on layered cohesive soil*

**Element type: CPE4R; Cohesion: $cu_1/cu_2=2$; $cu_1=20kPa$; $cu_2=10kPa$.*

**Friction angle=0^o; Self-weight $\gamma_1= \gamma_2= 0$*

**Elastic modulus: $E_1=40MPa$, $E_2=20MPa$; Possions' ratio=0.499.*

**Area=40m*20m*

**von Mises yield criterion*

****

** NODES DEFINING

****

*******All dimension in meter and stress is kPa*

*NODE, NSET=NA1

1001,0,0

1011,5,0

1021,12.5,0

1031,22.5,0

1041,40,0

4401,0,18

4411,5,18

4421,12.5,18

4431,22.5,18

4441,40,18

5001,0,20

5011,5,20

5021,12.5,20

5031,22.5,20

5041,40,20

*NGEN, NSET=NBOT

1001,1011,1

1011,1021,1

1021,1031,1

1031,1041,1

*NGEN, NSET=NMID

4401,4411,1

4411,4421,1

4421,4431,1

4431,4441,1

```
*NGEN, NSET=NTOP
5001,5011,1
5011,5021,1
5021,5031,1
5031,5041,1
*NFILL, BIAS=1.00, NSET=NSOIL
NBOT, NMID,34,100
*NFILL, BIAS=1.00, NSET=NSOIL
NMID, NTOP,6,100
*NSET, NSET=NSIDE, GENERATE
1001,4401,100
4401,5001,100
1041,4441,100
4441,5041,100
*NSET, NSET=F1
5001,
*NSET, NSET=F2, GENERATE
5002,5005
**********************************
** SOIL ELEMENT DEFINING
**********************************
*ELEMENT, TYPE=CPE4R, ELSET=ELSOIL
1001,1001,1002,1102,1101
```

```
*ELGEN, ELSET=ELSOIL

1001,40,1,1,34,100,100

*ELEMENT, TYPE=CPE4R, ELSET=ELSOIL1

4401,4401,4402,4502,4501

*ELGEN, ELSET=ELSOIL1

4401,40,1,1,6,100,100

*ELSET, ELSET=ELST, GENERATE

4901,4940

*SOLID SECTION, ELSET=ELSOIL, MATERIAL=MSOIL

*MATERIAL, NAME=MSOIL

*ELASTIC

20.0E3,0.499

*PLASTIC

17.32

*SOLID SECTION, ELSET=ELSOIL1, MATERIAL=MSOIL1

*MATERIAL, NAME=MSOIL1

*ELASTIC

40.0E3,0.499

*PLASTIC

34.641

*ELSET, ELSET=ELOAD, GENERATE

4901,4904,1

**********
```

```
*RESTART, WRITE, FREQUENCY=1
*EQUATION
2
F2,2,1.0,5001,2,-1
*BOUNDARY
NBOT, ENCASTRE
NSIDE,1,1
F2,1
*STEP, INC=1000, UNSYMM=YES
*STATIC
0.001,1,,0.005
*CONTROLS, ANALYSIS=DISCONTINUOUS
*CONTROLS, PARAMETERS=LINE SEARCH
20
*BOUNDARY
5001,2,2,-1
*EL PRINT, FREQUENCY=0
*NODE PRINT, NSET=F1, FREQUENCY=1, SUMMARY=NO, TOTAL=YES
U2, RF2
*NODE PRINT, FREQUENCY=0
*END STEP
**********************************
```

***The input file 1.2d also can be used for nonlinear analyses of bearing capacity of strip*

***foundation on layered cohesive soil with same H/B and different cu_1/cu_2.*

****

1.2e Input File for Layered Cohesive Soils (H/B=0.25)

*HEADING

****

***Bearing capacity of strip foundation on layered cohesive soil*

***Element type: CPE4R; Cohesion: cu_1/cu_2=2; cu_1=20kPa; cu_2=10kPa.*

***Friction angle=0°; Self-weight γ_1= γ_2= 0*

***Elastic modulus: E_1=40MPa, E_1=20MPa; Possions' ratio=0.499.*

***Area=40m*20m*

***von Mises yield criterion*

****

** NODES DEFINING

****

*****All dimension in meter and stress is kPa*

*NODE, NSET=NA1

1001,0,0

1011,5,0

1021,12.5,0

1031,22.5,0

1041,40,0

4701,0,19

4711,5,19

4721,12.5,19

4731,22.5,19

4741,40,19

5001,0,20

5011,5,20

5021,12.5,20

5031,22.5,20

5041,40,20

*NGEN, NSET=NBOT

1001,1011,1

1011,1021,1

1021,1031,1

1031,1041,1

*NGEN, NSET=NMID

4701,4711,1

4711,4721,1

4721,4731,1

4731,4741,1

*NGEN, NSET=NTOP

5001,5011,1

5011,5021,1

5021,5031,1

5031,5041,1

*NFILL, BIAS=1.00, NSET=NSOIL

NBOT, NMID,37,100

*NFILL, BIAS=1.00, NSET=NSOIL

NMID, NTOP,3,100

*NSET, NSET=NSIDE, GENERATE

1001,4701,100

4701,5001,100

1041,4741,100

4741,5041,100

*NSET, NSET=F1

5001,

*NSET, NSET=F2, GENERATE

5002,5005

****

** SOIL ELEMENT DEFINING

****

*ELEMENT, TYPE=CPE4R, ELSET=ELSOIL

1001,1001,1002,1102,1101

*ELGEN, ELSET=ELSOIL

1001,40,1,1,37,100,100

*ELEMENT, TYPE=CPE4R, ELSET=ELSOIL1

4701,4701,4702,4802,4801

```
*ELGEN, ELSET=ELSOIL1

4701,40,1,1,3,100,100

*ELSET, ELSET=ELST, GENERATE

4901,4940

*SOLID SECTION, ELSET=ELSOIL, MATERIAL=MSOIL

*MATERIAL, NAME=MSOIL

*ELASTIC

20.0E3,0.499

*PLASTIC

17.32

*SOLID SECTION, ELSET=ELSOIL1, MATERIAL=MSOIL1

*MATERIAL, NAME=MSOIL1

*ELASTIC

40.0E3,0.499

*PLASTIC

34.641

*ELSET, ELSET=ELOAD, GENERATE

4901,4904,1

**********************************************************

*RESTART, WRITE, FREQUENCY=1

*EQUATION

2

F2,2,1.0,5001,2,-1
```

*BOUNDARY

NBOT, ENCASTRE

NSIDE,1,1

F2,1

*STEP, INC=1000, UNSYMM=YES

*STATIC

0.001,1,,0.005

*CONTROLS, ANALYSIS=DISCONTINUOUS

*CONTROLS, PARAMETERS=LINE SEARCH

20

*BOUNDARY

5001,2,2,-1

*EL PRINT, FREQUENCY=0

*NODE PRINT, NSET=F1, FREQUENCY=1, SUMMARY=NO, TOTAL=YES

U2, RF2

*NODE PRINT, FREQUENCY=0

*END STEP

****

**The input file 1.2e also can be used for nonlinear analyses of bearing capacity of strip*

**foundation on layered cohesive soil with same H/B and different cu_1/cu_2.*

****

1.3 Input Files for Cohesive-Frictional Soils

1.3a Input File for Cohesive-Frictional Soil (c=10kPa, ø=10^0)

*HEADING

****

**Bearing capacity of strip foundation on uniform cohesive-frictional soil*

**Element type: CPE4R; Cohesion=10kPa; Friction angle=10^o;*

**Effective self-weight γ'= 9KN/m^3*

**Elastic modulus=20MPa; Possions' ratio=0.3, Area=40m*20m*

**Mohr-Coulomb yield criterion*

****

** NODES DEFINING

****

*******All dimension in meter and stress is kPa*

*NODE, NSET=NA1

1001,0,0

1011,5,0

1021,12.5,0

1031,22.5,0

1041,40,0

5001,0,20

5011,5,20

5021,12.5,20

5031,22.5,20

5041,40,20

*NGEN, NSET=NBOT

1001,1011,1

1011,1021,1

1021,1031,1

1031,1041,1

*NGEN, NSET=NTOP

5001,5011,1

5011,5021,1

5021,5031,1

5031,5041,1

*NFILL, BIAS=1.025, NSET=NSOIL

NBOT, NTOP,40,100

*NSET, NSET=NSIDE, GENERATE

1001,5001,100

1041,5041,100

*NSET, NSET=F1

5001,

*NSET, NSET=F2, GENERATE

5002,5005

****

** SOIL ELEMENT DEFINING

****

*ELEMENT, TYPE=CPE4R, ELSET=ELSOIL

1001,1001,1002,1102,1101

```
*ELGEN, ELSET=ELSOIL
1001,40,1,1,40,100,100
*ELSET, ELSET=ELST, GENERATE
4901,4940
*SOLID SECTION, ELSET=ELSOIL, MATERIAL=MSOIL
*MATERIAL, NAME=MSOIL
*ELASTIC
20.0E3,0.3
*MOHR COULOMB
10.0,0.0
*MOHR COULOMB HARDENING
10.0
**********************************************************
*RESTART, WRITE, FREQUENCY=1
*EQUATION
2
F2,2,1.0,5001,2,-1
*BOUNDARY
NBOT, ENCASTRE
NSIDE,1,1
F2,1
*STEP
*GEOSTATIC
```

*DLOAD

ELSOIL, BY,-9

*END STEP

*STEP, INC=5000, UNSYMM=YES, AMPLITUDE=RAMP

*STATIC

0.001,1,,0.005

*CONTROLS, ANALYSIS=DISCONTINUOUS

*CONTROLS, PARAMETERS=LINE SEARCH

20

*BOUNDARY

5001,2,2,-1

*EL PRINT, FREQUENCY=0

*NODE PRINT, NSET=F1, FREQUENCY=1, SUMMARY=NO, TOTAL=YES

U2, RF2

*NODE PRINT, FREQUENCY=0

*END STEP

1.3b Input File for Cohesive-Frictional Soil (c=10kPa, ø=20^o)

*HEADING

****

**Bearing capacity of strip foundation on uniform cohesive-frictional soil*

**Element type: CPE4R; Cohesion=10kPa; Friction angle=20^o;*

**Effective self-weight γ'= 9KN/m^3*

**Elastic modulus=20MPa; Possions' ratio=0.3; Area=40m*20m*

**Mohr-Coulomb yield criterion*

****

** NODES DEFINING

****

*******All dimension in meter and stress is kPa*

*NODE, NSET=NA1

1001,0,0

1011,5,0

1021,12.5,0

1031,22.5,0

1041,40,0

5001,0,20

5011,5,20

5021,12.5,20

5031,22.5,20

5041,40,20

*NGEN, NSET=NBOT

1001,1011,1

1011,1021,1

1021,1031,1

1031,1041,1

*NGEN, NSET=NTOP

5001,5011,1

5011,5021,1

5021,5031,1

5031,5041,1

*NFILL, BIAS=1.025, NSET=NSOIL

NBOT, NTOP,40,100

*NSET, NSET=NSIDE, GENERATE

1001,5001,100

1041,5041,100

*NSET, NSET=F1

5001,

*NSET, NSET=F2, GENERATE

5002,5005

****

** SOIL ELEMENT DEFINING

****

*ELEMENT, TYPE=CPE4R, ELSET=ELSOIL

1001,1001,1002,1102,1101

*ELGEN, ELSET=ELSOIL

1001,40,1,1,40,100,100

*ELSET, ELSET=ELST, GENERATE

4901,4940

*SOLID SECTION, ELSET=ELSOIL, MATERIAL=MSOIL

*MATERIAL, NAME=MSOIL

```
*ELASTIC
20.0E3, 0.3
*MOHR COULOMB
20.0,  0.0
*MOHR COULOMB HARDENING
10.0
**********************************************************
*RESTART, WRITE, FREQUENCY=1
*EQUATION
2
F2,2,1.0,5001,2,-1
*BOUNDARY
NBOT, ENCASTRE
NSIDE,1,1
F2,1
*STEP
*GEOSTATIC
*DLOAD
ElSOIL, BY,-9
*END STEP
*STEP, INC=5000,UNSYMM=YES, amplitude=ramp
*STATIC
0.0001,1,1e-10,0.005
```

*CONTROLS,ANALYSIS=DISCONTINUOUS

*CONTROLS, PARAMETERS=LINE SEARCH

20

*BOUNDARY

5001,2,2,-1

*EL PRINT, FREQUENCY=0

*NODE PRINT, NSET=F1, FREQUENCY=1, SUMMARY=NO, TOTAL=YES

U2, RF2

*NODE PRINT, FREQUENCY=0

*END STEP

1.3c Input Files for Cohesive–Frictional Soil (c=50kPa, ø=10^{o})

*HEADING

****

**Bearing capacity of strip foundation on uniform cohesive-frictional soil*

**Element type: CPE4R; Cohesion=50kPa; Friction angle=10^{o}*

**Effective self-weight γ'= 9KN/m^{3}*

**Elastic modulus=100MPa; Possions' ratio=0.3; Area=40m*20m*

**Mohr-Coulomb yield criterion*

****

** NODES DEFINING

****

********All dimension in meter and stress is kPa*

*NODE, NSET=NA1

1001,0,0

1011,5,0

1021,12.5,0

1031,22.5,0

1041,40,0

5001,0,20

5011,5,20

5021,12.5,20

5031,22.5,20

5041,40,20

*NGEN, NSET=NBOT

1001,1011,1

1011,1021,1

1021,1031,1

1031,1041,1

*NGEN, NSET=NTOP

5001,5011,1

5011,5021,1

5021,5031,1

5031,5041,1

*NFILL, BIAS=1.025, NSET=NSOIL

NBOT, NTOP,40,100

*NSET, NSET=NSIDE, GENERATE

1001,5001,100

1041,5041,100

*NSET, NSET=F1

5001,

*NSET, NSET=F2, GENERATE

5002,5005

****

** SOIL ELEMENT DEFINING

****

*ELEMENT, TYPE=CPE4R, ELSET=ELSOIL

1001,1001,1002,1102,1101

*ELGEN, ELSET=ELSOIL

1001,40,1,1,40,100,100

*ELSET, ELSET=ELST, GENERATE

4901,4940

*SOLID SECTION, ELSET=ELSOIL, MATERIAL=MSOIL

*MATERIAL, NAME=MSOIL

*ELASTIC

100.0E3,0.3

*MOHR COULOMB

10.0,0.0

*MOHR COULOMB HARDENING

50.0

```
**********************************************************
*RESTART, WRITE, FREQUENCY=1
*EQUATION
2
F2,2,1.0,5001,2,-1
*BOUNDARY
NBOT, ENCASTRE
NSIDE,1,1
F2,1
*STEP
*GEOSTATIC
*DLOAD
ELSOIL, BY,-9
*END STEP
*STEP, INC=1000, UNSYMM=YES, AMPLITUDE=RAMP
*STATIC
1e-5,1,1e-12,0.005
*CONTROLS, ANALYSIS=DISCONTINUOUS
*CONTROLS, PARAMETERS=LINE SEARCH
20
*BOUNDARY
5001,2,2,-1
*EL PRINT, FREQUENCY=0
```

*NODE PRINT, NSET=F1, FREQUENCY=1, SUMMARY=NO, TOTAL=YES

U2, RF2

*NODE PRINT, FREQUENCY=0

*END STEP

1.3d Input File for Cohesive-frictional Soil (c=50kPa, ø=20^o)

*HEADING

****

**Bearing capacity of strip foundation on uniform cohesive-frictional soil*

**Element type: CPE4R; Cohesion=50kPa; Friction angle=20^o*

**Effective self-weight γ'= 9KN/m^3*

**Elastic modulus=20MPa; Possions' ratio=0.3; Area=40m*20m*

**Mohr-Coulomb yield criterion*

****

** NODES DEFINING

****

*******All dimension in meter and stress is kPa*

*NODE, NSET=NA1

1001,0,0

1011,5,0

1021,12.5,0

1031,22.5,0

1041,40,0

5001,0,20

5011,5,20

5021,12.5,20

5031,22.5,20

5041,40,20

*NGEN, NSET=NBOT

1001,1011,1

1011,1021,1

1021,1031,1

1031,1041,1

*NGEN, NSET=NTOP

5001,5011,1

5011,5021,1

5021,5031,1

5031,5041,1

*NFILL, BIAS=1.025, NSET=NSOIL

NBOT, NTOP,40,100

*NSET, NSET=NSIDE, GENERATE

1001,5001,100

1041,5041,100

*NSET, NSET=F1

5001,

*NSET, NSET=F2, GENERATE

5002,5005

```
**********
** SOIL ELEMENT DEFINING
**********
*ELEMENT, TYPE=CPE4R, ELSET=ELSOIL
1001,1001,1002,1102,1101
*ELGEN, ELSET=ELSOIL
1001,40,1,1,40,100,100
*ELSET, ELSET=ELST, GENERATE
4901,4940
*SOLID SECTION, ELSET=ELSOIL, MATERIAL=MSOIL
*MATERIAL, NAME=MSOIL
*ELASTIC
100.0E3, 0.3
*MOHR COULOMB
20.0,0.0
*MOHR COULOMB HARDENING
50.0
**********
*RESTART, WRITE, FREQUENCY=1
*EQUATION
2
F2,2,1.0,5001,2,-1
*BOUNDARY
```

NBOT, ENCASTRE

NSIDE,1,1

F2,1

*STEP

*GEOSTATIC

*DLOAD

ELSOIL, BY,-9

*END STEP

*STEP, INC=5000, UNSYMM=YES, AMPLITUDE=RAMP

*STATIC

1e-5,1,1e-12,0.001

*CONTROLS, ANALYSIS=DISCONTINUOUS

*CONTROLS, PARAMETERS=LINE SEARCH

20

*BOUNDARY

5001,2,2,-1

*EL PRINT, FREQUENCY=0

*NODE PRINT, NSET=F1, FREQUENCY=1, SUMMARY=NO, TOTAL=YES

U2, RF2

*NODE PRINT, FREQUENCY=0

*END STEP

1.3e Input File for Cohesive-frictional Soil (c=50kPa, ø=30^{o})

*HEADING

****

***Bearing capacity of strip foundation on uniform cohesive-frictional soil*

***Element type: CPE4R; Cohesion=50kPa; Friction angle=20^{o}*

***Effective self-weight γ'= 9KN/m^{3}*

***Elastic modulus=20MPa; Possions' ratio=0.3; Area=40m*20m*

***Mohr-Coulomb yield criterion*

****

** NODES DEFINING

****

********All dimension in meter and stress is kPa*

*NODE, NSET=NA1

1001,0,0

1011,5,0

1021,12.5,0

1031,22.5,0

1041,40,0

5001,0,20

5011,5,20

5021,12.5,20

5031,22.5,20

5041,40,20

*NGEN, NSET=NBOT

1001,1011,1

1011,1021,1

1021,1031,1

1031,1041,1

*NGEN, NSET=NTOP

5001,5011,1

5011,5021,1

5021,5031,1

5031,5041,1

*NFILL, BIAS=1.025, NSET=NSOIL

NBOT,NTOP,40,100

*NSET, NSET=NSIDE, GENERATE

1001,5001,100

1041,5041,100

*NSET,NSET=F1

5001,

*NSET, NSET=F2, GENERATE

5002,5005

****

** SOIL ELEMENT DEFINING

****

*ELEMENT, TYPE=CPE4R, ELSET=ELSOIL

1001,1001,1002,1102,1101

*ELGEN, ELSET=ELSOIL

```
1001,40,1,1,40,100,100
*ELSET, ELSET=ELST, GENERATE
4901,4940
*SOLID SECTION, ELSET=ELSOIL, MATERIAL=MSOIL
*MATERIAL, NAME=MSOIL
*ELASTIC
100.0E3, 0.3
*MOHR COULOMB
30.0,0.0
*MOHR COULOMB HARDENING
50.0
**********************************************************
*RESTART, WRITE, FREQUENCY=1
*EQUATION
2
F2,2,1.0,5001,2,-1
*BOUNDARY
NBOT, ENCASTRE
NSIDE,1,1
F2,1
*STEP
*GEOSTATIC
*DLOAD
```

ELSOIL, BY,-9

*END STEP

*STEP, INC=10000, UNSYMM=YES, AMPLITUDE=RAMP

*STATIC

1e-5,1,1e-12,0.001

*CONTROLS, ANALYSIS=DISCONTINUOUS

*CONTROLS, PARAMETERS=LINE SEARCH

*BOUNDARY

5001,2,2,-1.5

*EL PRINT, FREQUENCY=0

*NODE PRINT, NSET=F1, FREQUENCY=1, SUMMARY=NO, TOTAL=YES

U2, RF2

*NODE PRINT, FREQUENCY=0

*END STEP

2 Linear Analysis

2.1 Input Files for Uniform Cohesive Soils

2.1a Input File for Uniform Cohesive Soils (Width of Foundation B=2m)

*HEADING

****

**The first elastic analysis for strip foundation on uniform cohesive soil*

**Element type: CPE4R; Cohesion=10kPa; Friction angle=0^o*

**Self-weight γ= 0*

**Elastic modulus=20MPa; Possions' ratio=0.499; Area=40m*20m*

****

** NODES DEFINING

****

*******All dimension in meter and stress is kPa*

*NODE, NSET=NA1

1001,0,0

1011,5,0

1021,12.5,0

1031,22.5,0

1041,40,0

5001,0,20

5011,5,20

5021,12.5,20

5031,22.5,20

5041,40,20

*NGEN, NSET=NBOT

1001,1011,1

1011,1021,1

1021,1031,1

1031,1041,1

*NGEN, NSET=NTOP

5001,5011,1

5011,5021,1

5021,5031,1

5031,5041,1

*NFILL, BIAS=1.025, NSET=NSOIL

NBOT, NTOP,40,100

*NSET, NSET=NSIDE, GENERATE

1001,5001,100

1041,5041,100

*NSET, NSET=F1

5001,

*NSET, NSET=F2, GENERATE

5002,5005

****

** SOIL ELEMENT DEFINING

****

*ELEMENT, TYPE=CPE4R, ELSET=ELSOIL

1001,1001,1002,1102,1101

*ELGEN, ELSET=ELSOIL

1001,40,1,1,40,100,100

*SOLID SECTION, ELSET=ELSOIL, MATERIAL=MSOIL

*MATERIAL, NAME=MSOIL

*ELASTIC

20E3,0.499

*ELSET, ELSET=ELST, GENERATE

4901,4940

*ELSET,ELSET=ELOAD, GENERATE

4901,4904,1

****

*RESTART, WRITE, FREQUENCY=1

*EQUATION

2

F2,2,1.0,5001,2,-1

*BOUNDARY

NBOT, ENCASTRE

NSIDE,1,1

F2,1

*STEP

*STATIC

*DLOAD

ELOAD, P3,100

*EL PRINT, FREQUENCY=1, SUMMARY=NO, TOTAL=NO

SP, MISES

*NODE PRINT, FREQUENCY=0

*END STEP

****

**The input file 2.1a also can be used for linear analyses of strip **foundation on uniform **cohesive soil with different* elastic modulus, cohesion, and applied pressure.

****

2.1b Input File for Uniform Cohesive Soils (Width of Foundation B=3m)

*HEADING

****

**The first elastic analysis for strip foundation on uniform cohesive soil*

**Element type: CPE4R; Cohesion=10kPa; Friction angle=0°;*

**Self-weight γ= 0*

**Elastic modulus=20MPa; Possions' ratio=0.499; Area=40m*20m*

****

** NODES DEFINING

****

*******All dimension in meter and stress is kPa*

*NODE, NSET=NA1

1001,0,0

1011,7.5,0

1021,18.75,0

1031,33.75,0

1041,60,0

5001,0,30

5011,7.5,30

5021,18.75,30

5031,33.75,30

5041,60,30

```
*NGEN, NSET=NBOT
1001,1011,1
1011,1021,1
1021,1031,1
1031,1041,1
*NGEN, NSET=NTOP
5001,5011,1
5011,5021,1
5021,5031,1
5031,5041,1
*NFILL, BIAS=1.025, NSET=NSOIL
NBOT, NTOP,40,100
*NSET, NSET=NSIDE, GENERATE
1001,5001,100
1041,5041,100
*NSET, NSET=F1
5001,
*NSET, NSET=F2, GENERATE
5002,5005
**********************************
** SOIL ELEMENT DEFINING
**********************************
*ELEMENT, TYPE=CPE4R, ELSET=ELSOIL
```

```
1001,1001,1002,1102,1101
*ELGEN, ELSET=ELSOIL
1001,40,1,1,40,100,100
*SOLID SECTION, ELSET=ELSOIL, MATERIAL=MSOIL
*MATERIAL, NAME=MSOIL
*ELASTIC
20E3,0.499
*PLASTIC
17.32
*ELSET, ELSET=ELST, GENERATE
4901,4940
*ELSET, ELSET=ELOAD, GENERATE
4901,4904,1
**********
*RESTART, WRITE, FREQUENCY=1
*EQUATION
2
F2,2,1.0,5001,2,-1
*BOUNDARY
NBOT, ENCASTRE
NSIDE,1,1
F2,1
*STEP
```

*STATIC

*DLOAD

ELOAD,p3,100

*EL PRINT, FREQUENCY==1, SUMMARY=NO, TOTAL=NO

SP, MISES

*NODE PRINT, FREQUENCY=0

*END STEP

****

**The input file 2.1b also can be used for linear analyses of strip foundation on uniform*

**cohesive soil with different elastic modulus, cohesion,and applied pressure.*

****

2.2 Input Files for Layered Cohesive Soils

2.2a Input File for Layered Cohesive Soils (H/B=1.5)

*HEADING

****

**The first elastic analysis for strip foundation on layered cohesive soil*

**Element type: CPE4R; Cohesion: $cu_1/cu_2=2$; $cu_1=20kPa$; $cu_2=10kPa$.*

**Friction angle=0^o, Self-weight $\gamma_1= \gamma_2= 0$*

**Elastic modulus: $E_1=40MPa$, $E_2=20MPa$; Possions' ratio=0.499.*

**Area=40m*20m*

****

** NODES DEFINING

****

*******All dimension in meter and stress is kPa*

*NODE, NSET=NA1

1001,0,0

1011,5,0

1021,12.5,0

1031,22.5,0

1041,40,0

3201,0,14

3211,5,14

3221,12.5,14

3231,22.5,14

3241,40,14

5001,0,20

5011,5,20

5021,12.5,20

5031,22.5,20

5041,40,20

*NGEN, NSET=NBOT

1001,1011,1

1011,1021,1

1021,1031,1

1031,1041,1

*NGEN, NSET=NMID

3201,3211,1

3211,3221,1

3221,3231,1

3231,3241,1

*NGEN, NSET=NTOP

5001,5011,1

5011,5021,1

5021,5031,1

5031,5041,1

*NFILL, BIAS=1.00, NSET=NSOIL

NBOT, NMID,22,100

*NFILL, BIAS=1.00, NSET=NSOIL

NMID,NTOP,18,100

*NSET, NSET=NSIDE, GENERATE

1001,3201,100

3201,5001,100

1041,3241,100

3241,5041,100

*NSET,NSET=F1

5001,

*NSET, NSET=F2, GENERATE

5002,5005

****

```
** SOIL ELEMENT DEFINING
************************************
*ELEMENT, TYPE=CPE4R, ELSET=ELSOIL
1001,1001,1002,1102,1101
*ELGEN, ELSET=ELSOIL
1001,40,1,1,22,100,100
*ELEMENT, TYPE=CPE4R, ELSET=ELSOIL1
3201,3201,3202,3302,3301
*ELGEN, ELSET=ELSOIL1
3201,40,1,1,18,100,100
*ELSET, ELSET=ELST, GENERATE
4901,4940
*SOLID SECTION, ELSET=ELSOIL, MATERIAL=MSOIL
*MATERIAL, NAME=MSOIL
*ELASTIC
20.0E3, 0.48
*SOLID SECTION, ELSET=ELSOIL1, MATERIAL=MSOIL1
*MATERIAL, NAME=MSOIL1
*ELASTIC
40.0E3, 0.48
*ELSET, ELSET=ELOAD, GENERATE
4901,4904,1
************************************
```

*RESTART, WRITE, FREQUENCY=1

*EQUATION

2

F2,2,1.0,5001,2,-1

*BOUNDARY

NBOT, ENCASTRE

NSIDE,1,1

F2,1

*STEP

*STATIC

*dLOAD

ELOAD, P3,100

*EL PRINT, FREQUENCY=1, SUMMARY=NO, TOTAL=NO

SP, MISES

*NODE PRINT, FREQUENCY=0

*END STEP

****

**The input file 2.2a also can be used for linear analyses of strip foundation layered*

***cohesive soil with different elastic modulus,cohesion,and applied pressure.*

****

2.2b Input File for Layered Cohesive Soils (H/B=1)

*HEADING

****

***The first elastic analysis for strip foundation on layered cohesive soil*

***Element type: CPE4R; Cohesion: $cu_1/cu_2=2$; $cu_1=20kPa$; $cu_2=10kPa$.*

***Friction angle=0^o, Self-weight $\gamma_1=\gamma_2=0$*

***Elastic modulus: $E_1=40MPa$, $E_2=20MPa$; Possions' ratio=0.499.*

***Area=40m*20m*

****

** NODES DEFINING

****

*******All dimension in meter and stress is kPa*

*NODE, NSET=NA1

1001,0,0

1011,5,0

1021,12.5,0

1031,22.5,0

1041,40,0

3801,0,16

3811,5,16

3821,12.5,16

3831,22.5,16

3841,40,16

5001,0,20

5011,5,20

5021,12.5,20

5031,22.5,20

5041,40,20

*NGEN, NSET=NBOT

1001,1011,1

1011,1021,1

1021,1031,1

1031,1041,1

*NGEN, NSET=NMID

3801,3811,1

3811,3821,1

3821,3831,1

3831,3841,1

*NGEN, NSET=NTOP

5001,5011,1

5011,5021,1

5021,5031,1

5031,5041,1

*NFILL, BIAS=1.00, NSET=NSOIL

NBOT, NMID,28,100

*NFILL, BIAS=1.00, NSET=NSOIL

NMID, NTOP,12,100

*NSET, NSET=NSIDE, GENERATE

1001,3801,100

3801,5001,100

1041,3841,100

3841,5041,100

*NSET, NSET=F1

5001,

*NSET, NSET=F2, GENERATE

5002,5005

****

** SOIL ELEMENT DEFINING

****

*ELEMENT, TYPE=CPE4R, ELSET=ELSOIL

1001,1001,1002,1102,1101

*ELGEN, ELSET=ELSOIL

1001,40,1,1,28,100,100

*ELEMENT, TYPE=CPE4R, ELSET=ELSOIL1

3801,3801,3802,3902,3901

*ELGEN, ELSET=ELSOIL1

3801,40,1,1,12,100,100

*ELSET, ELSET=ELST, GENERATE

4901,4940

*SOLID SECTION, ELSET=ELSOIL, MATERIAL=MSOIL

*MATERIAL, NAME=MSOIL

*ELASTIC

```
20.0E3, 0.48
*SOLID SECTION, ELSET=ELSOIL1, MATERIAL=MSOIL1
*MATERIAL, NAME=MSOIL1
*ELASTIC
40.0E3, 0.48
*ELSET, ELSET=ELOAD, GENERATE
4901,4904,1
**********************************
*RESTART, WRITE, FREQUENCY=1
*EQUATION
2
F2,2,1.0,5001,2,-1
*BOUNDARY
NBOT, ENCASTRE
NSIDE,1,1
F2,1
*STEP
*STATIC
*DLOAD
 ELOAD, P3,100
*EL PRINT, FREQUENCY=1, SUMMARY=NO, TOTAL=NO
SP, MISES
*NODE PRINT, FREQUENCY=0
```

*END STEP

****

***The input file 2.2b also can be used for linear analyses of strip foundation layered*

***cohesive soil with different elastic modulus,cohesion,and applied pressure.*

****

2.2c Input File for Layered Cohesive Soils (H/B=0.75)

*HEADING

****

***The first elastic analysis for strip foundation on layered cohesive soil*

***Element type: CPE4R; Cohesion: $cu_1/cu_2=2$; $cu_1=20kPa$; $cu_2=10kPa$.*

***Friction angle=0^o,Self-weight $\gamma_1= \gamma_2= 0$*

***Elastic modulus: $E_1=40MPa$, $E_2=20MPa$; Possions' ratio=0.499.*

***Area=40m*20m*

****

** NODES DEFINING

****

********All dimension in meter and stress is kPa*

*NODE, NSET=NA1

1001,0,0

1011,5,0

1021,12.5,0

1031,22.5,0

1041,40,0

4101,0,17

4111,5,17

4121,12.5,17

4131,22.5,17

4141,40,17

5001,0,20

5011,5,20

5021,12.5,20

5031,22.5,20

5041,40,20

*NGEN, NSET=NBOT

1001,1011,1

1011,1021,1

1021,1031,1

1031,1041,1

*NGEN, NSET=NMID

4101,4111,1

4111,4121,1

4121,4131,1

4131,4141,1

*NGEN, NSET=NTOP

5001,5011,1

5011,5021,1

5021,5031,1

5031,5041,1

*NFILL, BIAS=1.00, NSET=NSOIL

NBOT, NMID,31,100

*NFILL, BIAS=1.00, NSET=NSOIL

NMID, NTOP,9,100

*NSET, NSET=NSIDE, GENERATE

1001,4101,100

4101,5001,100

1041,4141,100

4141,5041,100

*NSET, NSET=F1

5001,

*NSET, NSET=F2, GENERATE

5002,5005

****

** SOIL ELEMENT DEFINING

****

*ELEMENT, TYPE=CPE4R, ELSET=ELSOIL

1001,1001,1002,1102,1101

*ELGEN, ELSET=ELSOIL

1001,40,1,1,31,100,100

*ELEMENT, TYPE=CPE4R, ELSET=ELSOIL1

```
4101,4101,4102,4202,4201
*ELGEN, ELSET=ELSOIL1
4101,40,1,1,9,100,100
*ELSET, ELSET=ELST, GENERATE
4901,4940
*SOLID SECTION, ELSET=ELSOIL,MATERIAL=MSOIL
*MATERIAL, NAME=MSOIL
*ELASTIC
20.0E3,0.499
*SOLID SECTION, ELSET=ELSOIL1, MATERIAL=MSOIL1
*MATERIAL, NAME=MSOIL1
*ELASTIC
40.0E3,0.499
*ELSET, ELSET=ELOAD, GENERATE
4901,4904,1
**********************************
*RESTART, WRITE, FREQUENCY=1
*EQUATION
2
F2,2,1.0,5001,2,-1
*BOUNDARY
NBOT, ENCASTRE
NSIDE,1,1
```

F2,1

*STEP

*STATIC

*DLOAD

ELOAD, P3,100

*EL PRINT, FREQUENCY=1, SUMMARY=NO, TOTAL=NO

SP, MISES

*NODE PRINT, FREQUENCY=0

*END STEP

****

**The input file 2.2c also can be used for linear analyses of strip foundation layered*

**cohesive soil with different elastic modulus, cohesion,and applied pressure.*

****

2.2d Input File for Layered Cohesive Soils (H/B=0.5)

*HEADING

****

**The first elastic analysis for strip foundation on layered cohesive soil*

**Element type: CPE4R; Cohesion: $cu_1/cu_2=2$; $cu_1=20kPa$; $cu_2=10kPa$.*

**Friction angle=0^o, Self-weight $\gamma_1= \gamma_2= 0$*

**Elastic modulus: $E_1=40MPa$, $E_2=20MPa$; Possions' ratio=0.499.*

**Area=40m*20m*

****

** NODES DEFINING

****

*******All dimension in meter and stress is kPa*

*NODE, NSET=NA1

1001,0,0

1011,5,0

1021,12.5,0

1031,22.5,0

1041,40,0

4401,0,18

4411,5,18

4421,12.5,18

4431,22.5,18

4441,40,18

5001,0,20

5011,5,20

5021,12.5,20

5031,22.5,20

5041,40,20

*NGEN, NSET=NBOT

1001,1011,1

1011,1021,1

1021,1031,1

1031,1041,1

*NGEN, NSET=NMID

4401,4411,1

4411,4421,1

4421,4431,1

4431,4441,1

*NGEN, NSET=NTOP

5001,5011,1

5011,5021,1

5021,5031,1

5031,5041,1

*NFILL, BIAS=1.00, NSET=NSOIL

NBOT, NMID,34,100

*NFILL, BIAS=1.00, NSET=NSOIL

NMID, NTOP,6,100

*NSET, NSET=NSIDE, GENERATE

1001,4401,100

4401,5001,100

1041,4441,100

4441,5041,100

*NSET, NSET=F1

5001,

*NSET, NSET=F2, GENERATE

5002,5005

```
**********************************
** SOIL ELEMENT DEFINING
**********************************
*ELEMENT, TYPE=CPE4R, ELSET=ELSOIL
1001,1001,1002,1102,1101
*ELGEN, ELSET=ELSOIL
1001,40,1,1,34,100,100
*ELEMENT, TYPE=CPE4R, ELSET=ELSOIL1
4401,4401,4402,4502,4501
*ELGEN, ELSET=ELSOIL1
4401,40,1,1,6,100,100
*ELSET, ELSET=ELST, GENERATE
4901,4940
*SOLID SECTION, ELSET=ELSOIL, MATERIAL=MSOIL
*MATERIAL, NAME=MSOIL
*ELASTIC
20.0E3,0.499
*SOLID SECTION, ELSET=ELSOIL1, MATERIAL=MSOIL1
*MATERIAL, NAME=MSOIL1
*ELASTIC
40.0E3,0.499
*ELSET, ELSET=ELOAD, GENERATE
4901,4904,1
```

****

*RESTART, WRITE, FREQUENCY=1

*EQUATION

2

F2,2,1.0,5001,2,-1

*BOUNDARY

NBOT, ENCASTRE

NSIDE,1,1

F2,1

*STEP

*STATIC

*DLOAD

ELOAD, P3,100

*EL PRINT, FREQUENCY=1, SUMMARY=NO, TOTAL=NO

SP, MISES

*NODE PRINT, FREQUENCY=0

*END STEP

****

**The input file 2.2d also can be used for linear analyses of strip foundation layered*

***cohesive soil with different elastic modulus,cohesion,and applied pressure.*

****

2.2e Input File for Layered Cohesive Soils (H/B=0.25)

*HEADING

****

***The first elastic analysis for strip foundation on layered cohesive soil*

***Element type: CPE4R; Cohesion: $cu_1/cu_2=2$; $cu_1=20kPa$; $cu_2=10kPa$.*

***Friction angle=0^o, Self-weight $\gamma_1= \gamma_2= 0$*

***Elastic modulus: $E_1=40MPa$, $E_2=20MPa$; Possions' ratio=0.499.*

***Area=40m*20m*

****

** NODES DEFINING

****

*****All dimension in meter and stress is kPa*

*NODE, NSET=NA1

1001,0,0

1011,5,0

1021,12.5,0

1031,22.5,0

1041,40,0

4701,0,19

4711,5,19

4721,12.5,19

4731,22.5,19

4741,40,19

5001,0,20

5011,5,20

5021,12.5,20

5031,22.5,20

5041,40,20

*NGEN, NSET=NBOT

1001,1011,1

1011,1021,1

1021,1031,1

1031,1041,1

*NGEN, NSET=NMID

4701,4711,1

4711,4721,1

4721,4731,1

4731,4741,1

*NGEN, NSET=NTOP

5001,5011,1

5011,5021,1

5021,5031,1

5031,5041,1

*NFILL, BIAS=1.00, NSET=NSOIL

NBOT, NMID,37,100

*NFILL, BIAS=1.00, NSET=NSOIL

NMID, NTOP,3,100

*NSET, NSET=NSIDE, GENERATE

1001,4701,100

4701,5001,100

1041,4741,100

4741,5041,100

*NSET, NSET=F1

5001,

*NSET, NSET=F2, GENERATE

5002,5005

****

** SOIL ELEMENT DEFINING

****

*ELEMENT, TYPE=CPE4R, ELSET=ELSOIL

1001,1001,1002,1102,1101

*ELGEN, ELSET=ELSOIL

1001,40,1,1,37,100,100

*ELEMENT, TYPE=CPE4R, ELSET=ELSOIL1

4701,4701,4702,4802,4801

*ELGEN, ELSET=ELSOIL1

4701,40,1,1,3,100,100

*ELSET, ELSET=ELST, GENERATE

4901,4940

*SOLID SECTION, ELSET=ELSOIL, MATERIAL=MSOIL

*MATERIAL, NAME=MSOIL

```
*ELASTIC
20.0E3,0.499
*SOLID SECTION, ELSET=ELSOIL1, MATERIAL=MSOIL1
*MATERIAL, NAME=MSOIL1
*ELASTIC
40.0E3,0.499
*ELSET, ELSET=ELOAD, GENERATE
4901,4904,1
**********************************
*RESTART, WRITE, FREQUENCY=1
*EQUATION
2
F2,2,1.0,5001,2,-1
*BOUNDARY
NBOT, ENCASTRE
NSIDE,1,1
F2,1
*STEP
*STATIC
*DLOAD
ELOAD, P3,100
*EL PRINT, FREQUENCY=1, SUMMARY=NO, TOTAL=NO
SP, MISES
```

*NODE PRINT, FREQUENCY=0

*END STEP

****

**The input file 2.2e also can be used for linear analyses of strip foundation layered*

**cohesive soil with different elastic modulus, cohesion,and applied pressure.*

****

2.3 Input Files for Cohesive-Frictional Soils

2.3a Input File for Cohesive-Frictional Soils (structure submitted to applied load)

*HEADING

****

**The first elastic analysis for strip foundation on cohesive-frictional soil*

**Element type: CPE4R;*

**Elastic modulus=20MPa; Possions' ratio=0.3*

**Area=40m*20m*

****

** NODES DEFINING

****

*******All dimension in meter and stress is kPa*

*NODE, NSET=NA1

1001,0,0

1011,5,0

1021,12.5,0

1031,22.5,0

1041,40,0

5001,0,20

5011,5,20

5021,12.5,20

5031,22.5,20

5041,40,20

*NGEN, NSET=NBOT

1001,1011,1

1011,1021,1

1021,1031,1

1031,1041,1

*NGEN, NSET=NTOP

5001,5011,1

5011,5021,1

5021,5031,1

5031,5041,1

*NFILL, BIAS=1.025, NSET=NSOIL

NBOT, NTOP,40,100

*NSET, NSET=NSIDE, GENERATE

1001,5001,100

1041,5041,100

*NSET, NSET=F1

5001,

```
*NSET, NSET=F2, GENERATE
5002,5005
**********
** SOIL ELEMENT DEFINING
**********
*ELEMENT, TYPE=CPE4R, ELSET=ELSOIL
1001,1001,1002,1102,1101
*ELGEN, ELSET=ELSOIL
1001,40,1,1,40,100,100
*ELSET, ELSET=ELST, GENERATE
4901,4940
*SOLID SECTION, ELSET=ELSOIL, MATERIAL=MSOIL
*MATERIAL, NAME=MSOIL
*ELASTIC
20.0E3, 0.3
**********
*RESTART, WRITE, FREQUENCY=1
*EQUATION
2
F2,2,1.0,5001,2,-1
*BOUNDARY
NBOT, ENCASTRE
NSIDE,1,1
```

F2,1

*STEP

*STATIC

*dLOAD

ELOAD, P3,100

*EL PRINT, FREQUENCY=1, SUMMARY=NO, TOTAL=NO

SP, MISES

*NODE PRINT, FREQUENCY=0

*END STEP

****

**The input file 2.3 also can be used for linear analyses of bearing capacity of strip*

**foundation on cohesive-frictional soil with different cohesion and friction angle*

****

2.3b Input File for Cohesive-Frictional Soils (structure submitted to self-weight)

*HEADING

****

**The first elastic analysis for strip foundation on cohesive-frictional soil*

**Element type: CPE4R;*

**Elastic modulus=20MPa; Possions' ratio=0.3*

**Area=40m*20m*

****

** NODES DEFINING

****

*******All dimension in meter and stress is kPa*

*NODE, NSET=NA1

1001,0,0

1011,5,0

1021,12.5,0

1031,22.5,0

1041,40,0

5001,0,20

5011,5,20

5021,12.5,20

5031,22.5,20

5041,40,20

*NGEN, NSET=NBOT

1001,1011,1

1011,1021,1

1021,1031,1

1031,1041,1

*NGEN, NSET=NTOP

5001,5011,1

5011,5021,1

5021,5031,1

5031,5041,1

*NFILL, BIAS=1.025, NSET=NSOIL

NBOT, NTOP,40,100

*NSET, NSET=NSIDE, GENERATE

1001,5001,100

1041,5041,100

*NSET, NSET=F1

5001,

*NSET, NSET=F2, GENERATE

5002,5005

****

** SOIL ELEMENT DEFINING

****

*ELEMENT, TYPE=CPE4R, ELSET=ELSOIL

1001,1001,1002,1102,1101

*ELGEN, ELSET=ELSOIL

1001,40,1,1,40,100,100

*SOLID SECTION, ELSET=ELSOIL, MATERIAL=MSOIL

*MATERIAL, NAME=MSOIL

*ELASTIC

100.0E3, 0.3

*ELSET, ELSET=ELST, GENERATE

4901,4940

*ELSET, ELSET=ELOAD, GENERATE

4901,4904,1

```
**********************************
*RESTART, WRITE, FREQUENCY=1
*EQUATION
2
F2,2,1.0,5001,2,-1
*BOUNDARY
NBOT, ENCASTRE
NSIDE,1,1
F2,1
*STEP
*STATIC
*DLOAD
 ELSOIL,BY,-9
*EL PRINT, FREQUENCY=1, SUMMARY=NO, TOTAL=NO
SP
*NODE PRINT, FREQUENCY=0
*END STEP
```

Matlab Modulus Changing and Stress Listing Macros

1 Script for Extracting Results from ABAQUS *.dat Files

```
Function ETS (f1, f2)
% Extracting stresses of each element from ABAQUS/Standard result file *.dat.
% f1 is the ABAQUS/Standard result file, the data extracted will be put into file f2.
```

```
fid=fopen(f1,'rt'); %Input the results obtained from ABAQUS
m=1;
ce=load(f2); %Creat a file to input the last results in
m1=1;
n1=0;
k=cell(1601,1);
while m<=1600 % Extract stresses of each element from ABAQUS result file
frewind(fid)
while feof(fid)==0
line=fgets(fid);
if m1<=1600
str=num2str(ce(m1,1));
else
fid1=fopen('2a.inp','w')
for m1=1:1600
fprintf(fid1,'%s',k{(m1+1),:});
end
fprintf(fid1,'%s',k{:,:});
fclose(fid);
fclose(fid1);
return
end
matches=findstr(line,str);
```

```
nm=9-matches;
num=nm*nm';
if num >0
nm(1,1);
if nm(1,1)> 0
m1=m1+1;
m=m+1;
fid2=fopen('3.inp','w');
fprintf(fid2,'%s',line);
fclose(fid2);
ce1=load('3.inp','w');
str1=num2str(ce1(1,1));
num1=strcmp(str,str1);
if num1>0
fprintf(1,'%d:%s',num,line);
k(m1,1)={line};
end
end
end
end
end
fid1=fopen('2a.inp','w')
for m1=1:1600
```

```
fprintf(fid1,'%s',k{(m1+1),:});
end
fclose(fid);
fclose(fid1);
```

2 Scripts for Moduli Modified

2.1a Moduli Modified for Uniform Cohesive Soils

```
Function read(f2,,e)
%Modifying the modulus of each element. From the file f2, stresses of each element are
%obtained, then according to theirs stresses modify the modulus of each element. New
%modulus of elements will be written into file y.inp by calling another Matlab script
%w.m. c is the cohesion of soil, e is the old Young's modulus of soil.
hg=load(f2); %Input the results obtained from ABAQUS
a1=hg(:,1);
b1=-hg(:,3);
b2=-hg(:,4);
b3=-hg(:,5);
for k=1:1600 %Modify the elastic modulus according to stresses
a2(k,1)=[(b1(k,1)-b2(k,1))^2+(b2(k,1)-b3(k,1))^2+(b3(k,1)-b1(k,1))^2]^0.5/2^0.5;
end
a=cat(2,a1,a2);
sy=min(a2);
[m,n]=size(a);
i=1;
```

```
for i=1:1600

CE(i,n)=sy*e/a(i,n);

end

ce=CE(:,2);

CE1=cat(2,a1,ce);

write(CE1);
```

2.1b Creating the Second Elastic Analysis Files for Uniform Cohesive Soils

```
Function write(CE1)

%Output the new modulus of each element  to file y.inp, which will be used for the second

%elastic analysis

str1a='**********************************';

str1b='**SOIL ELEMENT DEFINING';

str1c='**********************************';

[m,n]=size(CE1);

m1=1;

n1=1;

fid=fopen('y.inp','w');

fprintf(fid,'%s\n',str1a);

fprintf(fid,'%s\n',str1b);

fprintf(fid,'%s\n',str1c);

while m1<=m;

str2=strcat('*ELEMENT, TYPE=CPE4R, ELSET=ELSOIL', num2str(CE1(m1,1)));

nd=CE1(m1,1);
```

```
nd1=CE1(m1,1);
nd2=CE1(m1,1)+1;
nd3=CE1(m1,1)+101;
nd4=CE1(m1,1)+100;
str3=strcat(num2str(nd),',',num2str(nd1),',',num2str(nd2),',',num2str(nd3),',',num2str(nd4)
);
str4=strcat('*SOLID
SECTION,ELSET=ELSOIL',num2str(CE1(m1,1)),',','MATERIAL=MSOIL',num2str(CE
1(m1,1)));
str5=strcat('*MATERIAL,NAME=MSOIL',num2str(CE1(m1,1)));
str6='*ELASTIC';
v=0.499; % Poisson's ratio
str7=strcat(num2str(CE1(m1,2)),',',num2str(v));
m1=m1+1;
fprintf(fid,'%s\n',str2);
fprintf(fid,'%s\n',str3);
fprintf(fid,'%s\n',str4);
fprintf(fid,'%s\n',str5);
fprintf(fid,'%s\n',str6);
fprintf(fid,'%s\n',str7);
end
str8=('*ELSET,ELSET=MLST, GENERATE');
str9=('1001,4940');
```

```
str10=('*ELSET,ELSET=ELOAD, GENERATE ');

str11=('4901,4904,1');

fprintf(fid,'%s\n',str8);

fprintf(fid,'%s\n',str9);

fprintf(fid,'%s\n',str10);

fprintf(fid,'%s\n',str11);

fclose(fid);
```

2.2a Moduli Modified for Layered Cohesive Soils

```
Function read1(f2,e1,e2)

%Modifying the modulus of each element. From the file f2, stresses of each element are

%obtained, then according to theirs stresses modify the modulus of each element. New

%modulus of  elements will be written into file y.inp by calling another Matlab  script

%w.m. c is the cohesion of soil, e1 is the old Young's modulus of lower soil, e2. is the old

%Young's modulus of upper soil

hg=load(f2);

a1=hg(:,1);

a2=hg(:,7);

a=cat(2,a1,a2);

sy=min(a2)

[m,n]=size(a);

i=1;

for i=1:1600

if i<=640
```

```
CE(i,n)=sy*e1/a(i,n);

else

CE(i,n)=sy*e2/a(i,n);

end

end

ce=CE(:,2);

CE1=cat(2,a1,ce);

write(CE1);
```

2.2b Creating the Second Elastic Analysis Files for Layered Cohesive Soils

```
Function write(CE1)

%Output the new modulus of each element  to file y.inp, which will be used for the second

%elastic analysis

str1a='**********************************';

str1b='**SOIL ELEMENT DEFINING';

str1c='**********************************';

[m,n]=size(CE1);

m1=1;

n1=1;

fid=fopen('y.inp','w');

fprintf(fid,'%s\n',str1a);

fprintf(fid,'%s\n',str1b);

fprintf(fid,'%s\n',str1c);

while m1<=m;
```

```
str2=strcat('*ELEMENT, TYPE=CPE4R, ELSET=ELSOIL',num2str(CE1(m1,1)));
nd=CE1(m1,1);
nd1=CE1(m1,1);
nd2=CE1(m1,1)+1;
nd3=CE1(m1,1)+101;
nd4=CE1(m1,1)+100;
str3=strcat(num2str(nd),',',num2str(nd1),',',num2str(nd2),',',num2str(nd3),',',num2str(nd4)
);
str4=strcat('*SOLID
SECTION,ELSET=ELSOIL',num2str(CE1(m1,1)),',','MATERIAL=MSOIL',num2str(CE
1(m1,1)));
str5=strcat('*MATERIAL,NAME=MSOIL',num2str(CE1(m1,1)));
str6='*ELASTIC';
v=0.499; % Poisson's ratio
str7=strcat(num2str(CE1(m1,2)),',',num2str(v));
m1=m1+1;
fprintf(fid,'%s\n',str2);
fprintf(fid,'%s\n',str3);
fprintf(fid,'%s\n',str4);
fprintf(fid,'%s\n',str5);
fprintf(fid,'%s\n',str6);
fprintf(fid,'%s\n',str7);
end
```

```
str8=('*ELSET,ELSET=MLST, GENERATE');

str9=('1001,4940');

str10=('*ELSET,ELSET=ELOAD, GENERATE');

str11=('4901,4904,1');

fprintf(fid,'%s\n',str8);

fprintf(fid,'%s\n',str9);

fprintf(fid,'%s\n',str10);

fprintf(fid,'%s\n',str11);

fclose(fid);
```

2.3a Moduli Modified for Cohesive-Frictional Soils

```
Function read1(f1,f2,c,phi,e)
% This function is used to modify the modulus of each element for trial one, trial two.
%The result of stresses of each element came from the first analysis, friction angle of soil
%and old elastic modulus are inputted, then the new elastic modulus for each element is
%solved for the second elastic analysis. The result will be written into file y.inp,which
%will be used as part of the second analysis.c is the cohesion of soil, phi is the frictional
%angle of soil, e is the old Young's modulus of soil.
ld=load(f1); % stresses of each element caused by applied load
sw=load(f2); % stresses of each element caused by self-weight
for k=1:1600
ql(k,1)=-0.5*(ld(k,3)-ld(k,5));
pl(k,1)=-0.5*(ld(k,3)+ld(k,5));
qw(k,1)=-0.5*(sw(k,3)-sw(k,5));
```

```
pw(k,1)=-0.5*(sw(k,3)+sw(k,5));

b(k,1)=(ql(k,1)+qw(k,1))/(pl(k,1)+pw(k,1)+c/tan(phi*3.14/180));

if b(k,1)>1

b(k,1)=0.99;

end

cd(k,1)=tan(asin(b(k,1)))*c/tan(phi*3.14/180)

K(k,1)=c/cd(k,1)

end

% Modify elastic modulus of each element

for i=1:1600

CE(i,1)=e*K(i,1);

end

a4=ld(:,1);

CE1=cat(2,a4,CE);

write1(CE1); % Call the function write1 to output the new modulus
```

2.3b Moduli Modified for Cohesive-Frictional Soils (for trial three, trial four)

```
Function read1(f1,f2,c,phi,e,v)

% This function is used to modify the modulus of each element for trial three, trial four.

%The result of stresses of each element came from the first analysis, friction angle of soil

%and old elastic modulus are inputted, then the new elastic modulus for each element is

%solved for the second elastic analysis. The result will be written into file y.inp,which

%will be used as part of the second analysis.c is the cohesion of soil, phi is the frictional

%angle of soil, e is the old Young's modulus of soil. v is the old Poissons' ratio of soil.
```

```
ld=load(f1); % stresses of each element caused by applied load
sw=load(f2); % stresses of each element caused by applied load
for k=1:1600
ql(k,1)=-0.5*(ld(k,3)-ld(k,5));
pl(k,1)=-0.5*(ld(k,3)+ld(k,5));
qw(k,1)=-0.5*(sw(k,3)-sw(k,5));
pw(k,1)=-0.5*(sw(k,3)+sw(k,5));
b(k,1)=(ql(k,1)+qw(k,1))/(pl(k,1)+pw(k,1)+c/tan(phi*3.14/180));
if b(k,1)>1
b(k,1)=0.99;
end
cd(k,1)=tan(asin(b(k,1)))*c/tan(phi*3.14/180);
F(k,1)=c/cd(k,1);
end
for i=1:1600
VE(i,1)=3/(2+F(i,1)*(1-2*v)/(1+v))-1;
if VE(i,1)>=0.5;
VE(i,1)=0.4999;
end
if VE(i,1)<=0.1;
VE(i,1)=0.1;
end
CE(i,1)=(1+VE(i,1))*e*F(i,1)/(1+v);
```

```
end
% Modify elastic modulus and poison's ratio of each element
a4=ld(:,1);
CE1=cat(2,a4,CE,VE);
write1(CE1);
% call the function write1 to output the new modulus
```

2.3c Creating the Second Elastic Analysis Files for Cohesive-Frictional Soils (for trial one, trial two)

```
Function write1 (CE1)
% Output the data to file y.inp, which will be taken as part of the second analysis.using
%for trial one and two
str1a='**********************************';
str1b='**SOIL ELEMENT DEFINING';
str1c='**********************************';
[m,n]=size(CE1);
m1=1;
n1=1;
fid=fopen('y.inp','w');
fprintf(fid,'%s\n',str1a);
fprintf(fid,'%s\n',str1b);
fprintf(fid,'%s\n',str1c);
while m1<=m;
str2=strcat('*ELEMENT, TYPE=CPE4R, ELSET=ELSOIL',num2str(CE1(m1,1)));
```

```
nd=CE1(m1,1);
nd1=CE1(m1,1);
nd2=CE1(m1,1)+1;
nd3=CE1(m1,1)+101;
nd4=CE1(m1,1)+100;
str3=strcat(num2str(nd),',',num2str(nd1),',',num2str(nd2),',',num2str(nd3),',',num2str(nd4)
);
str4=strcat('*SOLID
SECTION,ELSET=ELSOIL',num2str(CE1(m1,1)),',','MATERIAL=MSOIL',num2str(CE
1(m1,1)));
str5=strcat('*MATERIAL, NAME=MSOIL',num2str(CE1(m1,1)));
str6='*ELASTIC';
v=0.3;% Poisson's ratio
str7=strcat(num2str(CE1(m1,2)),',',num2str(v));
m1=m1+1;
fprintf(fid,'%s\n',str2);
fprintf(fid,'%s\n',str3);
fprintf(fid,'%s\n',str4);
fprintf(fid,'%s\n',str5);
fprintf(fid,'%s\n',str6);
fprintf(fid,'%s\n',str7);
end
str8=('*ELSET, ELSET=ELSOIL, GENERATE');
```

```
str9=('1001,4940');

str10=('*ELSET, ELSET=ELOAD, GENERATE');

str11=('4901,4904,1');

fprintf(fid,'%s\n',str8);

fprintf(fid,'%s\n',str9);

fprintf(fid,'%s\n',str10);

fprintf(fid,'%s\n',str11);

fclose(fid);
```

2.3d Creating the Second Elastic Analysis Files for Cohesive-Frictional Soils (for trial three, trial four)

Function write1 (CE1)

```
% Output the data to file y.inp, which will be taken as part of the second analysis.using

%for trial three and four

str1a='**********************************';

str1b='**SOIL ELEMENT DEFINING';

str1c='**********************************';

[m,n]=size(CE1);

m1=1;

n1=1;

fid=fopen('y.inp','w');

fprintf(fid,'%s\n',str1a);

fprintf(fid,'%s\n',str1b);

fprintf(fid,'%s\n',str1c);
```

```
while m1<=m;
str2=strcat('*ELEMENT, TYPE=CPE4R, ELSET=ELSOIL',num2str(CE1(m1,1)));
nd=CE1(m1,1);
nd1=CE1(m1,1);
nd2=CE1(m1,1)+1;
nd3=CE1(m1,1)+101;
nd4=CE1(m1,1)+100;
str3=strcat(num2str(nd),',',num2str(nd1),',',num2str(nd2),',',num2str(nd3),',',num2str(nd4)
);
str4=strcat('*SOLID
SECTION,ELSET=ELSOIL',num2str(CE1(m1,1)),',','MATERIAL=MSOIL',num2str(CE
1(m1,1)));
str5=strcat('*MATERIAL, NAME=MSOIL',num2str(CE1(m1,1)));
str6='*ELASTIC';
str7=strcat(num2str(CE1(m1,2)),',',num2str(CE1(m1,3)));
m1=m1+1;
fprintf(fid,'%s\n',str2);
fprintf(fid,'%s\n',str3);
fprintf(fid,'%s\n',str4);
fprintf(fid,'%s\n',str5);
fprintf(fid,'%s\n',str6);
fprintf(fid,'%s\n',str7);
end
```

```
str8=('*ELSET,ELSET=ELSOIL, GENERATE');

str9=('1001,4940');

str10=('*ELSET,ELSET=ELOAD, GENERATE');

str11=('4901,4904,1');

fprintf(fid,'%s\n',str8);

fprintf(fid,'%s\n',str9);

fprintf(fid,'%s\n',str10);

fprintf(fid,'%s\n',str11);

fclose(fid);
```

3 Scripts for Finding R-node Elements and Plotting

3.1 Finding R-node Elements and Plotting for Uniform Cohesive Soils

```
Function [b]=try3(file1,file2)

[d1]=try1(file1);

[d2]=try2(file2);

b=zeros(40,2);

c=zeros(40,1);

for i=1:40;

a1=d1(:,:,i);

a2=d2(:,:,i);

a3=a1(:,2)-a2(:,2);

a3=abs(a3);

a4=a2(:,2);

for h=1:40
```

```
a3(h)/a4(h);

a5(h,1)=ans;

end

[m,n]=min(a5);

b(i,1)=a1(n,1);

if m <=1;

b(i,3)=m*100;

b(i,2)=[a1(n,2)+a2(n,2)]/2;

c(i)=n;

end

end

subplot(1,2,1);

plot(c,'o');

axis([1 40 1 40]);

grid on;

xlabel('Segment number');

ylabEL('Row number');

TITLE('R-nodes Locations');

subplot(1,2,2);

plot(b(:,2));

axis([1 40 0 100]);

grid on;

xlabel('Segment number');
```

```
ylabEL('R-node von Mises stresses(kPa)');

TITLE('R-node von Mises Stresses');

fclose('all')

[m,n]=size(c);

m1=1;

n1=1;

fid=fopen('E.inp','w');

while m1<=m;

str7=strcat(num2str(c(m1,1)));

fprintf(fid,'%s\n',str7);

m1=m1+1;

end

fclose(fid);


Function [d1]=try1(file1)

a1=load(file1);

b1=a1(:,1);

c1=-a1(:,3);

c2=-a1(:,4);

c3=-a1(:,5);

for k=1:1600

b2(k,1)=[(c1(k,1)-c2(k,1))^2+(c2(k,1)-c3(k,1))^2+(c3(k,1)-c1(k,1))^2]^0.5/2^0.5;

end
```

```
b3=cat(2,b1,b2);

m=40;

n=40;

m1=1;

m2=1;

d=zeros(m,2,n);

n1=1;

n2=1;

for i=1:n;

for i=1:m;

d(m2,1,n2)=b3(m1,1);

d(m2,2,n2)=b3(m1,2);

m1=m1+40;

m2=m2+1;

end

n2=n2+1;

n1=n1+1;

m1=n1;

m2=1;

end

d1=d;


Function [d2]=try2(file2)
```

```
a1=load(file2);
b1=a1(:,1);
c1=-a1(:,3);
c2=-a1(:,4);
c3=-a1(:,5);
for k=1:1600
b2(k,1)=[(c1(k,1)-c2(k,1))^2+(c2(k,1)-c3(k,1))^2+(c3(k,1)-c1(k,1))^2]^0.5/2^0.5;
end
b3=cat(2,b1,b2);
m=40;
n=40;
m1=1;
m2=1;
d=zeros(m,2,n);
n1=1;
n2=1;
for i=1:n;
for i=1:m;
d(m2,1,n2)=b3(m1,1);
d(m2,2,n2)=b3(m1,2);
m1=m1+40;
m2=m2+1;
end
```

```
n2=n2+1;

n1=n1+1;

m1=n1;

m2=1;

end

d2=d;
```

3.2 Finding R-node Elements and Plotting for Layered Cohesive Soils

```
Function [b]=try3(file1,file2)

[d1]=try1(file1);

[d2]=try2(file2);

b=zeros(40,2);

c=zeros(40,1);

mm=zeros(40,40);

for i=1:40;

a1=d1(:,:,i);

a2=d2(:,:,i);

a3=a1(:,2)-a2(:,2);

a4=a1(:,2);

for h=1:40

a3(h)/a4(h);

a5(h,1)=ans;

end

for h=1:39
```

```
if and(abs(a5(h,1))<=0.1,abs(a5(h+1,1))<=0.1)
if
and(or(and(a5(h,1)>=0,a5(h+1,1)<0),and(a5(h,1)<0,a5(h+1,1)>=0)),abs((a5(h,1)+a5(h+1,
1))<=0.1))
mm(h,i)=a1(h,2)-(a1(h,2)-a1(h+1,2))*a5(h,1)/(a5(h,1)-a5(h+1,1));
else
mm(h,i)=0;
end
end
end
[m1,n1]=min(abs(a5));
[m,n]=max(mm(:,i));
if m >= a1(n1,2)
b(i,1)=a1(n,1);
b(i,3)=m;
c(i)=n;
else
b(i,1)=a1(n1,1);
b(i,3)=a1(n1,2);
c(i)=n1;
end
b(i,4)=m1*1000;
b(i,5)=m;
```

```
b(i,2)=[a1(n,2)+a2(n,2)]/2;
end
subplot(1,2,1);
plot(c,'o');
axis([1 40 1 40]);
grid on;
xlabel('Segment number');
ylabEL('Row number');
TITLE('R-node Locations');
subplot(1,2,2);
plot(b(:,3));
axis([1 40 0 100]);
grid on;
xlabel('Segment number');
ylabEL('R-node von Mises Stresses(kPa)');
TITLE('R-node von Mises Stresses');
fclose('all')
[m,n]=size(c);
m1=1;
n1=1;
fid=fopen('E.inp','w');
while m1<=m;
str7=strcat(num2str(c(m1,1)));
```

```
fprintf(fid,'%s\n',str7);

m1=m1+1;

end

fclose(fid);


Function [d1] = try1(file1)

a1=load(file1);

b1=a1(:,1);

b2=a1(:,7);

b3=cat(2,b1,b2);

m=40;

n=40;

m1=1;

m2=1;

d=zeros(m,2,n);

n1=1;

n2=1;

for i=1:n;

for i=1:m;

d(m2,1,n2)=b3(m1,1);

d(m2,2,n2)=b3(m1,2);

m1=m1+40;

m2=m2+1;
```

```
end
n2=n2+1;
n1=n1+1;
m1=n1;
m2=1;
end
d1=d;

Function [d2] = try2(file2)
a1=load(file2);
b1=a1(:,1);
b2=a1(:,7);
b3=cat(2,b1,b2);
m=40;
n=40;
m1=1;
m2=1;
d=zeros(m,2,n);
n1=1;
n2=1;
for i=1:n;
for i=1:m;
d(m2,1,n2)=b3(m1,1);
```

```
d(m2,2,n2)=b3(m1,2);

m1=m1+40;

m2=m2+1;

end

n2=n2+1;

n1=n1+1;

m1=n1;

m2=1;

end

d2=d;
```

3.3 Finding R-node Elements and Plotting for Cohesive-frictional Soils

3.3a For Trial One and Two

```
Function [b]=try3(file1,file2,file3,c,phi)

[d1]=try1(file1,file3,c,phi);

[d2]=try2(file2,file3,c,phi);

b=zeros(40,2);

c=zeros(40,1);

mm=ones(40,40)*10001;

for i=1:40;

a1=d1(:,:,i);

a2=d2(:,:,i);

a3=a1(:,2)-a2(:,2);
```

```
a4=a1(:,2);
for h=1:40
a3(h)/a4(h);
a5(h,1)=ans;
end
for h=1:39
if and(abs(a5(h,1))<=0.1,abs(a5(h+1,1))<=0.1)
if
and(or(and(a5(h,1)>=0,a5(h+1,1)<0),and(a5(h,1)<0,a5(h+1,1)>=0)),abs((a5(h,1)+a5(h+1,
1))<=0.1))
mm(h,i)=a1(h,2)-(a1(h,2)-a1(h+1,2))*a5(h,1)/(a5(h,1)-a5(h+1,1));
else
mm(h,i)=10001;
end
end
end
[m,n]=min(mm(:,i));
if m > 10000
m = 0;
else
m=m;
end
b(i,1)=a1(n,1);
```

```
if m >= 10000
b(i,3)=0;
c(i)=n;
else
b(i,3)=a1(n,2);
c(i)=n;
end
end
subplot(1,2,1);
plot(c,'o');
axis([1 40 1 40]);
grid on;
xlabel('Segment number');
ylabEL('Row number');
TITLE('R-node Locations');
subplot(1,2,2);
plot(b(:,3));
axis([1 40 0 30]);
grid on;
xlabel('Segment number');
ylabEL('R-node Moblized Cohension Cd(kPa)');
TITLE('R-node Moblized Cohension Cd');fclose('all')
[m,n]=size(c);
```

```
m1=1;

n1=1;

fid=fopen('E.inp','w');

while m1<=m;

str7=strcat(num2str(c(m1,1)));

fprintf(fid,'%s\n',str7);

m1=m1+1;

end

fclose(fid);


Function [d1] = try1(file1,file3,c,phi)

ld=load(file1);

sw=load(file3);

b1=ld(:,1);

for k=1:1600

ql(k,1)=-0.5*(ld(k,3)-ld(k,5));

pl(k,1)=-0.5*(ld(k,3)+ld(k,5));

qw(k,1)=-0.5*(sw(k,3)-sw(k,5));

pw(k,1)=-0.5*(sw(k,3)+sw(k,5));

b(k,1)=(ql(k,1)+qw(k,1))/(pl(k,1)+pw(k,1)+ c/tan(phi*3.14/180));

if b(k,1)>1

b(k,1)=0.99;

k;
```

```
b(k,1);

pause

end

cd(k,1)=tan(asin(b(k,1)))*c/tan(phi*3.14/180);

end

b2=cd;

b3=cat(2,b1,b2);

m=40;

n=40;

m1=1;

m2=1;

d=zeros(m,2,n);

n1=1;

n2=1;

for i=1:n;

for i=1:m;

d(m2,1,n2)=b3(m1,1);

d(m2,2,n2)=b3(m1,2);

m1=m1+40;

m2=m2+1;

end

n2=n2+1;

n1=n1+1;
```

```
m1=n1;

m2=1;

end

d1=d;


Function [d2] = try2(file2,file3,c,phi)

ld=load(file2);

sw=load(file3);

b1=ld(:,1);

for k=1:1600

ql(k,1)=-0.5*(ld(k,3)-ld(k,5));

pl(k,1)=-0.5*(ld(k,3)+ld(k,5));

qw(k,1)=-0.5*(sw(k,3)-sw(k,5));

pw(k,1)=-0.5*(sw(k,3)+sw(k,5));

b(k,1)=(ql(k,1)+qw(k,1))/(pl(k,1)+pw(k,1)+ c/tan(phi*3.14/180));

if b(k,1)>1

b(k,1)=0.99;

k;

b(k,1);

end

cd(k,1)=tan(asin(b(k,1)))*c/tan(phi*3.14/180);

end

b2=cd;
```

```
b3=cat(2,b1,b2);

m=40;

n=40;

m1=1;

m2=1;

d=zeros(m,2,n);

n1=1;

n2=1;

for i=1:n;

for i=1:m;

d(m2,1,n2)=b3(m1,1);

d(m2,2,n2)=b3(m1,2);

m1=m1+40;

m2=m2+1;

end

n2=n2+1;

n1=n1+1;

m1=n1;

m2=1;

end

d2=d;
```

3.3b For Trial Three and Four

```
Ffunction  [b]=try3(file1,file2,file3,c,phi)
[d1]=try1(file1,file3,c,phi);
[d2]=try2(file2,file3,c,phi);
b=zeros(40,2);
c=zeros(40,1);
mm=ones(40,40)*0;
for i=1:40;
a1=d1(:,:,i);
a2=d2(:,:,i);
a3=a1(:,2)-a2(:,2);
a4=a1(:,2);
for h=1:40
a3(h)/a4(h);
a5(h,1)=ans;
end
for h=1:39
if and(abs(a5(h,1))<=0.1,abs(a5(h+1,1))<=0.1)
if
and(or(and(a5(h,1)>=0,a5(h+1,1)<0),and(a5(h,1)<0,a5(h+1,1)>=0)),abs((a5(h,1)+a5(h+1,
1))<=0.1))
mm(h,i)=a1(h,2)-(a1(h,2)-a1(h+1,2))*a5(h,1)/(a5(h,1)-a5(h+1,1));
else
mm(h,i)=0;
```

```
end

end

end

mm;

[m1,n1]=min(abs(a5));

[m,n]=min(abs(mm(:,i)));

if m == 0

b(i,1)=a1(n1,1);

b(i,3)=a1(n1,2)*1000;

c(i)=n1;

else

b(i,1)=a1(n,1);

b(i,3)=m*1000;

c(i)=n;

end

end

subplot(1,2,1);

plot(c,'o');

axis([1 40 1 40]);

grid on;

xlabel('Segment number');

ylabEL('Row number');

TITLE('R-node Locations');
```

```
subplot(1,2,2);

plot(b(:,3));

axis([1 40 0 2]);

grid on;

xlabel('Segment number');

ylabEL('R-node Safety Factor K');

TITLE('R-node Safety Factor K');

fclose('all')

[m,n]=size(c);

m1=1;

n1=1;

fid=fopen('E.inp','w');

while m1<=m;

str7=strcat(num2str(c(m1,1)));

fprintf(fid,'%s\n',str7);

m1=m1+1;

end

fclose(fid);


Function [d1] = try1(file1,file3,c,phi)

ld=load(file1);

sw=load(file3);

b1=ld(:,1);
```

```
for k=1:1600

ql(k,1)=-0.5*(ld(k,3)-ld(k,5));

pl(k,1)=-0.5*(ld(k,3)+ld(k,5));

qw(k,1)=-0.5*(sw(k,3)-sw(k,5));

pw(k,1)=-0.5*(sw(k,3)+sw(k,5));

b(k,1)=(ql(k,1)+qw(k,1))/(pl(k,1)+pw(k,1)+ c/tan(phi*3.14/180));

if b(k,1)>1

b(k,1)=0.99;

k;

b(k,1);

pause

end

tan(asin(b(k,1)));

c1(k,1)=c/tan(phi*3.14/180);

c2(k,1)=sin(phi*3.14/180)*(pw(k,1)+c1(k,1))-qw(k,1);

K(k,1)=c2(k,1)/(ql(k,1)-sin(phi*3.14/180)*pl(k,1));

end

b2=K;

b3=cat(2,b1,b2);

m=40;

n=40;

m1=1;

m2=1;
```

```
d=zeros(m,2,n);

n1=1;

n2=1;

for i=1:n;

for i=1:m;

d(m2,1,n2)=b3(m1,1);

d(m2,2,n2)=b3(m1,2);

m1=m1+40;

m2=m2+1;

end

n2=n2+1;

n1=n1+1;

m1=n1;

m2=1;

end

d1=d;


Function [d2] = try2(file2,file3,c,phi)

ld=load(file2);

sw=load(file3);

b1=ld(:,1);

for k=1:1600

ql(k,1)=-0.5*(ld(k,3)-ld(k,5));
```

```
pl(k,1)=-0.5*(ld(k,3)+ld(k,5));

qw(k,1)=-0.5*(sw(k,3)-sw(k,5));

pw(k,1)=-0.5*(sw(k,3)+sw(k,5));

b(k,1)=(ql(k,1)+qw(k,1))/(pl(k,1)+pw(k,1)+ c/tan(phi*3.14/180));

if b(k,1)>1

b(k,1)=0.99;

k;

b(k,1);

pause

end

tan(asin(b(k,1)));

c1(k,1)=c/tan(phi*3.14/180);

c2(k,1)=sin(phi*3.14/180)*(pw(k,1)+c1(k,1))-qw(k,1);

K(k,1)=c2(k,1)/(ql(k,1)-sin(phi*3.14/180)*pl(k,1));

end

b2=K;

b3=cat(2,b1,b2);

m=40;

n=40;

m1=1;

m2=1;

d=zeros(m,2,n);

n1=1;
```

```
n2=1;
for i=1:n;
for i=1:m;
d(m2,1,n2)=b3(m1,1);
d(m2,2,n2)=b3(m1,2);
m1=m1+40;
m2=m2+1;
end
n2=n2+1;
n1=n1+1;
m1=n1;
m2=1;
end
d2=d;
```